Design Analysis of a Lomolding Machine

Charl Leonard Goussard

Dissertation presented in partial fulfillment of the requirements for the degree of Doctor of Philosophy in Engineering at the Stellenbosch University

Department of Mechanical and Mechatronic Engineering
Stellenbosch University

Promoter: Prof A.H. Basson

December 2007

Declaration

I, the undersigned, hereby declare that the work contained in this dissertation is my own original work and that I have not previously in its entirety or in part submitted it at any university for a degree.

Signature: .....
C.L. Goussard

Date: .....

Abstract

Design Analysis of a Lomolding Machine

C.L. Goussard

Department of Mechanical and Mechatronic Engineering
Stellenbosch University
Private Bag X1, 7602 Matieland, South Africa

Dissertation: PhD (Mechanical Engineering)

December 2007

This dissertation describes the design analysis of a lomolder (a machine similar to an injection moulding machine). It focuses on key design aspects that will drive the purchase cost of the machine and that will also influence the maintenance and operating cost. The main objective of the study is to provide an understanding of the key factors that influence the cost of a lomolder as well as the factors that contributes to a quality manufactured part.

A semi-analytical flow model was developed to predict cavity pressure drops for a range of part sizes. This model was necessary to eliminate time consuming numeric simulations required for machine optimisation. Numerous machine concept designs were developed and a final layout design chosen. A parametric CAD model was built for the lomolder. Layout designs for different sized lomolders can be generated with this model. The dissertation concludes with a cost study that focuses on the purchase cost of a lomolder unit. Key elements such as choice of actuator and piston to part area ratio are described.

Uittreksel

Ontwerpsanalise van 'n Lomolding Masjien

("Design Analysis of a Lomolding Machine")

C.L. Goussard

Departement Meganiese en Megatroniese Ingenieurswese
Stellenbosch Universiteit
Privaatsak X1, 7602 Matieland, Suid Afrika

Proefskrif: PhD (Meganiese Ingenieurswese)

Desember 2007

Hierdie proefskrif beskryf die ontwerpsanalise van 'n lomolder ('n masjien soortgelyk aan 'n inspuitgietmasjien). Dit fokus op sleutel ontwerpsaspekte wat die aankoopkoste van die masjien dryf asook die onderhouds- en bedryfskoste beïnvloed. Die hoofdoel van die studie is om die sleutel faktore te verstaan wat die koste van 'n lomolder beïnvloed, asook die bydraende faktore wat lei tot 'n kwaliteit vervaardigde produk.

'n Semi-analitiese vloeimodel is ontwikkel om die drukval in die holte te bepaal vir 'n reeks van produk groottes. Die model is nodig om tydrowende numeriese simulasies wat vir masjienoptimering benodig word, te elimineer. Verskeie masjienkonsepontwerpe is ontwikkel en 'n finale uitlegontwerp is gekies. 'n Parametriese RGO (rekenaargesteunde-ontwerp) model is ontwikkel vir die lomolder. Uitlegontwerpe vir verskillende groottes lomolders kan met die model genereer word. Die proefskrif sluit af met 'n kostestudie wat fokus op die aankoopkoste van 'n lomolder eenheid. Sleutel elemente soos die aktueerder keuse en suier-tot-part-area verhouding word bespreek.

Acknowledgements

I wish to express my sincere gratitude to everyone who has contributed to this dissertation in any way. In particular, I would like to convey my thanks to the persons, institutions and companies below:

- Professor A.H. Basson for his valuable advice, criticisms and guidance throughout the research.
- My fellow students, Jacques Dymond, Brett Johnson and Pieter van Wyk, for their advice and support.
- Lomotek Polymers, the National Research Foundation (NRF) and Stellenbosch University for financial assistance.
- Everyone at the Mechanical and Mechatronic Engineering department, thank you for your friendliness and help throughout my many years of tertiary education. It was indeed a wonderful experience.
- Grant Hailmer and Koot Kotze of TF Design for their help regarding costing of the lomolders. Their comments and advice from industry are appreciated.
- Kevin Lombard, Colin Rothery and Georg Venter of Tectra Automation for their advice and costing of the Rexroth linear screws, servo electric motors and drives.
- Steven Claase of Yale Engineering Products for information on Spiracon roller screws.
- Leon Christians and Jolene Hall of Zest for the AC motor costs.
- Herman van Rensburg of Hytec Engineering for helping me with different hydraulic layout choices and costing of the units.
- Wolfgang Viehweg of Circuit Breaker Industries for his valuable input regarding maintenance of injection moulding machines in practice.
- Patrick Bracke of Engel South Africa for his advice on choosing between hydraulic and electric machines in practice.

- Victor Marques of Yelland Control and Gregory Donelly of Siemens Automation and Drives for their valuable advice regarding control systems.

- My family and friends, for their love, patience and encouragement throughout these years.

Finally to my Creator, Saviour and Heavenly Father. My praise and thanks for the life that I have.

Contents

List of Figures

List of Tables

Nomenclature

Variables

b	shortest side of rectangle
c_L	polymer melt specific heat capacity
c_S	frozen polymer specific heat capacity
F	force
Gz	Graetz number
h	half-height of cavity
h^*	half-height of the polymer melt region
k_L	thermal conductivity of polymer melt
k_S	thermal conductivity of frozen polymer
l	longest side of rectangle
L	length of thermal entrance region
m	viscosity shear rate coefficient or mass
$\triangle P$	pressure drop
p	lead
P	power
Q	constant material volume flow rate
R	radius
R_i	average radius of control volume i
Sf	Stefan number
T	torque
T_i	polymer inlet melt temperature
T_m	polymer melting temperature
T_w	uniform cavity wall temperature
u_x	polymer velocity in the flow direction
v	velocity
w	width of flow channel

w_i	width of flow channel of control volume i
x	axial coordinate in channel
x_f	melt front position in channel
y	coordinate in height direction
α	polymer melt thermal diffusivity
$\Gamma()$	gamma function
δ	dimensionless thickness of frozen polymer
Θ^*	dimensionless wall temperature
ε	dimensionless axial coordinate in channel
ε_f	dimensionless melt front position in channel
Λ	latent heat of fusion
ϕ	diameter
ρ_L	polymer melt density
ρ_S	frozen melt density
μ^*	material unit shear rate viscosity

Subscripts

lom	lomolder
max	maximum
met	metering cylinder
min	minimum
mol	moulding cylinder

Chapter 1

Introduction

1.1 The Lomolding Process

Lomolding is a piston moulding process aimed at making similar parts to injection moulding. The classical injection moulding process shown in Figure 1.1 (Weir, 1975) will be described first as many similarities exist between injection moulding and lomolding.

Injection moulding consists of four phases: a material melting phase, an injection phase, a packing and cooling phase and a part ejection phase. The polymer material is fed in a granular form from a hopper into a plasticising unit. The plasticising unit consists of a screw, barrel, heater bands and a hydraulic or electrical motor. Heater bands are necessary to melt the polymer material. The temperature of the melt is also raised by the viscous shear action generated by the screw. As the material is melted, the melt travels towards the front of the screw. The screw moves backwards at the same time until the required volume of material is reached to fill the part cavity. This volume is called the material shot. Once the required shot is measured the screw is pushed forward and the melt is injected through a sprue into the cavity. The sprue is typically a few millimetres in diameter. The mould is in

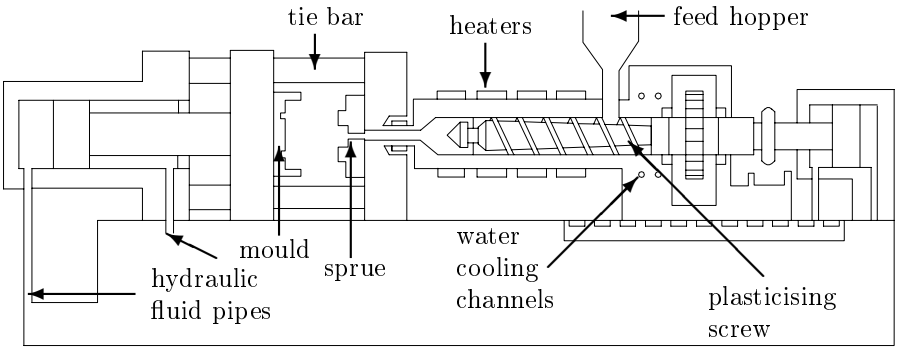

Figure 1.1: Injection moulding process

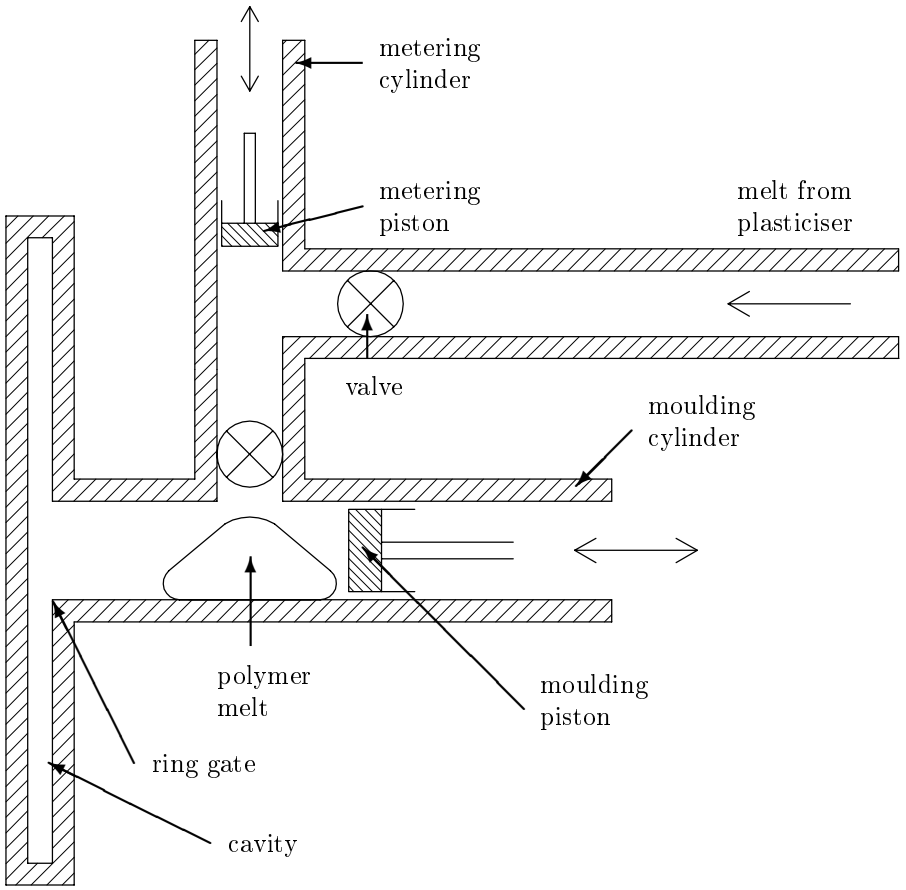

Figure 1.2: Lomold process

the closed position while the melt is injected. Once the melt injection is completed, it is necessary to pack the material as material cooling results in shrinkage. During packing the screw is pushed forward very slowly to account for the smaller melt volume. Once the cooling phase is completed, the mould is opened and the part ejected by ejector pins. The material in the sprue is completely solidified at this time and the part breaks lose at the sprue. The sprue diameter must be small enough to ensure that the manufactured part parts easily from it.

Traditionally hydraulics is used to turn the plasticising screw and to push the screw forward. Today, on typically small and medium sized injection machines, electric servo motors are used instead of hydraulics.

Lomolding's main operational sequence (illustrated in Figure 1.2) starts by measuring off in the metering cylinder the exact amount of molten thermoplastic required for a part (the shot). Next, the melt is transferred to the moulding cylinder and then pushed into the moulding cavity by a piston. The material entry point into the cavity is similar to a fully open external ring gate in injection moulding. During solidification, the moulding piston holds the cavity under pressure (to en-

sure sufficient packing) and the piston face forms part of the cavity wall. Once the solidification phase is completed the part is ejected. Note that no sprue exists in lomolding.

An exact measuring phase is necessary, as there is no chance of adding or removing molten material from the shot once the moulding cylinder started pushing the melt into the cavity. This is different from injection moulding where more material can be pushed into the part cavity during the packing stage for instance. The area where the melt enters the cavity is much larger than the typical sprue of injection moulding, which brings expected advantages such as moulding of longer fibres, lower material shear rates, and lower clamping force requirements. Chapter 3 discusses the potential advantages and expected disadvantages of lomolding in detail.

1.2 Background

Lomotek Polymers and Stellenbosch University formed a partnership in 2002 to further develop lomolding. A patent from parts of Lomotek's initial research was filed by Eckardt and Stemke (2000). The patent describes a similar sequence of accumulating melt in a first melt-collecting chamber where the material shot is measured. The melt is then moved to a second melt-collecting chamber in front of a moulding piston which subsequently pushes the melt into the cavity. Part of the invention was to make it possible to easily convert an existing injection moulding machine into one having the characteristics described above. The main aim was to reduce variations in melt injection pressure needed to fill the cavity.

The first lomolder (LM1) design was done before Stellenbosch University became involved in the project. Based on the experience gained with LM1, a second lomolder (LM2) was designed and built as a retrofit Engel injection moulder. All lomolding research at Stellenbosch University was done on LM2 and was focused in four subprojects described below.

1.2.1 Process know-how and thermo-fluid modelling

The objectives of this subproject were to develop a sound understanding of lomolding and the capability to numerically model the mould cavity filling process. It was driven by the fact that little experience existed for this novel process and the effects of process parameters (such as mould filling rate, maximum injection pressure, number of moulding pistons, etc) were unknown. Furthermore, it would have been impractical to obtain answers for these questions by only carrying out experimental work. Dymond (2004) successfully developed a numerical model that can be used to predict injection pressures, melt temperatures, etc.

1.2.2 Process-material-product interaction

Since this is a novel process the polymer materials most suitable for lomolding had to be identified. The objectives of this subproject were to develop a knowledge data base of different materials suitable to the lomolding process. Focus was placed on determining the material properties required as an input to the numerical model described in Subsection 1.2.1, understanding the impact of material properties and process characteristics on product properties and understanding the role, application and limitations of long fibre reinforcement in polymer products (Johnson, 2006).

1.2.3 Rapid tooling

Lomolding competes with products manufactured by injection and compression moulding processes. Therefore, once suitable profitable products were identified, it was necessary to be able to quickly manufacture mould cavities for prototype parts. Joubert (2005) investigated current rapid tooling technologies with emphasis on high-speed milling for manufacturing cavities for small production runs. The goal of this subproject was to reduce time-to-market of lomolding parts.

1.2.4 Machine design and costing

The second prototype lomolder had many disadvantages as a result of a few design errors that became evident during experimental work done on this machine. Part of this subproject was to rethink the whole concept and to design a better machine. The focus of the machine design was to determine elements that greatly influence the cost of the machine as a whole. Emphasis was placed on purchase cost, maintenance cost and operating cost. This subproject of lomolding is what comprises this dissertation by Goussard.

The redesigned concept was further developed and a third prototype was built by a company that manufactures injection moulding machines commercially. A few minor changes were done on the design described in this dissertation.

1.3 Objectives

The objective of this dissertation is to determine design critical factors that have a large impact on machine cost for a range of different sized manufactured parts. Many machine component configurations exist that will be able to successfully manufacture a part. However, finding cost optimal solutions prove to be difficult, since no prior design and cost knowledge exists for this new invention. Three main cost design issues exist: What is the optimal ratio of part effective area to moulding piston face area, what is the optimal number of melt injection moulding

cylinders when larger parts are manufactured and what type of actuator (hydraulic or electric) must be used? This dissertation narrows down the options for these questions for a variety of part sizes.

1.4 Motivation

The lomolding machine size is mainly driven by the injection pressure needed to fill the mould cavity as well as the clamping force needed to resist the cavity pressures to avoid material flashing. These pressures are strongly influenced by the fill rate, the solidification rate against the mould walls during mould filling and the non-Newtonian character of the flow. Research has been done intensively in this field to predict for instance cavity pressures during mould filling, material filling profiles and temperature distribution during filling and cooling to name a few. Richardson has shown interest in this field and has mainly contributed from 1980 to 1987 on this topic. His main interest was to predict cavity pressures for simple geometric models analytically. His research will be described in Chapter 2.

During this time the computer capability was reached to compute these solutions numerically. Computer aided engineering (CAE) for injection moulding emerged as a highly intensive research field (Bernhardt, 1983)(Manzione, 1987)(Schacht *et al.*, 1985). This research mainly focussed on improvisations that could be made to part cavity design in the early design phases before costly manufacturing commenced. Wang *et al.* (1986) reported research on the filling process of the melt in the cavity and Singh and Wang (1982) analysed mould cooling during processing. Review articles covering the research done in this field were published by Mavridis *et al.* (1986) and Kim and Turng (2004).

Several numerical simulation programs (Cadmould, Mouldflow, etc.) have been developed to assist the mould designer in analysing the behaviour of the molten material before expensive moulds are manufactured. These programs typically require a large amount of user interaction (creating a mesh, setting large numbers of process and material parameters, cumbersome post processing, etc.) to accurately simulate a specific part. Therefore, it was soon realised that numerical simulations will take too long to be used to explore overall machine design decisions and optimising of the lomolding machines. A semi-analytical flow model was developed (Goussard and Basson, 2006a)(Goussard and Basson, 2006c) to quickly obtain the injection pressure and clamp force needed to produce a certain part for a range of operating parameters (i.e. cycle time, melt and mould temperatures, and material properties). User intervention is kept to a minimum to facilitate automation of the optimisation process.

The semi-analytical model answers are verified by numerical simulation at the optimum operating parameters. These answers are then used as input to a parametric CAD model that assists the designer in producing a lomolding machine

according to various parameters. The parametric model (Goussard and Basson, 2006b) focuses on the lomolding unit (metering cylinder, moulding cylinder) and attention is paid to factors such as runner design and material flow areas. This is necessary to exploit the advantages of lomolding as mentioned earlier. Quite a few design concepts were developed and carefully evaluated (Goussard and Basson, 2007) to ensure that an optimal machine configuration was selected.

A cost model with focus on purchase cost of equipment, maintenance cost and operating cost during operation was developed. This was particularly challenging as no prior knowledge existed for the lomolding machines. Collection of these data from literature proved impossible since this information is proprietary to machine manufacturing companies and is vital in such a competitive market. Costing research in injection moulding concentrates mostly on part features and mould design (Chen and Liu, 1999)(Lee *et al.*, 1997).

1.5 Strategy and Overview of Dissertation

Note that a literature review is not included as a separate chapter. Background and literature relevant to each chapter are given at each chapter's start as each chapter's contents differ substantially.

It was necessary to develop a quick method to predict the cavity pressure drop occurring during the injection phase sufficiently accurate for machine design issues. Chapter 2 describes the development of this semi-analytical flow model in detail. Background to the problem is given as well as a description of how models found in literature have been adopted to fit the needs of the author. A few case studies show the applicability of the flow model.

Chapter 3 presents all the concepts that were evaluated in the design of the lomolding machine. Particular emphasis was placed on the metering unit, hot runner configuration and moulding unit design.

The selected machine concept was further refined in Chapter 4. A parametric sizing model of the lomolding machine was developed. This model enables the designer to efficiently create a layout model of the runner areas, metering unit and moulding unit for a machine that will be able to manufacture a certain sized part. Case studies are given for a small and large lomolder configuration.

Chapter 5 presents a parametric cost model of the lomolding machine. It focuses on the initial purchase cost of a typical machine. Aspects regarding maintenance cost and operating cost are also highlighted.

Chapter 6 reports some case studies to show the applicability and use of the parametric costing model.

Finally, Chapter 7 contains a few extensions that can be made to the cost model and concludes the dissertation.

Chapter 2

Semi-analytical Flow Model

2.1 Introduction

The necessity of an analytical flow model to predict cavity pressures during mould filling was described in Section 1.4. A solidified layer of material forms on the inside of the cold cavity walls during the melt injection phase. This effectively reduces the flow area available to the melt and results in a pressure drop across the melt flow path. The analytical model provides a means of calculating the height of this solidification layer and estimating the subsequent melt injection pressure drop. This estimation can be done in a fraction of the time compared to answers obtained by numerical analysis. Therefore, the model is very useful for optimisation studies.

2.2 Literature Review

Researchers have shown interest in theoretical and experimental studies involving fluid flow with solidification in circular tubes and on the walls of parallel plate channels. The effect of this solidification layer on laminar flow heat transfer was reported by Zerkle and Sunderland (1968), Hsing-Lung and Hwang (1977) and Weigand and Beer (1991). Zerkle and Sunderland (1968) and Lee and Zerkle (1969) studied the steady solidification of fluid flow for Newtonian fluids with constant physical properties and no viscous heating. They cast the energy equation into a form which is similar to one that describes the classical Graetz problem. The solution is found by the method of separation of variables and it takes the form of an infinite sum of eigenvalues. Janeschitz-Kriegl (1977) and Dietz *et al.* (1978) proposed methods to calculate the thickness of the frozen layer which is formed on the cold cavity walls during the injection moulding process. Janeschitz-Kriegl (1977) used a steady-state heat transfer coefficient and the viscous heat generated was estimated from the average melt velocity and the pressure gradient under isothermal conditions. Dietz *et al.* (1978) estimated the thickness of the frozen solid

layer by applying the solution for an infinite solid slab. Janeschitz-Kriegl (1979) showed in a later paper that a more detailed study with the aid of coupled motion and energy equations will not improve the accuracy of the solid layer thickness estimation. Effects such as glass transition or crystallisation kinetics at extreme rates of cooling and shearing heavily influence these results.

Richardson *et al.* (1980) described the benefits of decomposing moulding networks into basic geometries and solving an analytical flow problem for each segment. This scheme aided mould maker decisions regarding hot runner, sprue and mould design. Richardson (1983) extended the solution of Zerkle and Sunderland (1968) and Lee and Zerkle (1969) to non-Newtonian fluids with viscous heating. Again the energy equation is transformed and the temperature and frozen layer thickness are expanded in a power series. The thickness of the frozen layer is then computed by substituting the first three terms of the power series into the energy equation. This solution is well suited for material flows with high Graetz (Gz) numbers, for example in the thermal entrance region. The Graetz number is the ratio between the heat convection in the flow direction and the heat conduction in the direction perpendicular to the flow. In the work presented here, the solutions for flow between parallel plates were used. These solutions and how they are adapted to compute flows in discs, for instance, are described in more detail in Section 2.3.

Richardson also published three papers on flows with freezing of variable-viscosity fluids. The first (Richardson, 1986a) described developing flows with very high heat generation due to viscous dissipation that is large enough to cause significant variations in viscosity. However, the difference between the polymer temperature at the inlet to a specific part of the mould network and the melting temperature of the polymer is assumed not to cause significant variations in polymer viscosity. The second paper (Richardson, 1986b) described developing flows with very low heat generation due to viscous dissipation. Further, the difference between the temperature of the polymer at entry to a specific part of the mould network and the melting temperature of the polymer is assumed to be sufficiently large to cause significant variations in polymer viscosity. Polymer flows in pipes, between discs and between parallel plates were considered. These results compare reasonably well with results obtained from Richardson's (1983) previous paper as long as the flow Graetz number is sufficiently large. In the third paper, (Richardson, 1986c) discussed solutions for cases where the polymer flow is fully developed.

The first models proposed by Richardson (1986a) did not produce good results for typical lomolding flows when compared to numerical simulation results. It could be argued that the variations in shear rate are over-shadowed by the large difference in polymer inlet temperature to polymer melt temperature ($\pm 70\,^{\circ}\mathrm{C}$) and therefore the second paper (Richardson, 1986b) produces more acceptable results. However, combining the closed form solutions for the three different geometry types of the second paper, as required for the work presented in this dissertation, is not feasible. The third paper's flow solutions are not applicable to lomolding as the

flows considered in the work presented here are generally undeveloped regarding the temperature field.

All of the above papers consider polymer injection at constant flow rate. This constant flow rate phase comprises approximately the first 80 % to 90 % of the polymer injection stage and is followed by polymer injection at constant pressure. Richardson published three more case studies involving cavity filling at constant pressure: freezing off at polymer injection gates (Richardson, 1985a), freezing off in round and flat cavities (Richardson, 1985b) and freezing off in disc cavities (Richardson, 1987). As cavity filling occurs at more or less constant polymer flow rate for such a large part of the injection stage, the focus in the work presented here was placed on filling at constant flow rate.

Hill (1996) proposed solutions to find the equilibrium height of the solidified polymer layer, where the polymer temperature increase due to viscous dissipation is in equilibrium with the temperature drop due to heat conduction to the cold cavity wall. However, attention was restricted to the Newtonian case for which numerical solutions are provided as well. Neither the equilibrium, nor the Newtonian flow assumptions are reasonable for the work presented here.

Today, far more complex cavities and flow geometries can be analysed with numerical methods (this is the reason why interest in analytical models gradually disappeared). Analytical models are often used to test numerical algorithms for simple case studies. Yang *et al.* (1991) compared results for the steady solidification of non-Newtonian fluids flowing in round tubes. Gao *et al.* (1994) studied the effect of variable injection speed during injection mould filling. They also tested their numerical algorithms against simple analytical solution case studies.

2.3 Derivation of the Semi-analytical Flow Model

This section describes Richardson's (1983) analytical model briefly as well as the adaptation of the model to flows in channels of varying width. Figure 2.1 shows a schematic of the polymer flow between parallel plates. The flow is symmetrical with respect to the centreline and therefore only half of the cavity is shown. The half-height of the cavity is given by h and the distance between the centreline and the solidified layer by h^*. The solution is split into two regions, a thermal entrance region and a melt front region. The melt front region comprises most of the total flow length in typical cases.

The pressure drop ($\triangle P$) from melt entry into the cavity to the melt flow front (i.e. the entire flow length in the part cavity) is given by Equation 2.3.1:

$$\triangle P = \mu^* \int_0^{x_f} \left(\frac{(m+2)Q}{2wh^{*(m+2)}} \right)^{\frac{1}{m}} dx \tag{2.3.1}$$

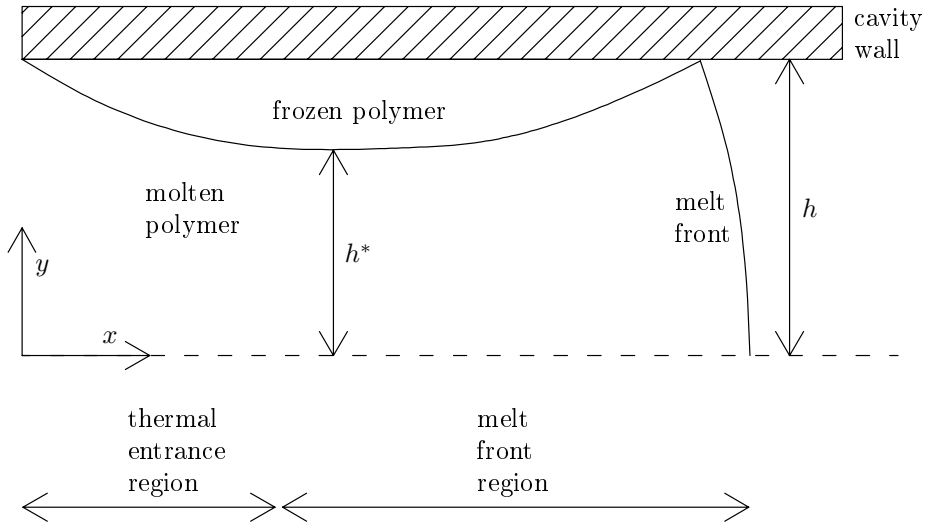

Figure 2.1: Polymer flow in a channel

The half-height of the polymer melt region h^* is found by introducing:

$$\delta = 1 - \frac{h^*}{h} \tag{2.3.2}$$

For the thermal entrance region δ is given by

$$\delta = 6\Theta^*\Gamma\left(\frac{4}{3}\right)\left(\frac{\varepsilon}{6(m+2)Gz}\right)^{\frac{1}{3}} + 0\left(Gz^{-\frac{2}{3}}\right) \tag{2.3.3}$$

and for the melt front region by

$$\delta = 4w^*\left(\frac{\varepsilon_f - \varepsilon}{Gz}\right)^{\frac{1}{2}} \tag{2.3.4}$$

where

$$\Theta^* = \frac{k_S(T_m - T_w)}{k_L(T_i - T_m)} \tag{2.3.5}$$

$$\Gamma\left(\frac{4}{3}\right) \approx 0{,}893 \tag{2.3.6}$$

$$\varepsilon = \frac{x}{L} \tag{2.3.7}$$

$$\varepsilon_f = \frac{x_f}{L} \tag{2.3.8}$$

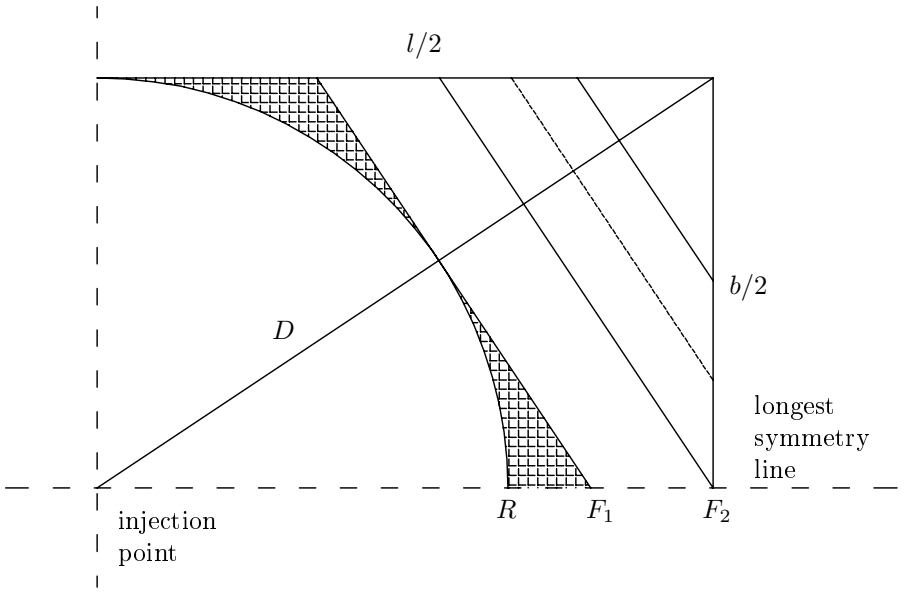

Figure 2.2: Schematic of the polymer flow front in a rectangular cavity (quarter segment shown)

$$w^* = \left(\frac{Sf}{2\kappa}\right)^{\frac{1}{2}} \tag{2.3.9}$$

$$Sf = \frac{c_S(T_m - T_w)}{\Lambda} \tag{2.3.10}$$

$$\kappa = \frac{k_L \rho_S c_S}{k_S \rho_L c_L} \tag{2.3.11}$$

The equations mentioned come from (Richardson, 1983). The Stefan number (Sf) is the ratio of the heat required to raise the polymer temperature from the cavity wall temperature to the polymer melting point, and the heat required to melt the polymer solid. Once the half-height of the polymer melt region is found for a control volume, the pressure drop can be calculated. These equations were derived for cases where the flow channel width remains constant and the flow front enters the cavity evenly over the whole channel width.

To develop the approach to apply the preceding to lomolding, consider a typical moulding case: a rectangular cavity with constant thickness is filled through a sprue in the centre of the cavity. Figure 2.2 shows a quarter of such a cavity.

Clearly the longest flow path is given by the diagonal line D running from the injection point to one corner. This longest flow path is divided into a number of control volumes. To calculate h^* for a specific control volume at a certain time, it is necessary to know the flow front position along D, the start point of the control

volume with respect to D, the length of this control volume along D and the average width of the control volume.

To place a particular control volume at an equivalent x-position in the analytic model, assumptions have to be made about the upstream and downstream conditions:

- The upstream flow path length in the semi-analytical model is taken to be the same as the true (geometric) length.
- The upstream and downstream flow path width is taken to be equal to the average width of the control volume under consideration.
- Once the melt front has passed through the control volume, its position is calculated using the above flow channel width (even though this will in general not coincide with the true flow front position).

Case studies, as shown in Section 2.4, have confirmed that the approximated upstream geometry gives reasonable results, even though any upstream variation in flow area will influence the time that the flow front takes to reach a control volume. The approximated downstream geometry can deviate from the true geometry without affecting the solidified layer thickness in the control volume under consideration since, for these cases where the flow rate is constant, the only upstream effect is in the pressure gradient.

The pressure drop and height of the solid layer are calculated for this control volume in a straight forward manner as described above. It is necessary to check if a control volume is positioned fully in the thermal entrance region, fully in the melt front region or contains both to solve Equation 2.3.1 correctly. Therefore it is necessary to calculate the equivalent width, volume and start position along D for each control volume. From Figure 2.2 it can be seen that the flow front will be circular until the nearest side of the rectangle ($b/2$) is met. Therefore the radius of the largest circular flow front is given by Equation 2.3.12.

$$R = \frac{b}{2} \tag{2.3.12}$$

Up to this point, the equivalent control volume width is given by Equation 2.3.13.

$$w_i = 2\pi R_i \tag{2.3.13}$$

From F_1 to F_2 (Figure 2.2, note F_2 is where the longest symmetry line meets the edge of the cavity) the equivalent flow widths are set equal to four times (note Figure 2.2 shows a quarter of the cavity) the length of a line perpendicular to D extending from the side of the cavity to the longest symmetry line. Note that these flow control volumes fall away when working with a square cavity (see Figure 2.3).

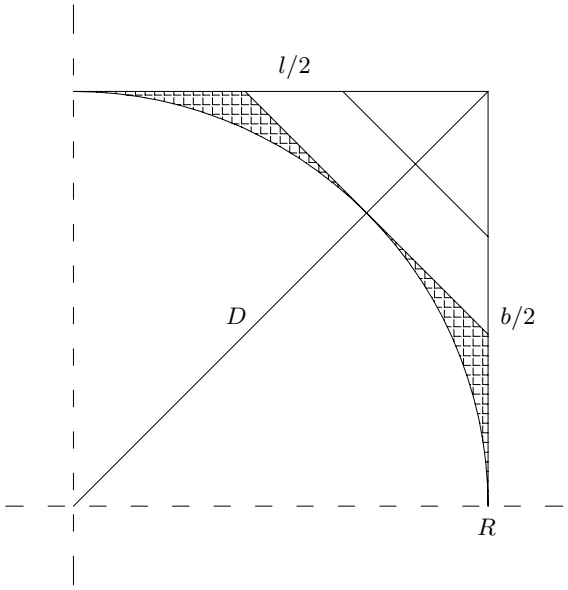

Figure 2.3: Schematic of the polymer flow front in a square cavity

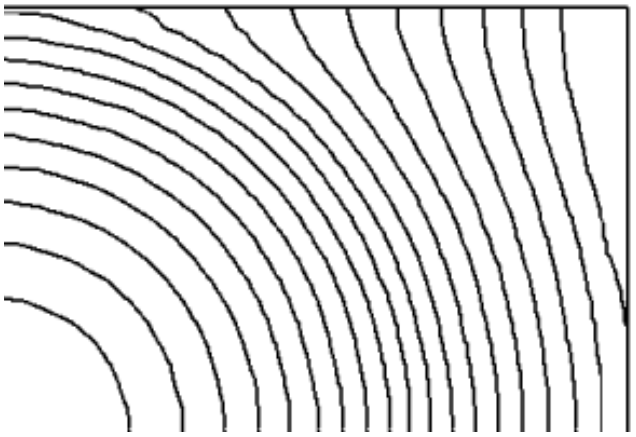

Figure 2.4: Flow lines for a rectangular cavity (one quarter showed) filled in the centre (lower left corner) as calculated with Cadmould (2002)

From position F_2 onwards the control volume width is calculated as four times the length of a line perpendicular to D extending from side to side.

Figure 2.4 shows that the assumptions made for the equivalent widths of the control volumes approximate the true flow case numerically calculated by Cadmould (2002).

It now remains to calculate the position of the melt flow front as closely as possible to the true flow phenomenon. As seen from Figure 2.2, the hatched area is

Table 2.1: Material properties

Property	**Novolen 1100 N**	**Celstran PP GF30**	**Unit**
Unit shear rate viscosity (μ^*)	5655	6958	Ns/m^2
Viscosity shear rate exponent (m)	2,63	3,31	
Melt inlet temperature (T_i)	220	260	℃
Polymer melting temperature (T_m)	154	170	℃
Cavity wall temperature (T_w)	40	55	℃
Polymer melt thermal conductivity (k_L)	0,236	0,150	W/mK
Polymer melt density (ρ_L)	910	994	kg/m^3
Polymer thermal diffusivity (α)	0,1043	0,0685	$1 \times 10^{-6}\,\mathrm{m}^2/\mathrm{s}$

the only area not accounted for in the control volumes. To preserve the filling time, the volume associated with the hatched area is added to all the control volumes on a per volume basis except for the round control volumes. Once this correction has been applied, it is easy to calculate the flow front position. The semi-analytical model is validated in the next section through different case studies.

2.4 Case Studies

This section shows some results to verify the semi-analytical model. The most restrictive requirement of the analysis presented above is that the flow Graetz number must be sufficiently high, which is explored later in this section. Two polymer materials suited for lomolding were selected for the case studies, i.e. Novolen 1100 N (a homogeneous polypropylene) and Celstran PP GF30 (a polypropylene with 30 % glass fibre component). The material properties for these materials given by Cadmould (2002) and Osswald and Menges (1995) were used and are summarised in Table 2.1.

Cadmould provides a Carreau viscosity model for these two materials. However, the analytical model developed here, needs a power law viscosity. The unit shear rate viscosity (μ^*) and the viscosity shear rate coefficient (m) are found by fitting a

Table 2.2: Range of shear rates to which power law is fitted

Fit number	Shear rate range [/sec]
1	1 - 500
2	5 - 2500
3	10 - 5000
4	100 - 50 000

power-law model to the Carreau model. However, as can be seen from Figure 2.5, the Carreau model is not a straight line on a log-log scale as it is a more complicated model. Therefore, it was necessary to determine in what range of shear rates the power law model needs to be fitted to achieve the most accurate results when compared to a numerical simulation. The power law viscosity model is given in Equation 2.4.1:

$$\mu = \mu^* \left| \frac{\partial u_x}{\partial y} \right|^{\frac{1}{m}-1} \tag{2.4.1}$$

Figure 2.5 shows four different fits of the power law to the Carreau viscosity model. Note that markers are only plotted at the start and end of each line for clarity. It is fitted for the Celstran material at a melt temperature equal to 260 ℃. This is a typical processing temperature for this fibre reinforced polymer. It is noted that the power law viscosity (used in Richardson's adapted model) is only a function of the material shear rate and not temperature or pressure. Therefore, a processing temperature is chosen.

The power law is fitted to four different ranges (given in Table 2.2) of shear rates. Case studies were performed for different sized parts where different viscosity fits were employed. On average, the best results for the predicted pressure drop during cavity filling were obtained when the power law viscosity model was fitted to the high shear rate portion of the Carreau model for both materials.

Figure 2.6 shows a typical case study where the sensitivity (as a result of the fitted power law viscosity) of the predicted cavity pressure drop during mould filling is compared to the numerical result of Cadmould that uses the Carreau viscosity model. Note that the power law that is fitted to the low shear rate region of the Carreau model results in a too high predicted pressure drop when used in the semi-analytical model.

Cadmould is used as a reference to check the accuracy of the analytical model throughout this research. Numerical models such as Cadmould are accepted in industry as analysis tools. They are validated according to known analytical solutions and experiments for simple mould cases. Therefore, results obtained from Cadmould are accepted as correct for the cases explored in this study. Limitations of the analytical model are also investigated with Cadmould.

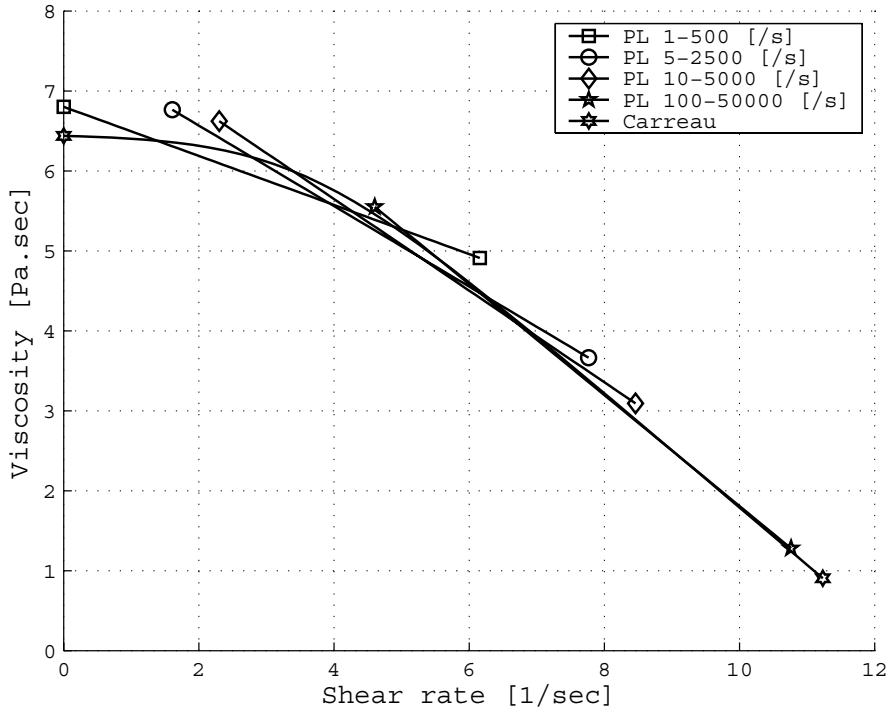

Figure 2.5: Power law viscosity fit to Carreau model for Celstran material

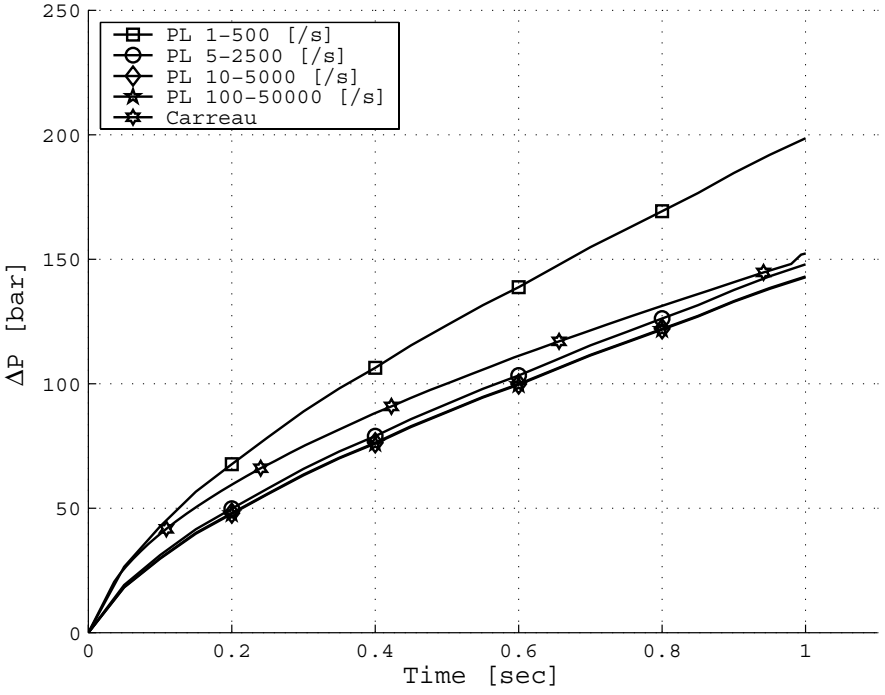

Figure 2.6: Pressure drop sensitivity as a result of power law fitted

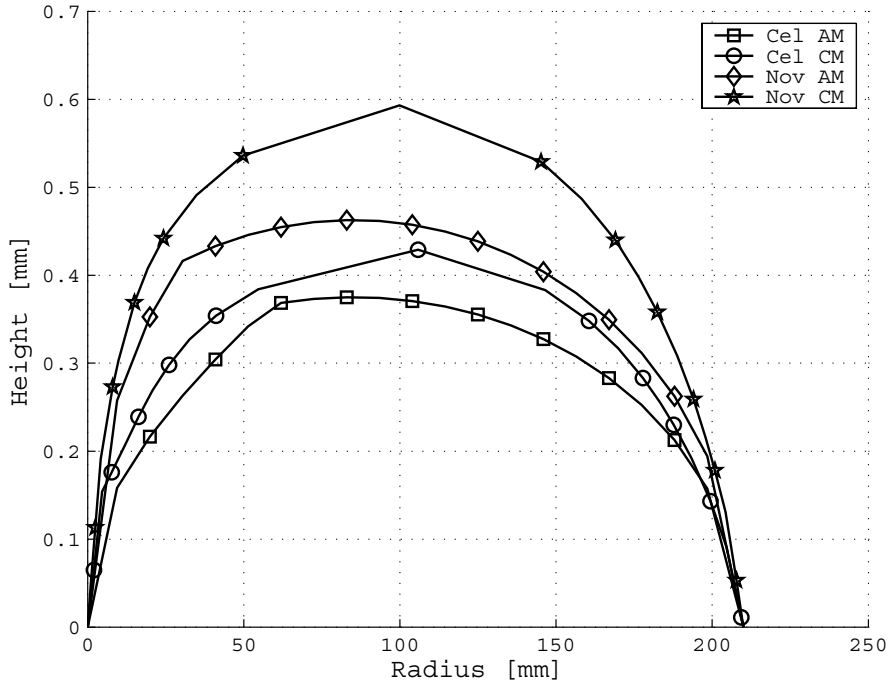

Figure 2.7: Growth of the solid layer in a disc cavity

Dymond (2004) showed that Cadmould can be used for simulating lomolding. The gate nodes have to be selected on the circumference of the ring gate. A few case studies were done comparing Cadmould's results to numerical results obtained from Moldflow (another widely used industry standard numerical package). Good comparison was found between the results.

The following figures showing the case study results use the following abbreviations: AM: Semi-analytical model result; CM: Cadmould numerical result; Cel: Celstran material; Nov: Novolen material.

The first case study is the filling of a 500 mm diameter disc, 3 mm thick and injection occurs along the circumference of an 80 mm diameter piston into the cavity. Therefore the flow path length is shown in Figure 2.7 as 210 mm. The disc is filled in one second at a constant flow rate. Figure 2.7 shows that the growth of the solid layer along the flow path (a radial line) is underestimated, relative to Cadmould for both materials. The pressure drop along the flow path relates well to the results obtained with Cadmould (Figure 2.8). The lowest calculated Graetz number was 209 for the Celstran material and 230 for Novolen.

The second case study involves a square cavity of 200 mm length and breadth, and 2 mm thick. The injection point is in the centre and the longest flow path D is equal to $100\sqrt{2}$ mm. The cavity is filled in 0,5 seconds. As can be seen from Figure 2.9, the semi-analytical model overestimates the growth of the solid layer in

this case, especially near the end of the flow path. This leads to higher predicted pressure drops for both materials as can be seen from Figure 2.10. The lowest calculated Graetz number was 134 for the Celstran material and 143 for Novolen. Note the sudden rise in pressure drop near the end of the filling phase due to the narrowing flow area.

The last case study is that of a rectangular cavity, 300 mm x 200 mm x 3 mm thick. The longest flow path D is equal to 180,28 mm. The cavity is filled in one second. Figure 2.11 shows that the solid layer height is reasonably well predicted for both materials. As a result of this, Figure 2.12 shows fair agreement between the analytical model and Cadmould for the pressure drop across the rectangular cavity. The lowest calculated Graetz number was 191 for the Celstran material and 209 for Novolen.

It is noted in the previous three case studies that a higher cavity pressure drop occurs under the same processing conditions when the homogeneous Novolen material is processed. However, this seems incorrect, since the Celstran material has added fibres that increase the viscosity. Therefore, logically, the Celstran material has to flow more difficult than the homogeneous polypropylene. The reason for this cavity pressure drop observation is that material scientists have added a flowing agent to the Celstran material. This additive decreases the melt viscosity below that of Novolen to make the material easier to mould.

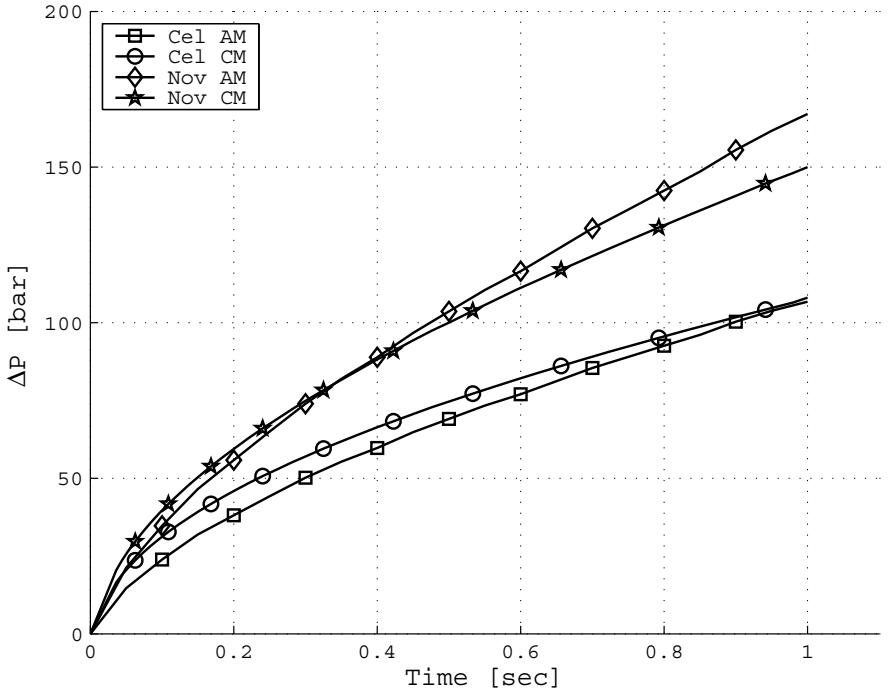

Figure 2.8: Pressure drop occurring in a disc cavity

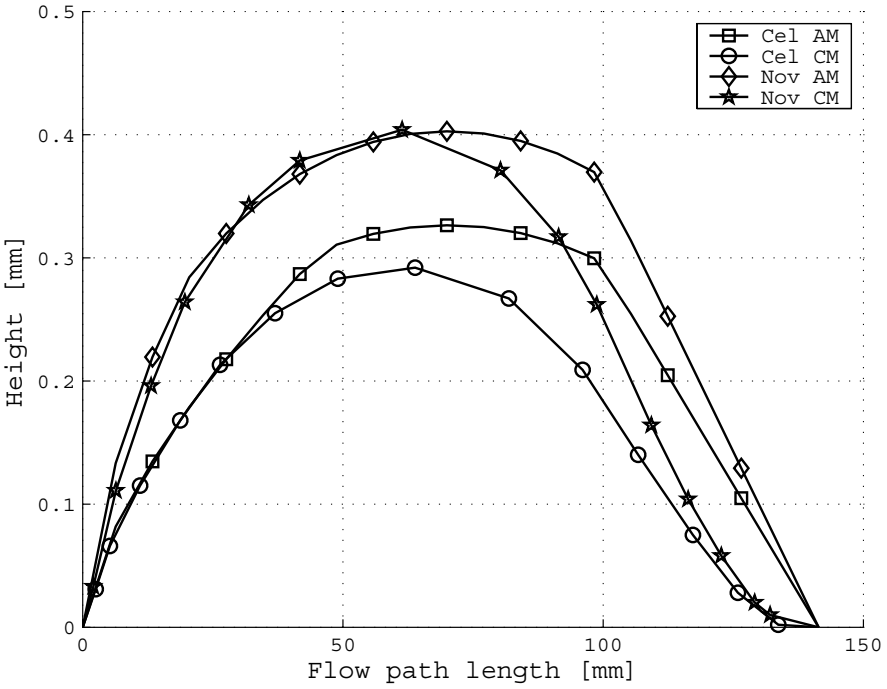

Figure 2.9: Growth of the solid layer in a square cavity

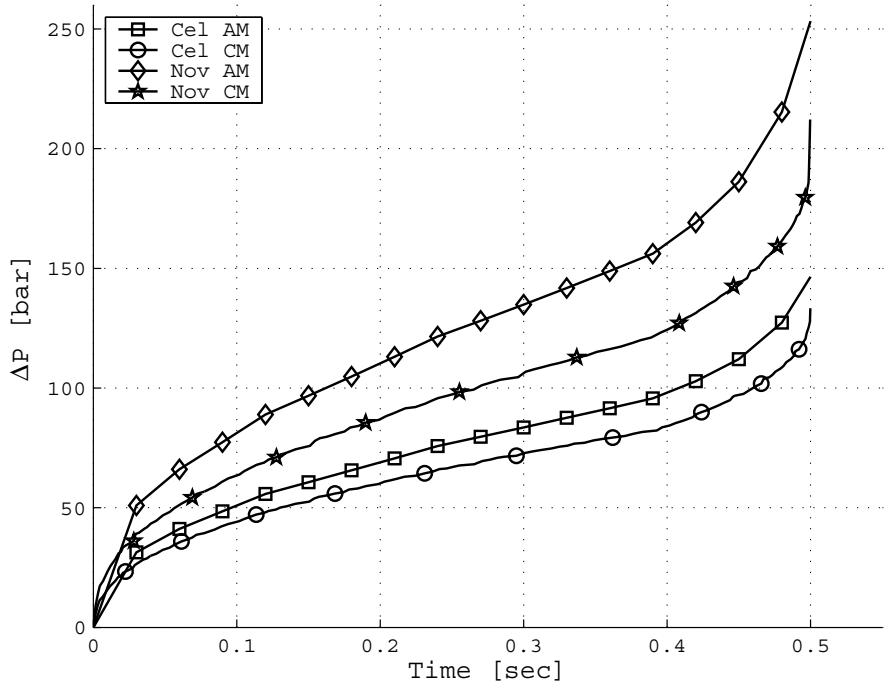

Figure 2.10: Pressure drop occurring in a square cavity

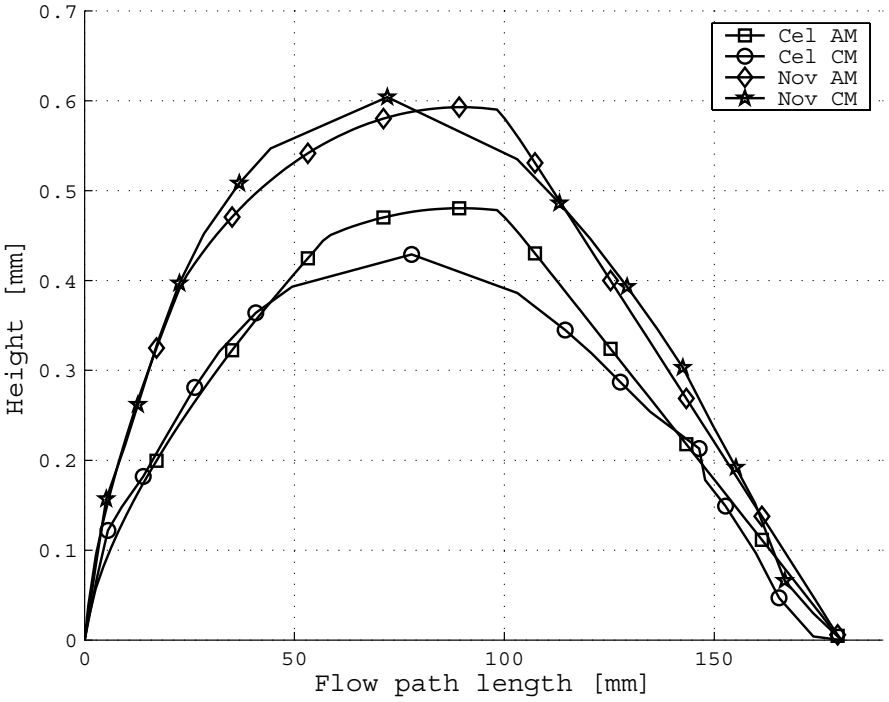

Figure 2.11: Growth of the solid layer in a rectangular cavity

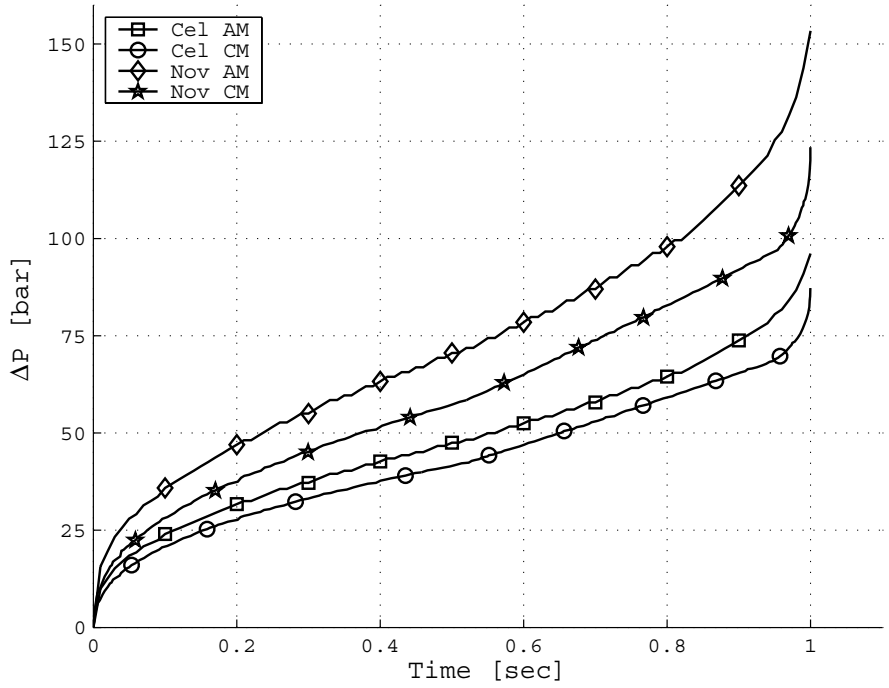

Figure 2.12: Pressure drop occurring in a rectangular cavity

In some situations, a cavity will be filled in a time that will minimise the pressure drop experienced during filling. However, if this filling time is too long, a larger injection pressure capacity machine may be used, since this will save cost during the machine life-time as the part cycle time will reduce. The fill rate directly influences the Graetz number, but the analytical model is only applicable to "large" Graetz numbers. It is therefore worth investigating what the influence is of the Graetz number on the accuracy of the semi-analytical model and what acceptable numerical values for the Graetz number would be.

The case studies conducted (Figures 2.13 to 2.18) show the influence of the Graetz number on the results obtained by the semi-analytical model for the same case studies shown in Figures 2.7 to 2.12. It is compared to numerical results obtained from Cadmould. The Graetz number reported in the figures is the smallest calculated at the end of the filling stage under constant flow rate. The objective was to find the filling time for which the pressure drop across the cavity will be a minimum when numerically calculated. These pressure drops are then compared to those found by the analytical model. It is also checked if this local minimum occurs at more or less the same filling time for both the analytical and numerical results. Again CM indicates to the results obtained from Cadmould and AM the semi-analytical model results.

Figures 2.13 and 2.14 show that for the disc cavity the pressure drop results differ strongly between the two models when the Graetz number drops below 100. The analytical model estimates the lowest pressured drop around a two seconds filling time. However, Cadmould estimates these minima at around four seconds for both materials. At two seconds the error of the semi-analytical model is 6 % in the case of the Novolen material and less in the case of Celstran. At 4 seconds this error grows to 59 % in the worst case which is again for the Novolen material. At this point the Graetz number is well below 100 at 37.

In the case of the square cavity shown in Figures 2.15 and 2.16, the analytical model predicts the smallest pressure drop at around a filling time of one second for both materials. This compares well to the filling times found by Cadmould, especially in the case of the Novolen material. The minimum pressure drop varies very little across a filling time of one to ten seconds in the case of the Celstran material. The error of the semi-analytical model is at most 33 % for the Novolen material case at a filling time of one second. At this point the Graetz number is equal to 57.

In the case of the rectangular cavity (Figures 2.17 and 2.18), both models predict a minimum pressure drop at around a two seconds cavity fill time. In the case of the Novolen material it is noted that the analytical model calculates a shorter optimal filling time corresponding to a minimum pressure drop compared to Cadmould. The semi-analytical model's error is 49 % at most for the Novolen case at a filling time of two seconds. At this point the Graetz number is equal to 83.

It can be seen from these results that the semi-analytical model is reasonably

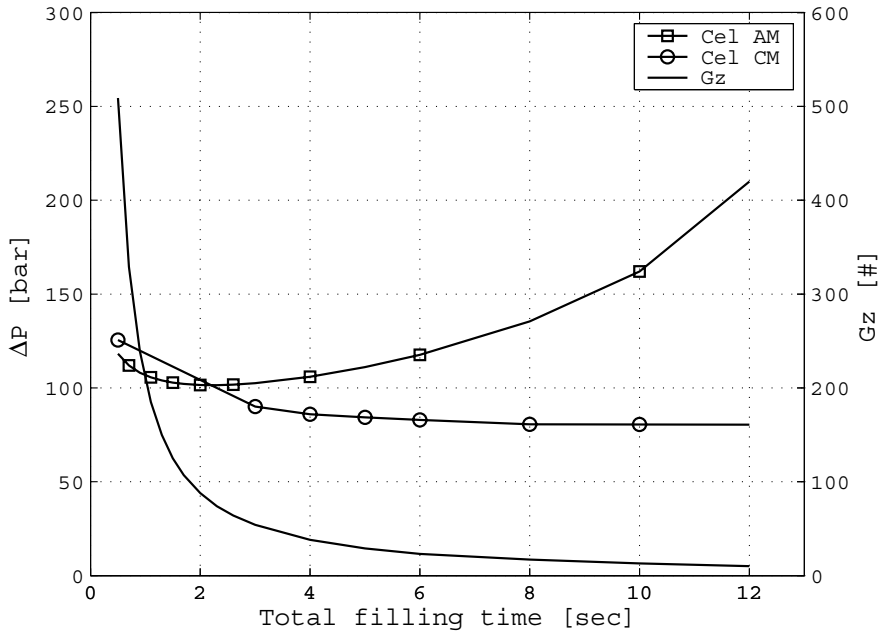

Figure 2.13: Pressure drop for different filling times in disc cavity for Celstran material

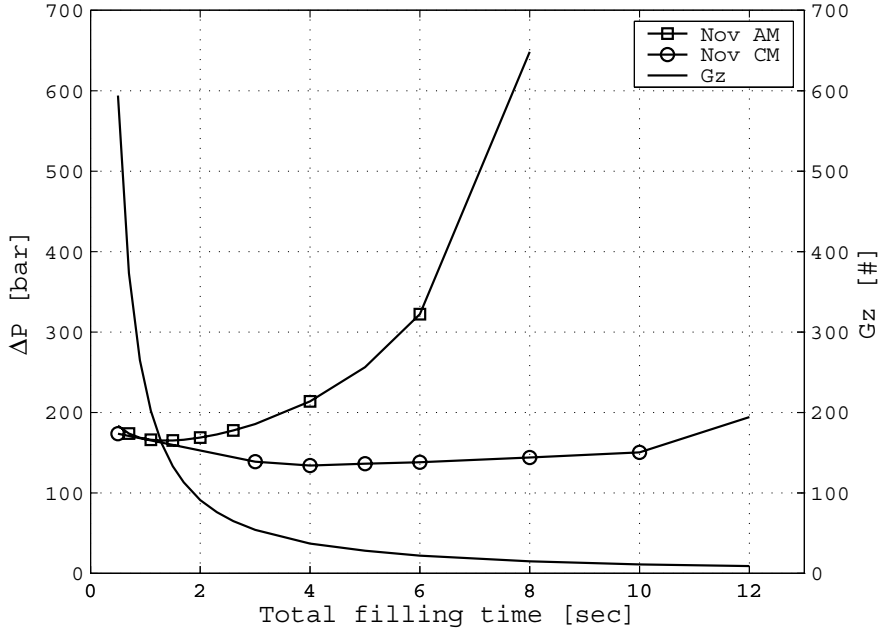

Figure 2.14: Pressure drop for different filling times in disc cavity for Novolen material

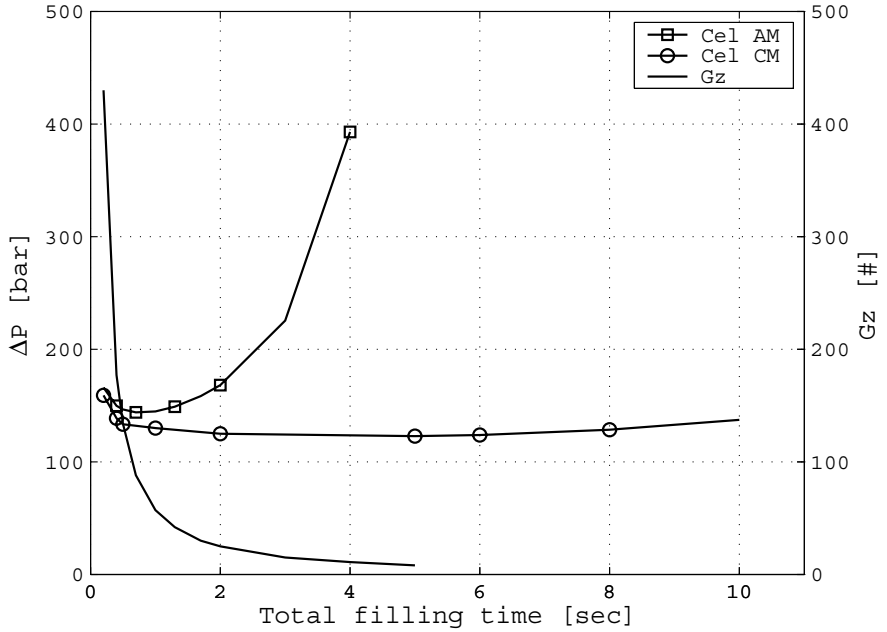

Figure 2.15: Pressure drop for different filling times in square cavity for Celstran material

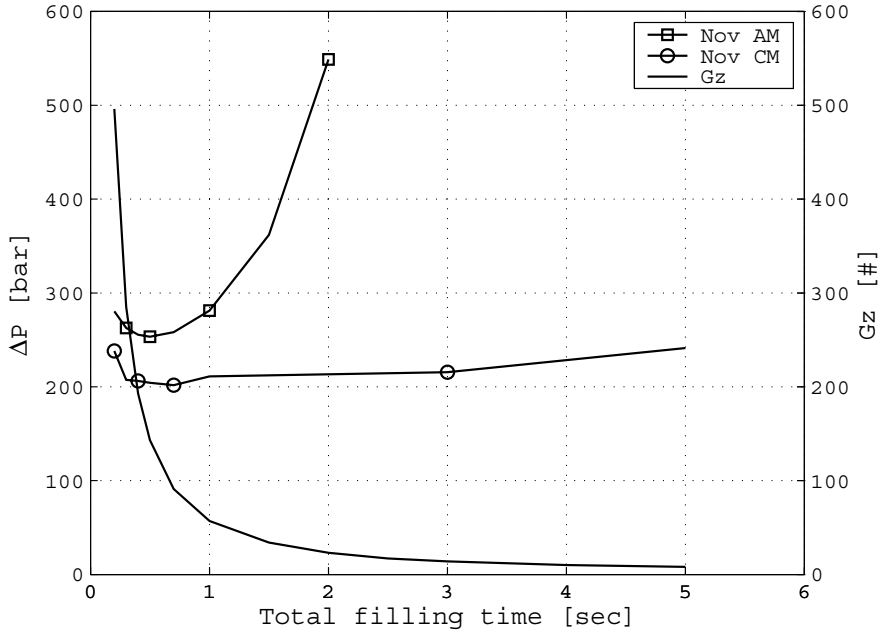

Figure 2.16: Pressure drop for different filling times in square cavity for Novolen material

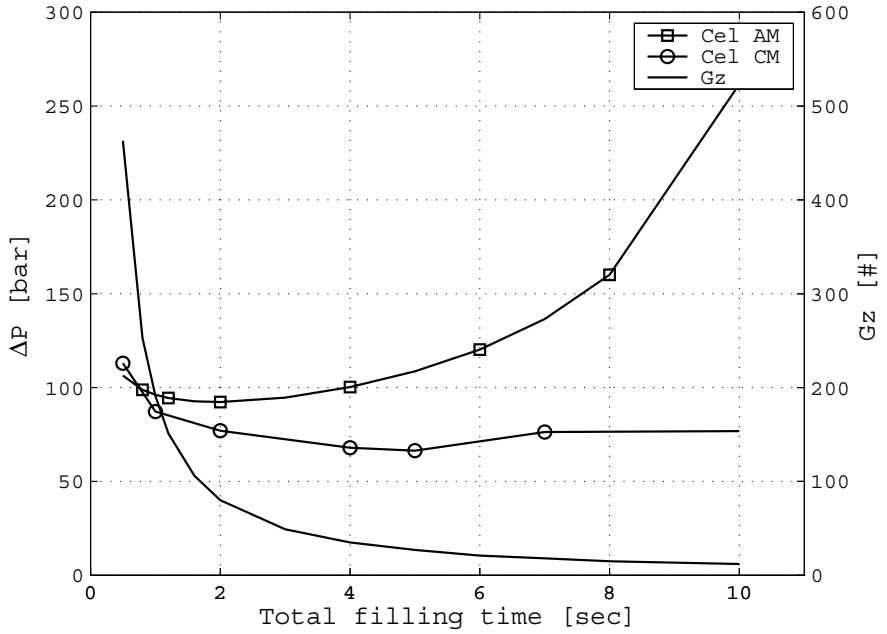

Figure 2.17: Pressure drop for different filling times in rectangular cavity for Celstran material

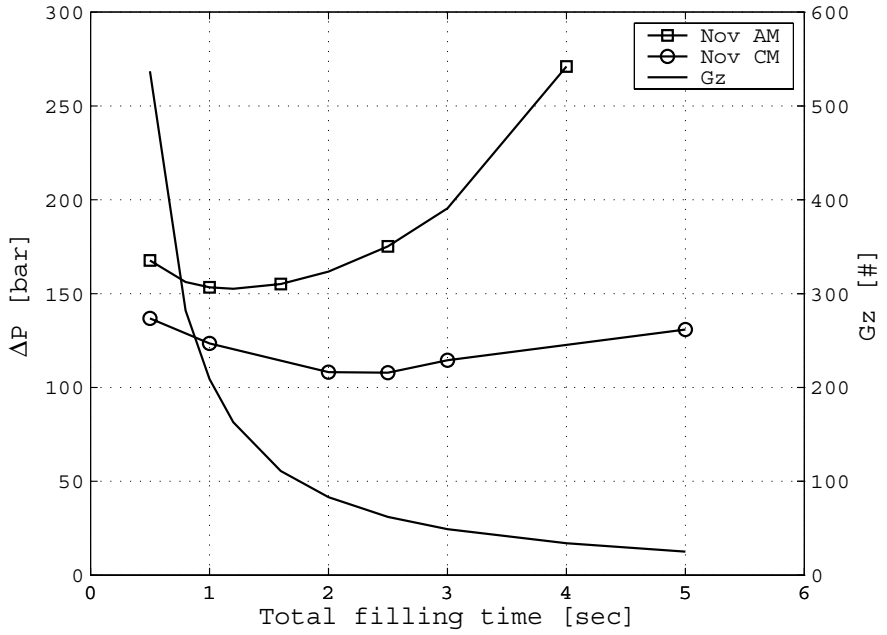

Figure 2.18: Pressure drop for different filling times in rectangular cavity for Novolen material

well suited to find the filling time that will correspond to a minimal pressure drop across the cavity as long as the Graetz number stays above 100 . Numerical simulations can then be carried out around this approximate optimum filling time and a better estimate for the pressure drop can be calculated. It is noted that the pressure drop computed by the semi-analytical model is higher than the pressure drop computed by Cadmould. This would mean that machines designed from these values will be slightly over designed and may be able to manufacture either slightly larger parts in the same time or produce the same part in a quicker cycle time.

2.5 Conclusion

The results presented in this chapter show that the semi-analytical model gives reasonable results for the pressure drop across the cavity when compared with numerical results obtained with Cadmould. The main restriction of the model is that too high pressure drops are predicted when the Graetz number drops below 100 . The reason for that is the overestimation of the solid layer thickness due to higher conduction between the molten material and the solid layer to the cavity wall. Due to the associated smaller flow area, the overestimated solid layer growth leads to a higher pressure drop than calculated with Cadmould. Otherwise, the model can be used for cavities with flow path length to cavity thickness aspect ratios in the range of the case studies presented here. The model provides a quick way of estimating the pressure drop across the cavity during filling, where numerical solutions would have been too cumbersome and time consuming.

The geometry creation and computation time for the models presented here are modest to insignificant. It is noted that the largest pressure errors occur towards the end of the filling phase. In practice a constant pressure control strategy is used for the last part of the filling phase. The machine sizing calculations are therefore based on the pressures encountered somewhat before the end of the filling phase. This filling method is shown in Figure 2.19. Case a shows a constant flow rate throughout the filling phase. In case b the flow rate is kept constant up to a certain time and it is followed then by filling under constant pressure until the cavity is completely filled.

Since the pressures encountered during mould filling are related to the filling rate, the filling rate can in practice be reduced if the pressures would have exceeded the design values for a given machine size. Also, the filling phase is normally much shorter than the cooling phase and the potential effects of the under/over prediction of pressure is restricted to a small part of the filling phase. Therefore, the influence of the largest pressure errors (i.e. those at the end of the filling phase) on the machine size and cycle time estimation is small. These pressure errors will have a small influence on the total machine cost, and the semi-analytical model can be expected to give useful results for machine sizing studies and cost assessments.

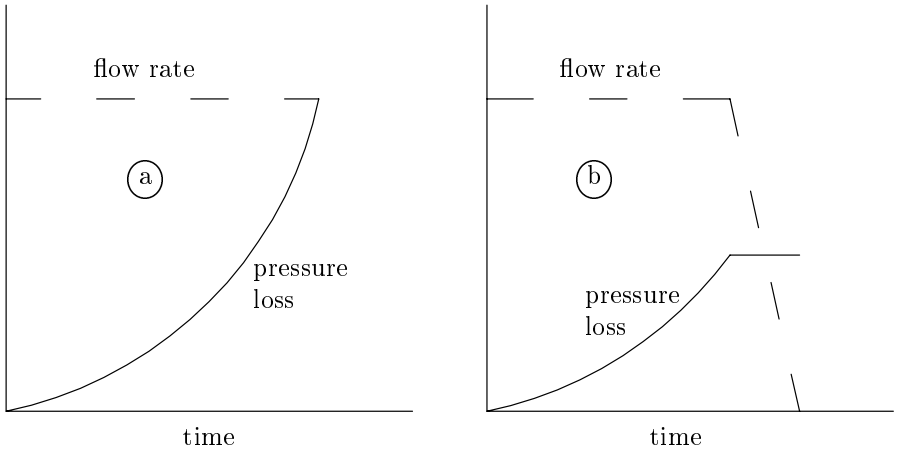

Figure 2.19: Cavity pressure loss and material flow rate during mould filling

Computing times for the analytical model is insignificant on a 3 GHz computer. The computation time for the numerical results is sensitive for the finite mesh density used to model the cavities. The case studies presented here comprised of relatively coarse meshes to keep the computation time reasonably low as many simulations were carried out. Computation time varied between 30 seconds and 3 minutes. The semi-analytical model will therefore yield substantially faster optimisation calculations, in addition to shorter pre- and post-processing times. Once a layout design has been selected, using the semi-analytical model presented here, final optimisation and design refinement can be done by using a numerical flow simulation package, such as Cadmould.

Chapter 3

Machine Design Concepts

3.1 Introduction

When the work presented in this dissertation started, two experimental machines had already been built and used for investigations of the lomolding process (Johnson, 2006). A few shortcomings of LM2 were identified during these investigations. These shortcomings were evaluated by various people involved in the project and led to the formulation and evaluation of new machine layout concepts (Goussard and Basson, 2006b). This was an essential step to ensure that a good concept was further developed and optimised. Sometimes it occurs in practice that a bad concept is optimised and made to work as a result of very tight time deadlines. Therefore, concepts were generated to maximise lomolding's potential advantages and minimise the effects of the expected disadvantages. Concepts were generated to fulfil the following required operations:

- transferring melt from metering phase to moulding phase
- minimising part defects caused by premature melt solidification
- elimination of accurate melt metering

This chapter explains and describes many of the design concepts that were evaluated as candidates for a new design of the lomolding machine. Each concept is described in detail: how it works, what the positive and negative aspects are and whether it was considered for further development. It explains why the design of the machine as described in Chapter 1 was chosen as a new design for further development. The next two sections describe lomolding's expected advantages and disadvantages. The design requirements against which the concepts were evaluated, were formulated with these advantages and disadvantages in mind.

3.1.1 Lomolding's expected advantages

Lomolding offers three distinct expected advantages when compared to injection moulding. Firstly, lower material shear rates are expected as a result of replacing the sprue with a large injection opening. Secondly, longer fibres can be injected into reinforced parts, since fibre attrition occurring in the sprue does not occur. Thirdly, the larger injection opening potentially reduces the needed injection pressure when compared to injection moulding. This, as well as the lower material shear rate at the material injection point, provides the ability to mould against skins (a thin delicate material inserted in the mould). These advantages are discussed in detail in the following paragraphs.

3.1.1.1 Lower material shear rates

Lomolding offers a lower material shear rate at the material entry point to the cavity compared to injection moulding. The reason for that is the larger flow area (the piston diameter is much larger than that of the sprue) that reduces the melt pressure gradient at the entry point. The material shear rate is directly influenced by the pressure gradient. Material shear stress results in the build up of residual stresses during processing which often leads to part warpage when the part is cooled and released from the mould (Matsuoka *et al.*, 1991).

3.1.1.2 Less fibre attrition

Thermoplastic materials are often reinforced with fibres to enhance their mechanical strength, stiffness, etc. This is done by adding short lengths (typical 1 mm to 2 mm) of fibre to the material that is plasticised in injection moulding. Longer lengths of fibre will either be broken in the plasticising screw, in the sprue or at the entry gate to the cavity. Fibre breakage due to bending (one of the reasons for fibre attrition) occurs as the fibres rotate against the material flow direction. These bending forces are proportional to the material shear rate (Zhang and Thompson, 2005). Therefore, less fibre attrition will occur during lomolding as the small sprue is replaced by a ring gate.

Material preparation for injection moulding is a very costly process. As an example: suppliers often combine the thermoplastic material with fibres and a flowing agent that changes the viscosity of the melt. Mixing of the material is done in a material extruder where the materials are heated and mixed. This process, called compounding, is similar to the material plasticising stage of injection moulding machines. The molten material is then pushed through small openings and fed through a water bath to allow the strings to cool down. The strings are then chopped into short lengths and dried. Short lengths are required, otherwise it will be impossible to remelt the material in a plasticiser. This chopping process and subsequent remelting in the plasticiser obviously reduces the average fibre length considerably.

The compounder can be coupled directly to a lomolder (or an injection moulder) if a melt accumulation chamber is added. As a result, the extruding of strings, cooling, chopping and drying process can be skipped.

Therefore, lomolding offers the advantage of less fibre attrition compared to injection moulding and even more if the lomolder is directly fed from a compounder in which case the plasticising stage (that accounts for a large portion of fibre attrition) is skipped.

3.1.1.3 Moulding against skins

The lower material shear rate during the cavity filling stage also lends itself to moulding against skins. During this process a thin skin of material (for example a printed logo) is put in the mould cavity on the opposite side of the injection point. The skin is bonded to the thermoplastic during injection. This process is difficult with injection moulding, since the high material shear rate and pressures at the entry gate often damage the skin. Moulding against skins results in non-uniform cooling of the part, since the skin restricts the heat transfer on one side. When injection moulding is used to mould against skins, the melt temperature is often increased to decrease the melt viscosity. This leads to a lower melt shear rate. However, this extra heat must be removed during the cooling phase and elevates the non-uniform cooling problem.

3.1.2 Lomolding's expected disadvantages

The exact amount of molten material has to be measured off in a metering device prior to the injection phase. This is necessary since the moulding piston's face forms part of the cavity wall once in the closed position. Too much material will result in an elevated piece of material ending up under the moulding piston. Too little material will either result in an under filled part or a part with insufficient packing (such a part will shrink more and part warpage might also be larger). Exact shot measurement can be overcome as the stopping position of the moulding piston to produce a good part will be known and can be measured during operation. With a closed loop control system, the amount of material needed can be easily corrected if necessary.

Since the moulding piston's face forms part of the cavity wall, it ideally needs to be at the same temperature as the cooled part cavity to ensure uniform cooling of the part, because different cooling gradients also contribute to part warpage (Matsuoka *et al.*, 1991). After material metering is completed, the melt is pushed in front of the moulding piston prior to the injection phase. During this time the moulding piston's face ideally needs to be hot to prevent melt solidification against it. This poses a problem, since it is impossible for both requirements to be met. Dymond (2004) showed that as long as the time the material spends in front of the

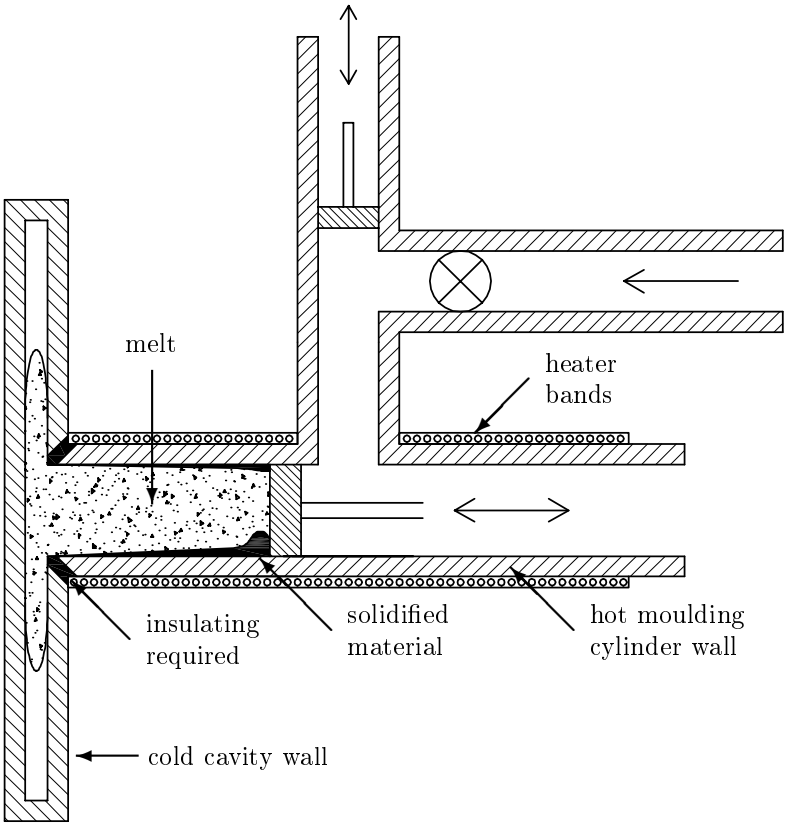

Figure 3.1: Insulation problem resulting in premature melt solidification

moulding piston is kept short, cooling of the piston face will not result in a part defect due to a solidified disc being pushed into the part.

The same type of problem is encountered where the moulding cylinder's wall is in contact with the part cavity (refer to Figure 3.1). The cylinder needs to be heated to prevent melt solidification prior to injection. However, the cavity wall must be cold, especially in the vicinity of the moulding cylinder to ensure uniform cooling. LM2 had a small opening between the mating surfaces of the part cavity and the cylinder. The opening had to be small enough to prevent melt leakage. A cylinder wall temperature gradient still existed and this lead to premature melt solidification mainly as a result of a too long material transferring time from the metering unit to the position in front of the moulding piston. This solidified material layer was scraped along when the moulding piston pushed the material into the cavity. This resulted in a part defect. A possible solution to this problem is to provide a small piece of insulating material between the moulding cylinder and the cavity. This adds a little complexity as well as maintenance due to wear of this extra insulation, especially if fibre reinforced material is processed. Another possible solution is to

make the contact area between the part cavity and the moulding cylinder as small as possible.

3.2 Design Requirements

This section analyses the needs of the client that the lomolder has to fulfil. The needs are translated into specifications. The specifications lead to several concepts that are discussed in the subsequent sections. The best one is chosen that potentially achieves all of the specifications. Focus is placed on the metering unit, hot runner configuration and the moulding unit, since these subsystems differ from injection moulding. Special attention is given to the existing disadvantages of LM2.

3.2.1 Prevention of premature melt solidification

The moulding cylinder temperature must transition from melt temperature (>200 ℃) where the melt is received, to mould wall temperature (<55 ℃) at the junction with the part cavity. The region below melt temperature should be kept as short as possible and the time that the melt is in contact with cold parts of the cylinder should be kept as short as possible to prevent premature solidification as discussed in Section 3.1.2.

3.2.2 Prevention of fibre attrition

Fibre attrition results in a lower average fibre length and this leads to weaker moulded parts than expected. Therefore, fibre breakage must be minimised since moulding long fibres is potentially a significant advantage of lomolding over injection moulding. Fibre breakage occurs in regions of high shear rate which causes bending moments on the fibres (Zhang and Thompson, 2005) (Jones, 1998). Therefore these regions of high shear rate are evaluated using equations published by Richardson (1983) to determine the pressure drop in runner sections.

3.2.3 Minimisation of part cycle time

A shorter cycle time means a better lomolder efficiency. It was decided to preferably do melt metering in parallel with the part cooling phase in order to reduce the overall cycle time. The part cycle time can also be shortened by having the metering cylinder inject some of the melt into the part cavity during the melt transfer phase. In order to accomplish this, the volume in front of the moulding piston must be less than the part volume.

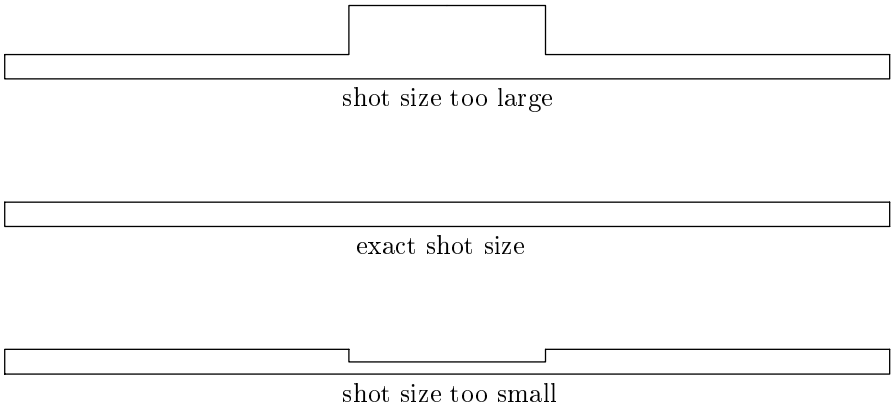

Figure 3.2: Part shapes as a result of different material shot sizes

3.2.4 Accurate metering

Inaccurate metering leads to the part defects shown in Figure 3.2. The varying part thickness under the moulding piston may be unacceptable when tight tolerances are needed. Measuring the exact amount of molten material needed is challenging, since thermoplastic materials expands and shrinks considerably with changes in temperature (Osswald and Menges, 1995).

3.2.5 Compactness of moulding unit

This was not a customer need as such, but is necessary as a design requirement. The moulding unit goes through the stationary platen. The stationary platen will partially loose its stiffness if the hole in the platen is too large as a result of a too bulky moulding and runner unit combination. Preferably, the ejection system must be situated on the same platen as the ring gate, otherwise the ejected part will have a piston mark on one side and ejection pin markings on the other side. A compact moulding unit provides more available space for the ejection system. This refinement is discussed in Chapter 4.

3.2.6 Easy material purging

It is important for the client to easily change between different materials or different colours as needed. Therefore, regions where molten material can remain instead of flowing through should be avoided as far as possible.

3.2.7 Easy maintenance

Easy maintenance of the lomolder is essential. Therefore, the lomolder must be able to make a large number of parts with the minimum of major maintenance (e.g. replacement or refurbishment of complex parts).

3.3 Concepts Developed to Transfer Melt

A number of concepts were generated to fulfil the goal of feeding molten material from a plasticiser or extruder into a metering cylinder where the exact amount of material to fill the cavity is measured off, followed by transferring the measured off material to in front of an injection piston, which then pushes this material into a part cavity. The main objective is to decrease the melt transfer time. Secondary objectives include minimising the number of parts (less complexity) and developing an as compact design as possible.

The concepts focus on a distinct aspect that were found lacking on LM2. The melt measuring time overshadowed the cycle time of the part with a volume of $589\,\mathrm{cm}^3$. The transfer unit runners were too small and this led to high pressures required to transfer the melt from the metering cylinder to a position in front of the moulding piston. It also led to high melt velocity speeds and therefore unnecessary high strain rates developed in the material that escalated fibre attrition. This aspect needed to be improved.

Concept 1 (Figure 3.3) shows an inline metering piston and moulding piston. The melt is moved by this double piston configuration and is measured between the two pistons. Once the correct volume of molten material has been measured, the melt is pushed through a valve in the moulding piston head and transferred to the front of the moulding piston. The valve in the piston then closes to prevent back flow of the melt and the moulding piston pushes the melt into the cavity to the point where its face forms part of the cavity wall at the end of the filling phase.

The concept's advantages include the compactness of the design (which reduces the size of the hole required in the stationary platen through which the moulding unit passes) and that material metering can be done in parallel with the part cooling phase.

The concept's main disadvantages are: The valve in the moulding piston creates a high melt velocity section. This increases the shear rate on the material and will cause fibre length attrition before the cavity even starts to fill. This smaller area may also be blocked by material with high fibre content. The inline metering piston and moulding piston leads to a complex mechanical design with increased maintenance times and maintenance difficulties expected. Insulating the hot side of the moulding piston facing the metering piston while metering is being done from the cold side (that forms part of the cavity wall) required for part cooling,

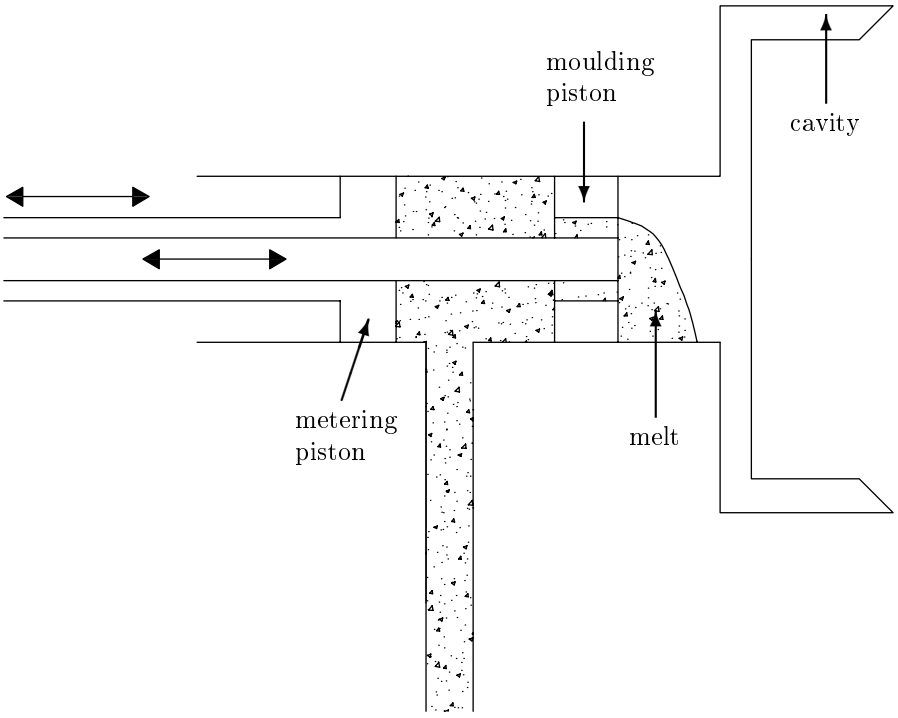

Figure 3.3: Concept 1: Inline pistons where melt is fed through the moulding piston

also poses difficulties. For instance, it will be difficult to cool the small valve head as the cooling tubes must run through the thin moulding shaft. The valve in the moulding piston head will result in an extra piston mark on the moulded part. Uniform cooling of the moulding piston on the cavity side will also be difficult to achieve due to the valve in the piston. Due to these disadvantages, concept 1 is not attractive.

Concept 2 (Figure 3.4) also has an inline metering piston and moulding piston, but the melt is measured behind the metering piston and pushed in front of the moulding piston via a bypass runner. Once the shot has been transferred in front of the moulding piston, a valve in the bypass runner closes to prevent backflow of material during the moulding phase. Next, the moulding piston pushes the melt into the cavity and its face forms part of the cavity wall at the end of the filling phase.

The main concept advantages include compactness of the design, although less than concept 1. Also, metering can be done while the part is being cooled. The hot melt is not in contact with the moulding piston during the measuring phase. Therefore, cooling of the moulding piston is less of a problem than in concept 1.

The disadvantages of the concept are: The inline metering piston and moulding piston leads to a complex design as in concept 1. Leakage of melt past the metering piston will accumulate between the metering piston and moulding piston. It will

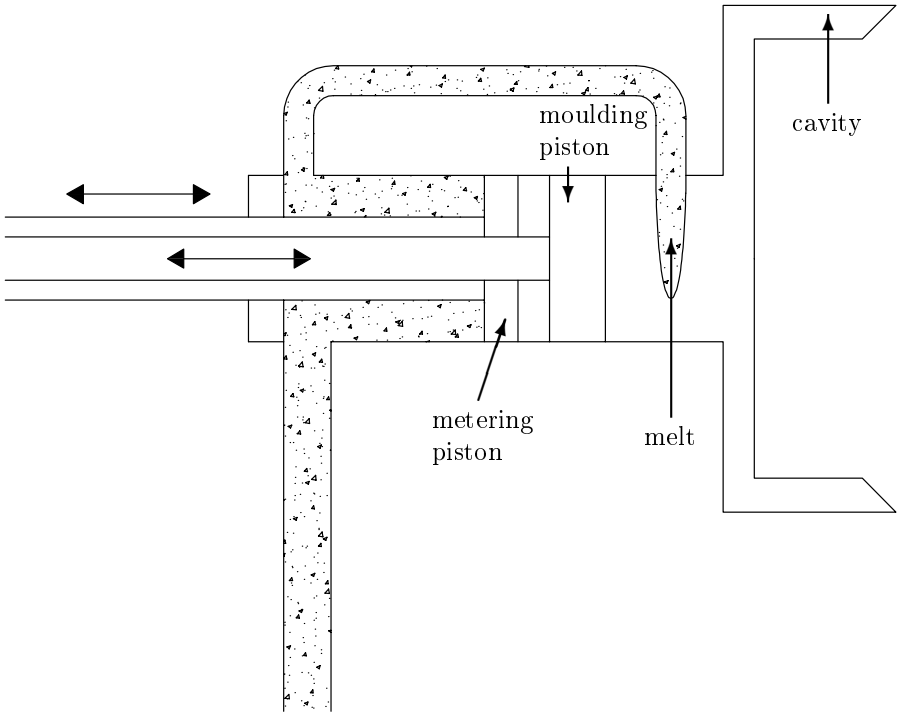

Figure 3.4: Concept 2: Inline pistons where melt is measured behind the metering piston and fed around the moulding piston

be very difficult to purge the melt from this position and this will lead to increased maintenance times. Concept 2 is therefore not attractive.

Concept 3 (Figure 3.5) is similar to concept 2, except that the melt is measured between the two pistons. It retains most of the disadvantages of concept 2, as well as the added complication that the moulding piston has to be hot on the metering side and cold on the cavity side. This concept holds no advantages above concept 2, except that the problem with melt leaking past the moulding piston in concept 2 has been eliminated. Therefore this concept is not considered further as well.

Concept 4 (Figure 3.6) shows a combined metering and moulding piston and a cross-fed shut-off valve. The melt is measured between the moulding piston and the shut-off valve and, once the correct volume of molten material has been measured, a valve closes in the melt inlet to prevent back flow of the melt during the cavity filling phase. After the shut-off valve opens, the moulding piston pushes the melt into the cavity and its face forms part of the cavity wall at the end of the filling phase.

The concept's advantages include the elimination of the metering cylinder. The shut-off valve does not need accurate position control over the range of movement, except that a precise stopping position is required, but this can be achieved with a mechanical stop.

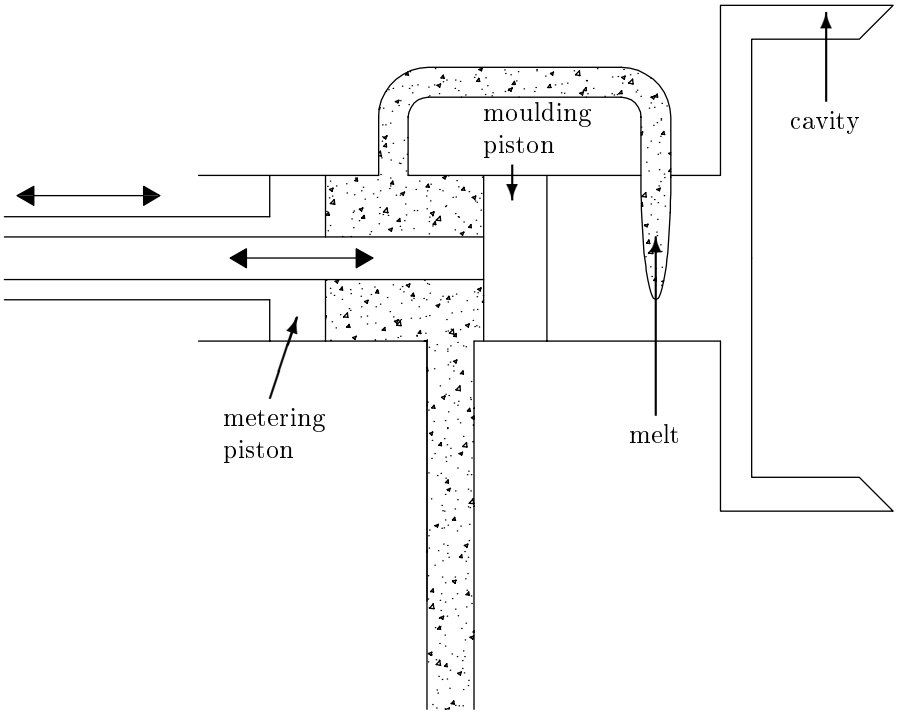

Figure 3.5: Concept 3: Inline pistons where melt is measured between the pistons and fed around the moulding piston

The concept's disadvantages are: Metering cannot be done in parallel with the part cooling phase and the moulding piston head is in contact with the melt during the whole metering phase. This concept is therefore not attractive.

Concept 5 (Figure 3.7) shows an inline moulding piston and rotating measuring cavity. Melt from the plasticiser fills the fixed volume measuring cavity. Once filled, it rotates through 90℃ and this allows the moulding piston to push the material shot into the cavity. The moulding piston face forms part of the cavity wall at the end of the filling phase.

The concept's advantages include the elimination of the metering cylinder. The rotating measuring cavity does not need accurate position control, except that the position in which it must stop before the moulding piston moves forward must be very accurate. The moulding piston is not heated during the melt measuring phase.

The concept's disadvantages are: The shot is a fixed volume and cannot compensate for density changes due to inevitable melt temperature variations. Further, only parts with one volume can be made on the machine. Metering cannot be done in parallel with the part cooling phase. Heating the rotating body to prevent melt solidification is also difficult. This concept was implemented in the first experimental lomolding machine, but was found unattractive for the reasons given above.

Concept 6 (Figure 3.8) shows a moulding piston and a section of moving cavity

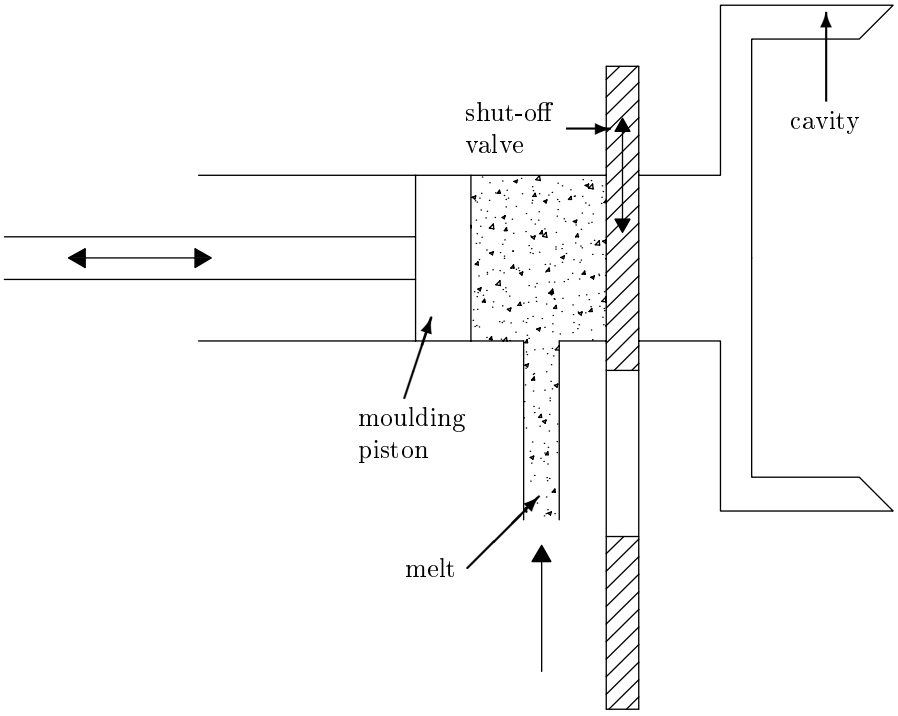

Figure 3.6: Concept 4: Inline moulding piston and shut-off valve

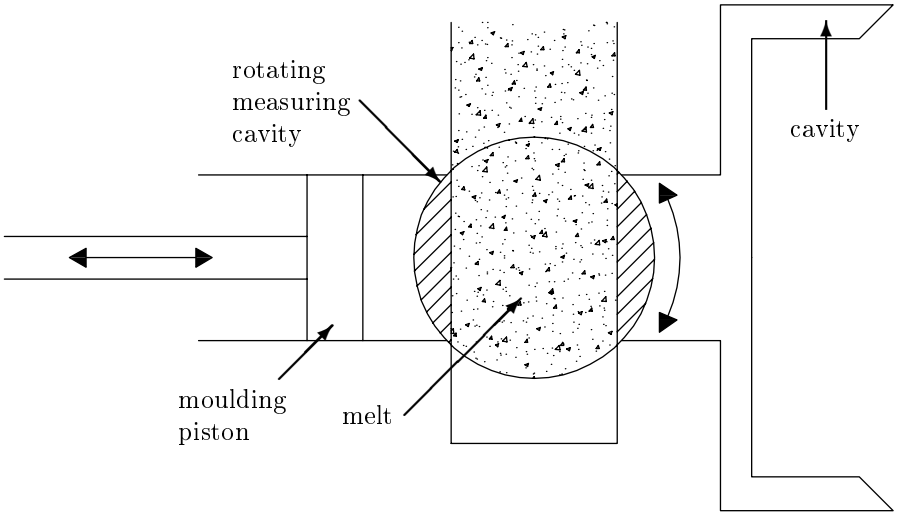

Figure 3.7: Concept 5: Inline moulding piston and rotating measuring cavity

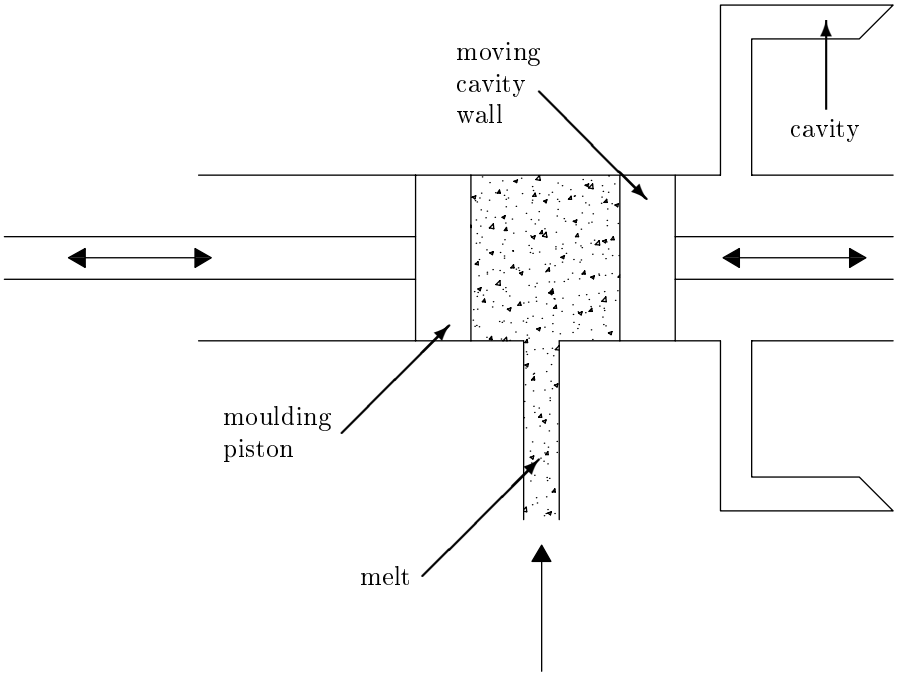

Figure 3.8: Concept 6: Inline moving cavity wall

wall opposite the moulding piston (i.e. another piston that moves relative to the moving platen). The melt is measured between the moulding piston and the moving cavity wall. Once the shot is measured, the moving cavity wall retracts and the moulding piston pushes the melt into the cavity. The moulding piston face forms part of the cavity wall at the end of the filling phase.

Concept advantages include the inline replacement of the metering cylinder (compactness). However the design on the moving platen side will be complex (e.g. actuators on moving platen required). It will also complicate the placement and operation of the part ejection system.

Further disadvantages included that metering cannot be done in parallel with the part cooling phase, that the cool moulding piston and the moving wall are in contact with the melt for the whole metering period and that both the moulding piston and the moving wall will leave marks on the part. The concept was discarded for these reasons.

Concept 7 (Figure 3.9) shows a configuration where metering is done with a positive displacement pump. The pump is heated to prevent melt solidification. The melt is transferred to in front of the moulding piston and then pushed into the cavity. The moulding piston face forms part of the cavity wall at the end of the filling phase. Whether replacing the metering cylinder with a positive displacement pump will increase the cycle time, is not certain.

However, fibre attrition is likely to occur in the pump when fibre reinforced

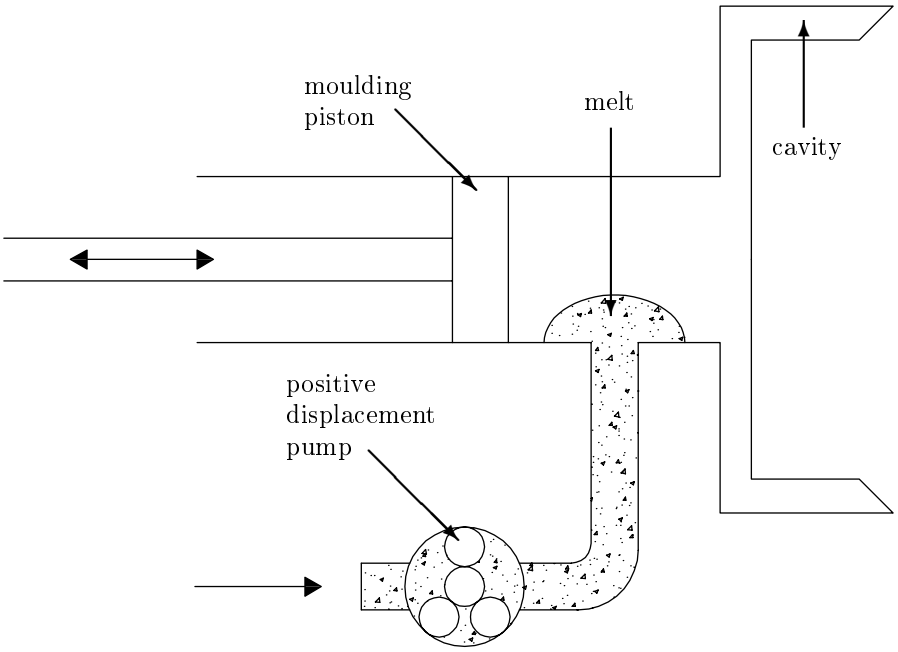

Figure 3.9: Concept 7: Positive displacement metering

material is processed. The accuracy of the metered shot is difficult to determine. This concept was deemed unattractive since it replaces a relatively simple and controllable metering cylinder with a more complex pump.

Concept 8 (Figure 3.10) has a separate metering cylinder and moulding cylinder. After the melt is measured off in the metering cylinder, a valve closes in the melt inlet runner (not shown) to prevent back flow of the melt during the moulding phase and a valve between the metering and moulding cylinders (also not shown) opens. The shot is then transferred to the front of the moulding piston. The moulding piston pushes the melt into the cavity and forms part of the cavity wall at the end of the filling stroke.

The concept's advantages include that metering can be done during the part cooling phase and that the moulding piston is not in contact with the melt during the metering phase.

The main disadvantage is that this concept is more bulky than the previous inline concepts.

3.4 Concepts Developed to Minimise Part Defects Caused by Premature Melt Solidification

All parts produced on the second prototype lomolder had a defect at the melt injection point. Analysis (Dymond, 2004) showed that the defect was caused by a

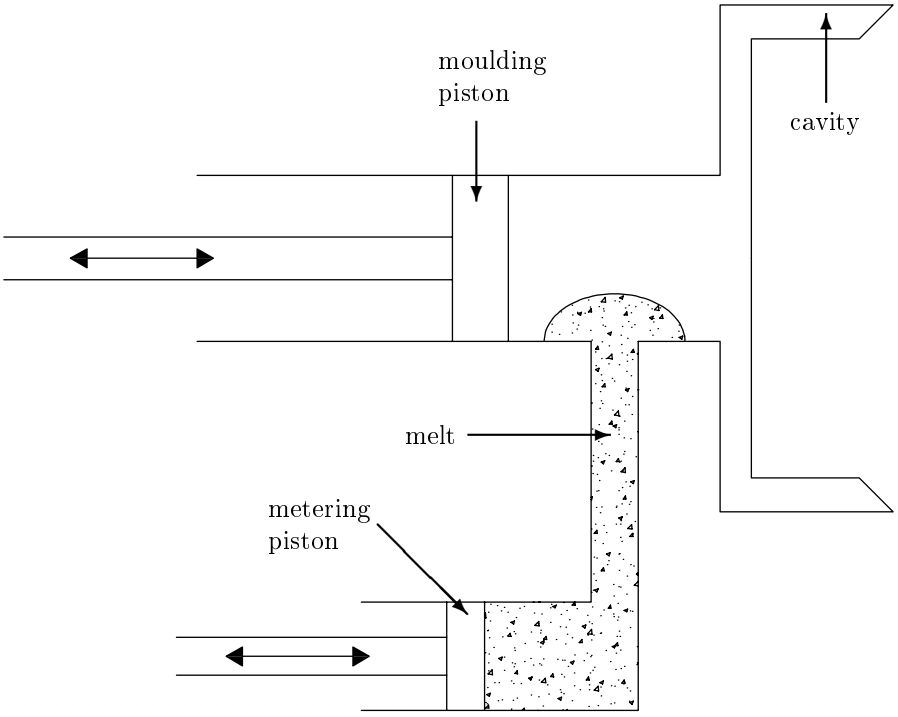

Figure 3.10: Concept 8: Separate metering and moulding cylinders

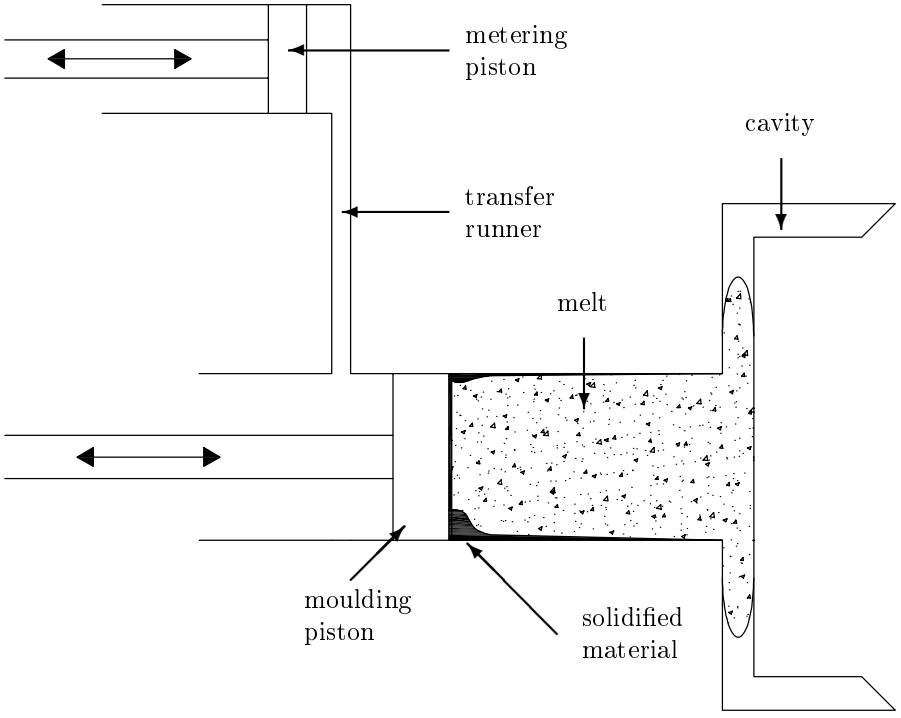

Figure 3.11: Solidified ring of material as a result of a too long metering transfer time

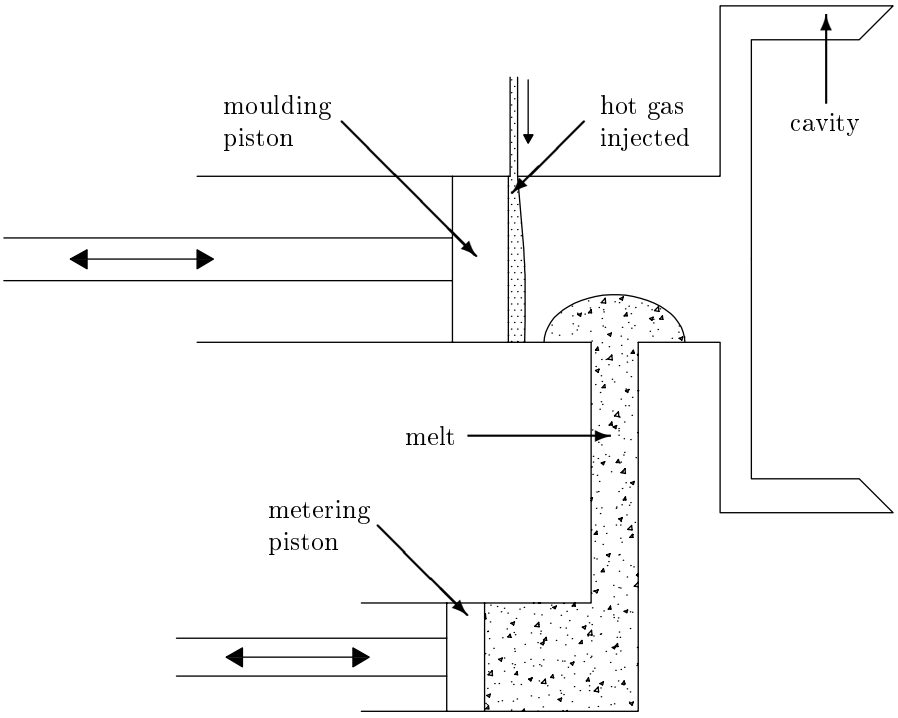

Figure 3.12: Concept 9: Heated piston face

solidified ring of material being pushed into the part at the end of the moulding piston stroke. Concepts developed here try to minimise the time that the melt spends in contact with the moulding piston (before completing mould filling) and the moulding cylinder respectively. Figure 3.11 shows this solidified ring of material in black on the sides of the moulding cylinder. The solidified layer is thicker on the bottom half of the moulding cylinder as the melt collects here during the long metering transfer phase.

Dymond (2004) showed that the largest contributor to this solidified ring of material was the solidified layer of material being scraped along by the moulding cylinder's face. It overshadowed the solidified layer that formed on the cooled moulding cylinder's face itself. The moulding piston has to be water cooled (not shown in the concepts) as it heats up during the melt injection phase. Preferably, it must be close to the cavity wall temperature at the end of the injection phase. Otherwise, irregular cooling will result in a part defect. The goal of concepts developed here, was to get rid of part defects caused by the moulding piston temperature.

Concept 9 (Figure 3.12) shows concept 8 (Figure 3.10) with the introduction of a hot gas being blown over the face of the moulding piston. The piston face is pre-heated by the hot gas stream before the melt is transferred to the front of the moulding piston. During the moulding phase the heat from the piston face will dissipate quickly into the piston head while the melt is injected into the cavity.

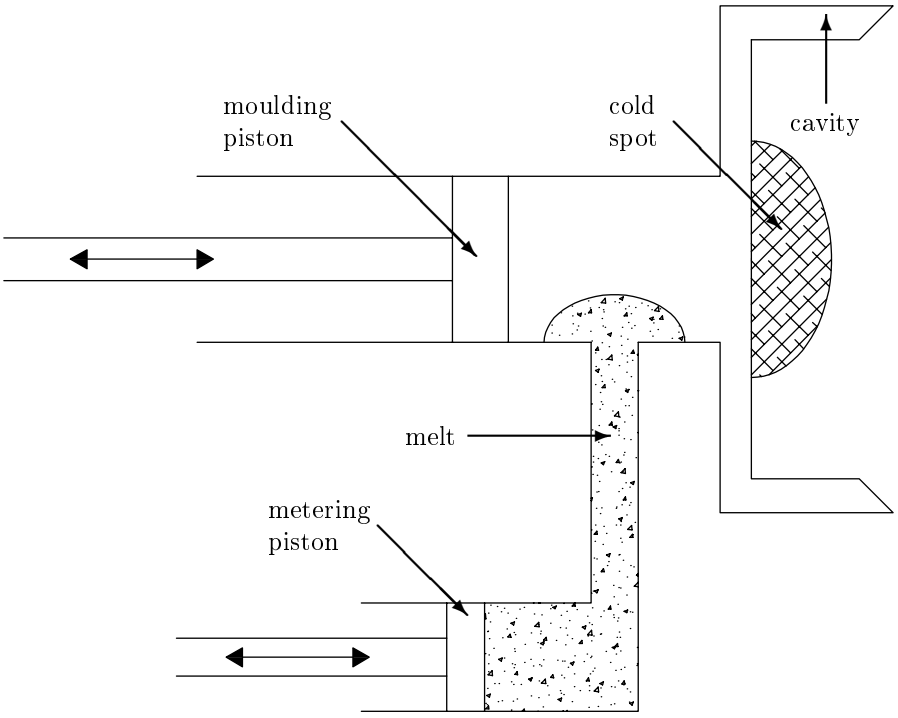

Figure 3.13: Concept 10: Cavity cold spot

The idea is that at the end of the injection phase, the piston head will be cooled down to the cavity wall temperature.

This concept was discarded as the hot gas may contaminate the melt and this will result in part defects. Heating of the piston face must be precise and therefore the temperature of the piston face has to be calculated/measured. This is very difficult, since the heating time interval will be very short. Therefore, control of the process proves to be difficult.

Concept 10 (Figure 3.13) shows concept 8 (Figure 3.10) with the introduction of a cold spot on the cavity wall opposite of where the moulding piston face forms part of the cavity wall. This area is cooler than the rest of the cavity wall. The heat from the moulding piston will dissipate into the part and will be equalised by this cooler cavity wall area. During the cooling phase these areas will reach the same temperature as the rest of the cavity wall. This concept was discarded as polymer melts do not conduct heat very well. Therefore, this concept will lead to irregular part cooling and this may lead to part warpage for instance. Again, the part ejection system layout will be complicated by this design.

Concept 11 (Figure 3.14) shows an extension of concept 4 (Figure 3.6) where an extra shut-off valve is added. Melt metering is done between these two shut-off valves. The advantage of this concept is that the metering unit is replaced and accurate position measuring of the valves is not necessary over their movement

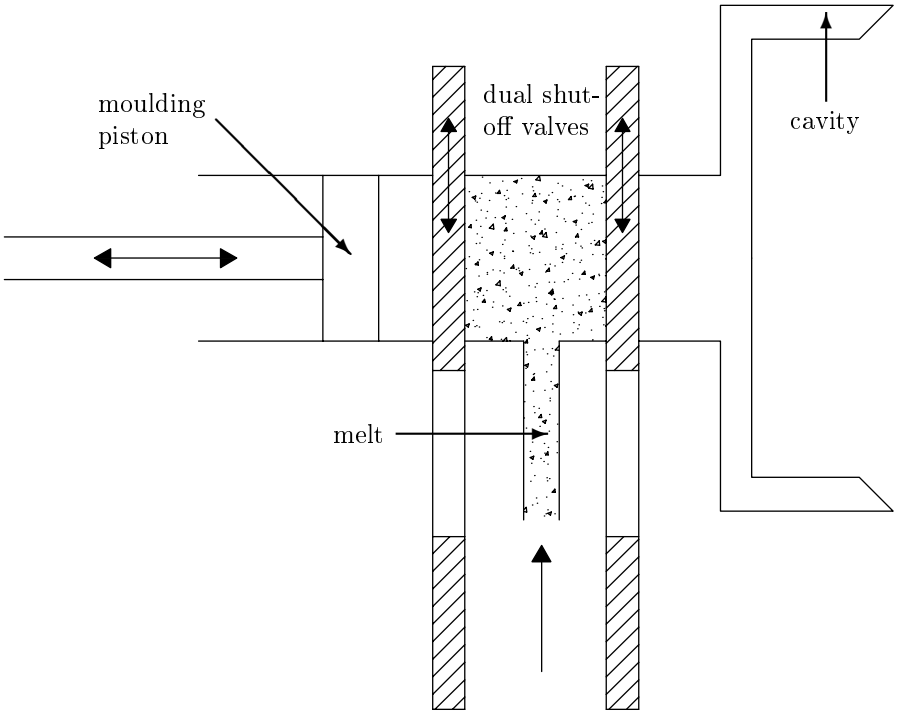

Figure 3.14: Concept 11: Inline moulding piston and dual shut-off valves

range. Also, the moulding piston is not heated during the metering phase. However, the stop position of the valves is critical, otherwise moulding piston damage will occur. A mechanical stop can be implemented to achieve this. On the negative side it is noted that this concept again has a fixed shot volume, which does not allow compensation for melt temperature variation or the production of thicker parts for instance. Therefore, concept 11 is discarded.

Dymond (2004) showed that complexity added by the above three concepts is not warranted. He showed that premature melt solidification is not a problem and will not cause part defects if the melt is transferred quickly in front of the moulding piston after the metering phase and if the melt is quickly injected into the part cavity.

3.5 Concepts Developed to Eliminate the Need for Accurate Metering

Concepts developed in this section provide the opportunity for adding or removing molten material after crude shot measuring is done.

Concept 12 (Figure 3.15) shows a moulding piston with a melt filling port and melt return port in front of the piston. The volume in front of the piston is larger

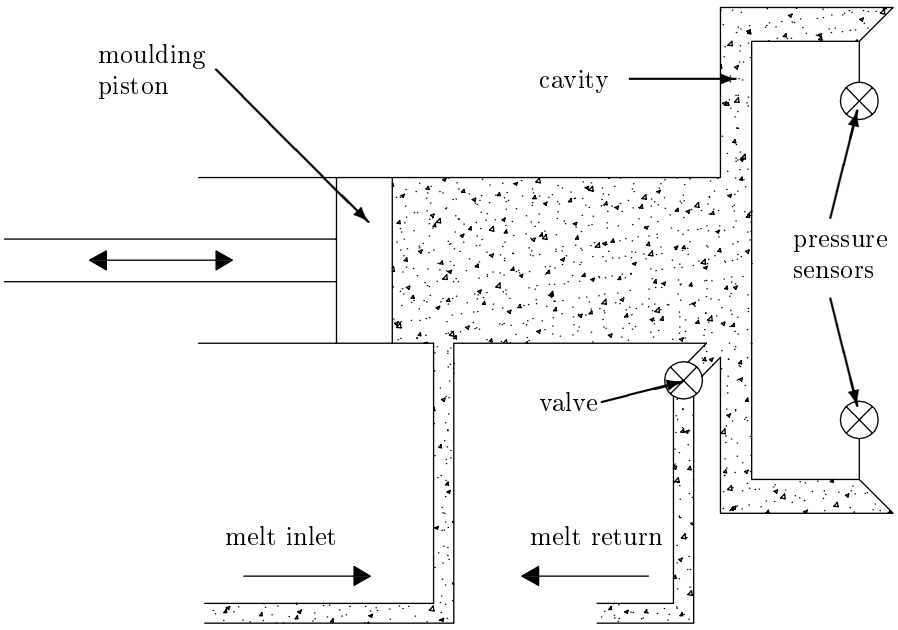

Figure 3.15: Concept 12: Pressure metering to replace accurate melt metering phase

than the part volume. This entire volume is filled with molten material and accurate melt metering is replaced by measuring the pressure at predetermined points in the part cavity during the injection phase. Once predetermined pressures are reached in the cavity the valve in the melt return line opens and the excess melt is transferred back to a melt accumulator until the moulding piston reaches its stopping position.

This concept was not further considered, since accurate pressure measurement in small time increments as required during part filling is very difficult. The melt may also block the metering points after some time and pressure measurement may be inaccurate. The repeatability of the process is also a point of concern.

Concept 13 (Figure 3.16) shows a smaller additional moulding piston added to the machine configuration. Melt is fed in front of the moulding piston and then pushed into the part cavity. This initial material shot has a volume slightly less than needed to produce a part. Once the moulding piston reaches its intended position, the cavity is completely filled by the additional piston. More than one secondary injection point can be used. When the part is removed after the cooling phase, it breaks off at these secondary filling gates similarly to injection moulding.

This concept was discarded as it becomes complex with too many parts, especially if more than one secondary injection point is used. Also, the small secondary injection points may block if fibre reinforced material is processed. This will result in machine down time. Both of these two concepts will also result in an additional mark left on the part.

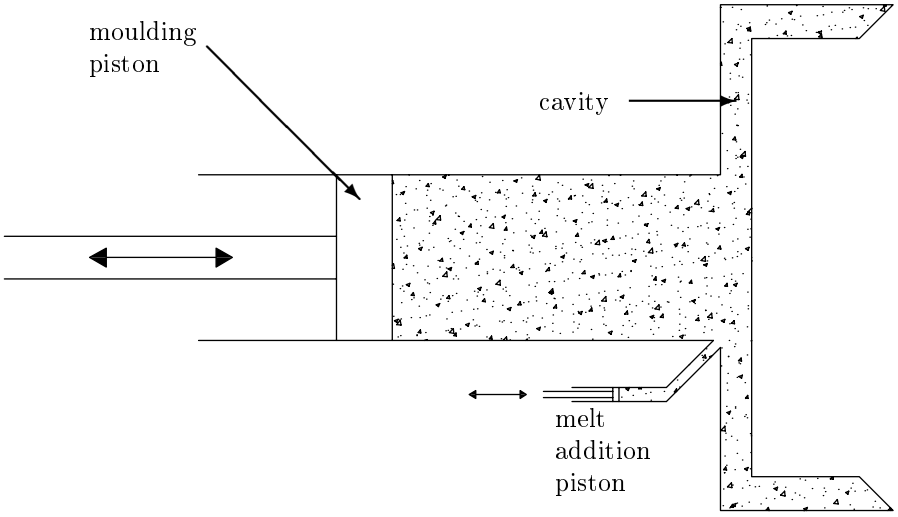

Figure 3.16: Concept 13: Melt injection after moulding piston reaches required position

3.6 Final Concept Selection

This chapter described the concepts that were evaluated as candidates for further development. Their working principles, advantages and disadvantages were explained as well as the reasons why they were discarded or used for further development. Concept 8 was chosen as the best candidate for further design development. It best satisfied the main design requirements listed in section 3.2 and had the simplest mechanical design (thus reducing development risks). Concepts attempting to prevent premature melt solidification (Section 3.4) were discarded as a result of Dymond's results. The concepts of Section 3.5 were discarded as a result off added complexity, increased cycle time and unreliability when repeatability and maintenance problems are considered.

Lomotek Polymers built a next prototype lomolder based on the chosen concept in partnership with an overseas company that manufactures injection moulding machines. This prototype is further used for machine refinement and research.

Chapter 4

Machine Design Refinement

4.1 Introduction

This chapter describes the refinement of the chosen machine concept discussed in Chapter 3. A parametric machine sizing model is developed that provides useful information to set up an initial machine cost model. The parametric machine model is configured to conceptualise different sizes of piston moulding machines. Once the machine component sizing is done, purchase cost estimation can be done for the different components. The parametric model concentrates on the design of the components of the lomolding unit, i.e. the metering- and moulding cylinders and the flow channels between them, since these components differ significantly from those found on general injection moulders. The plasticiser and clamping unit (the part of the machine that opens and closes the mould halves) are essentially the same as in injection moulding. Even though costing research in injection moulding concentrates mostly on part features and mould design (Chen and Liu, 1999) (Lee *et al.*, 1997) and research related to machine costing and optimisation is usually proprietary to machine manufacturing companies (and therefore rarely published), the vast experience in the injection moulding industry can be relied on to provide these subsystems. The chapter outlines important aspects regarding machine layout that influences the cost of the lomolding unit. The lomolding unit consists of the metering unit, moulding unit and the runner flow areas to transfer the melt to the moulding unit. Focus is then placed on the effects of cavity filling time. Then melt flow area calculations and critical material selection for different machine parts are discussed. This is followed by two extreme sizes of lomolders that are analysed as case studies.

4.2 Layout Design

Machine design and cost are mostly influenced by the diameter of the moulding piston. A small diameter piston means a smaller available area and therefore a lower injection force is needed to inject the material compared to the case when a larger diameter piston is used. Choosing a moulding piston diameter is not a trivial task and is limited by boundaries. First, if the diameter is too small, the whole process is comparable to traditional injection moulding where material is fed through the sprue and therefore, most of the advantages of lomolding as discussed in Chapter 3 are lost. Alternatively, if the diameter is too large, the process is comparable to compression moulding and therefore very large forces are needed to produce parts. Lomolding unit cost is strongly influenced by injection forces and therefore the cost of the machine will also rise. It may even become impossible to use electric actuators as the power requirements may fall outside the ranges that are currently available. The actuator sizing and cost issues are discussed in detail in Chapter 5.

Figure 4.1 shows a typical layout design provided by the parametric model. The figure will be referred during the discussion of typical machine layout design issues.

4.2.1 Stationary platen hole

It was decided to put the metering cylinder behind the stationary platen, to reduce the required hole size in the stationary platen. As mentioned in Section 3.2, the hole reduces the stiffness of the platen and therefore it must be as small as possible. Melt is delivered through an annular runner to a position in front of the moulding piston to ensure compactness.

4.2.2 Piston skirt

A skirt is fitted around the moulding piston and made of a softer material (more about the materials in Section 4.5) than the moulding cylinder. This skirt is extended to serve as the valve between the metering cylinder and the moulding cylinder. It must be long enough to completely seal of the port between the annular runner and the moulding cylinder when the moulding piston is in the closed position (i.e. during the part cooling phase).

4.2.3 Metering unit orientation

The metering unit in Figure 4.1 shows a metering unit that is perpendicularly placed to the moulding unit. This configuration makes the lomolding unit as a whole less compact, but has advantages. Having the metering unit parallel to the moulding unit, creates difficulties to position the actuators of both in the smaller

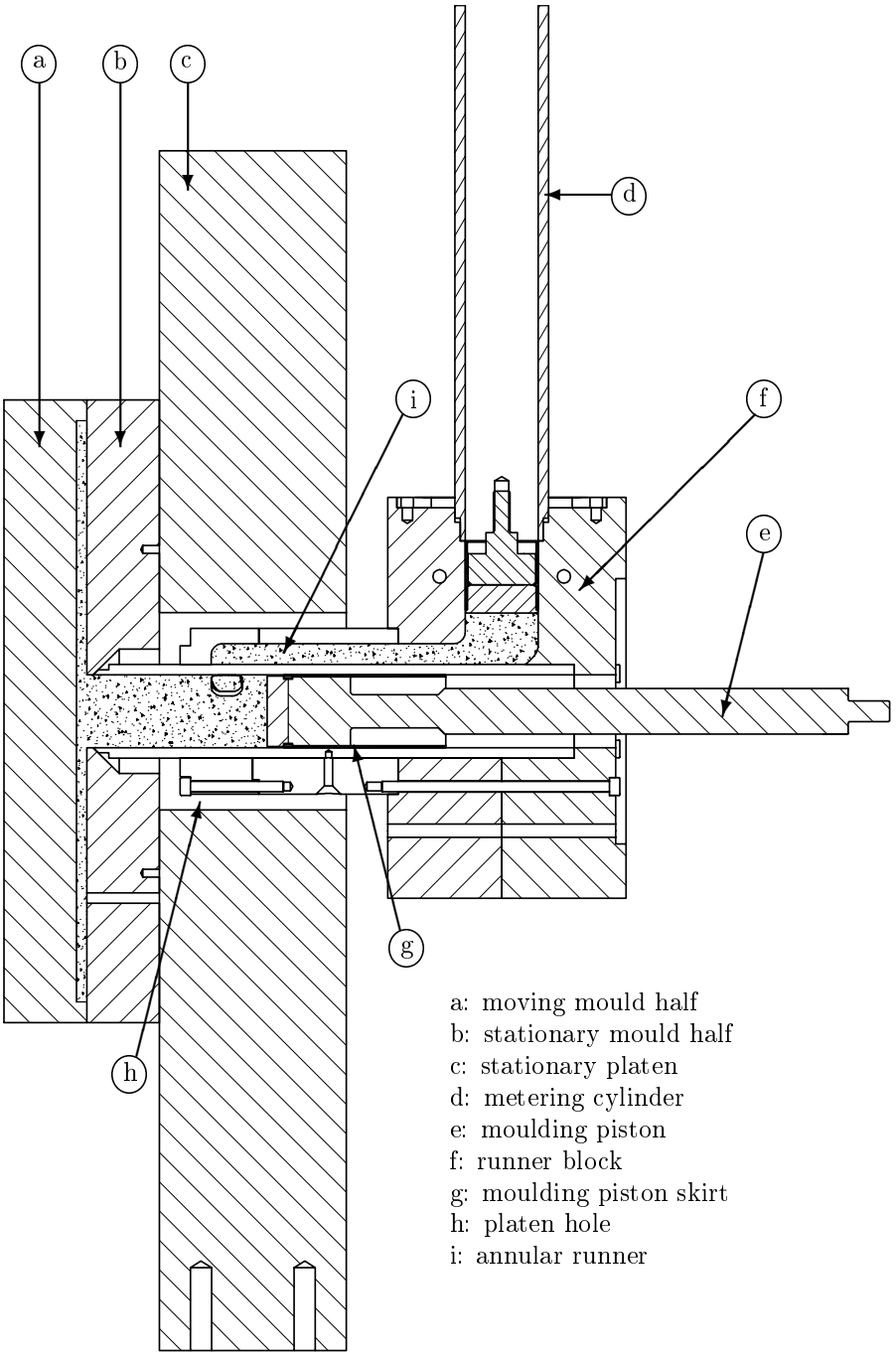

Figure 4.1: Moulding unit layout

space available. Especially, the placement of the belts and pulleys in the case of electric drives will be challenging. Therefore, the perpendicular layout was chosen. It is noted that a perpendicular layout may also influence the operation of the ejection system on the stationary platen.

4.2.4 Temperature gradients

The problem with having a hot moulding cylinder in close proximity to the cold stationary moulding half was discussed in Chapter 3. It was decided against using an insulation section (as shown previously in Figure 3.1) as this adds complexity and extra maintenance. The insulation material will wear more quickly than the moulding cylinder and fibres (when reinforced material is processed) will get caught at this point. It will also be difficult to keep the moulding cylinder and the cavity ring gate concentric to each other as close tolerances exists. Therefore, a thin circular contact area is introduced that will restrict heat transfer. Solidification is not a problem as long as the metering and moulding phase are done rapidly.

4.3 Machine Design Issues

This section describes different issues regarding machine design that are applicable to all sizes of lomolders, e.g. forces in the main machine components. The range of machine sizes considered starts at a machine that is capable of manufacturing a disc with a diameter of 150 mm. This is approximately equivalent to a bread board size product. A pallet of 1,0 m x 1,0 m forms the upper part threshold. These pallets are used in the packaging industry for instance.

4.3.1 Effect of cavity filling time

The piston moulding process is performed by the actions as described in Chapter 3 (Figure 3.10). The semi-analytical model (Chapter 2) provides the pressure drop experienced in the part cavity during the moulding phase as an input to the parametric sizing model.

The cavity pressure loss, i.e. the difference between the cavity pressure under the piston and that at the flow front, is an important machine design parameter. The idealised relationship between the cavity pressure loss and the corresponding flow rate time history are shown by the solid and dashed lines, respectively, in Figure 4.2 (repeated here for clarity).

Figure 4.2a shows a constant flow rate and increasing pressure loss over time due to the progression of mould filling. These profiles would give the minimum fill time (which would give a cycle time advantage), but the machine would have to be able to deliver a high moulding pressure and flow rate simultaneously. Also, controlling

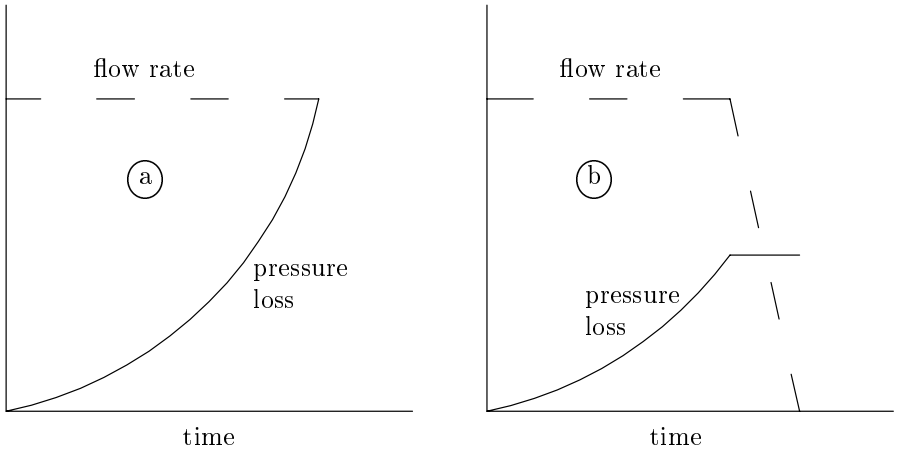

Figure 4.2: Cavity pressure loss and material flow rate during mould filling

the machine when the shot is even slightly too large or too small, would be very challenging. Injection moulding is therefore not normally done in this manner and instead a constant flow rate is prescribed for only a certain part of the filling phase (80 % to 90 % of the injection stroke) followed by filling under constant pressure until the cavity is completely filled (as shown in Figure 4.2b).

The change over point between the constant flow rate phase and the constant pressure drop phase is treated as a user-specified parameter in the parametric model. Once the cavity is completely filled the part is packed under constant pressure. This step is necessary to minimise warpage and to avoid sink marks resulting from the material shrinkage during solidification.

It can be seen from these graphs that a specific sized machine might be able to produce larger (same thickness, larger area) parts than it was designed for by reducing the material flow rate. However, it must be kept in mind that a minimum melt flow rate is required to prevent a frozen melt front (no further cavity filling is possible) that will result in a short shot. Therefore, the longer flow path is filled in a longer time, resulting in the same melt pressure drop across the part cavity that the machine was designed for. Thicker parts (i.e. larger volume) can also be manufactured, since the larger flow area results in a lower cavity melt pressure drop. The metering unit capacity places a limit on the higher volume parts.

The calculated maximum pressure drop (by the semi-analytical model) is used to determine the force on the moulding piston. The clamping force that the clamping unit has to withstand is calculated in a similar manner.

The metering piston does not have to exert a pressure as large as that of the moulding piston since it only has to cope with the runner pressure losses and the earliest part of the filling phase (only when the shot volume exceeds the swept

volume of the moulding piston).

The moulding and metering pistons can be driven either by hydraulic cylinders or electric servo motors with ball screws. In both cases the following aspects have to be kept in mind:

- The shaft of the hydraulic actuator or the rotating ball screw must withstand the maximum axial force without buckling.
- The actuator must be able to deliver the required linear speed (determined by the required flow rate) combined with the required force (determined by the cavity pressure and a friction allowance) at the point in Figure 4.2b where the change over from constant speed to constant pressure occurs. This point typically constitutes a critical design point, since the maximum energy transfer from the actuator to the piston occurs at that point in the filling phase.

4.4 Melt Flow Areas

The melt flow area directly influences the pressure gradient that the melt withstands during transfer. The material shear rate is directly proportional to melt flow pressure gradient. Fibre breakage due to bending (one of the reasons for fibre attrition) occurs as the fibres rotate against the material flow direction. These bending forces are also proportional to the material shear rate (Zhang and Thompson, 2005). The retention of longer fibres is expected to be one of the advantages of lomolding and therefore it is important that shear rates are lower everywhere in flow path upstream of the ring gate.

Concept 8 (Figure 3.10) was identified as the most favourable for further development and Figure 4.1 shows a refinement of that concept. The melt flow path is strongly influenced by the machine layout details: molten material is pushed from the plasticiser through a round hole (part of the runner block, Figure 4.1:f) upwards into the metering cylinder. The material cannot flow into the moulding cylinder at this stage, since the ports in the moulding cylinder wall are closed by the moulding piston skirt during the part cooling phase (see Figure 4.3). After the part has solidified, the mould opens, the part is ejected, the mould closes again, and the moulding piston withdraws to its rear position. Then the melt is pushed by the metering cylinder through the runner block circular opening (Figure 4.4:a), through the semi-annular runner (Figure 4.4:b) and into the moulding cylinder through two ports in the moulding cylinder wall (Figure 4.4:c).

The semi-annular runner (Figure 4.4:b and Figure 4.5, where the hatched area on the left shows the net flow area) is included in the layout to minimise the swept volume of the moulding cylinder, the time that the melt is in contact with the moulding cylinder, and the length of the moulding piston skirt. The melt enters the moulding cylinder through the two ports in the moulding cylinder wall (Figure 4.6).

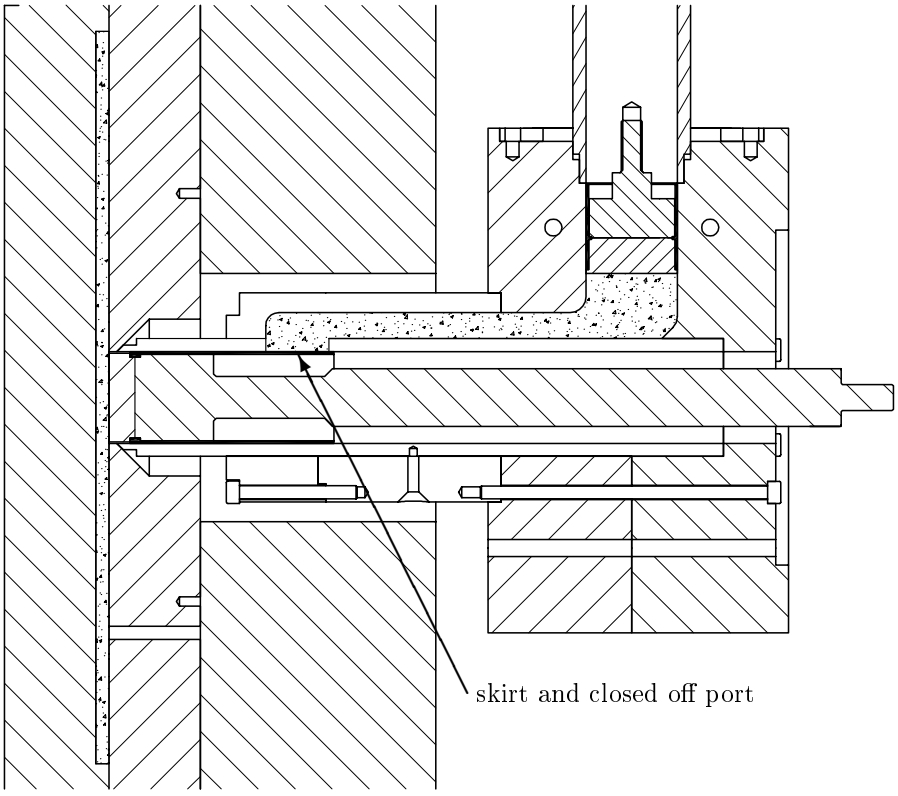

Figure 4.3: Moulding piston skirt closes off port during cooling phase

The land between the ports helps to ensure concentricity of the moulding cylinder when the moulding piston starts moving forward.

Since many of lomold's advantages are derived from keeping the shear stresses that the melt is exposed to well below that encountered in injection moulding, the main flow areas described have to be sized in such a way that the highest material shear rate occurs where the material enters the mould cavity. The shear rate at that point is controlled by the cylinder diameter, part thickness and fill rate. Richardson (1983) published the following formulae that relate the pressure gradient to the material flow rate for non-Newtonian fluids in round tubes (Equation 4.4.1) and between parallel plates (Equation 4.4.2):

$$\frac{\partial p}{\partial z} = 2\mu^* \left[\frac{Q(m+3)}{\pi R^{(m+3)}}\right]^{\frac{1}{m}} \tag{4.4.1}$$

$$\frac{\partial p}{\partial x} = \mu^* \left[\frac{Q(m+2)}{2wh^{(m+2)}}\right]^{\frac{1}{m}} \tag{4.4.2}$$

The viscosity at unit shear rate is given by μ^*. Q is the material volume flow rate, m is the viscosity shear rate exponent (in a power law viscosity model), R

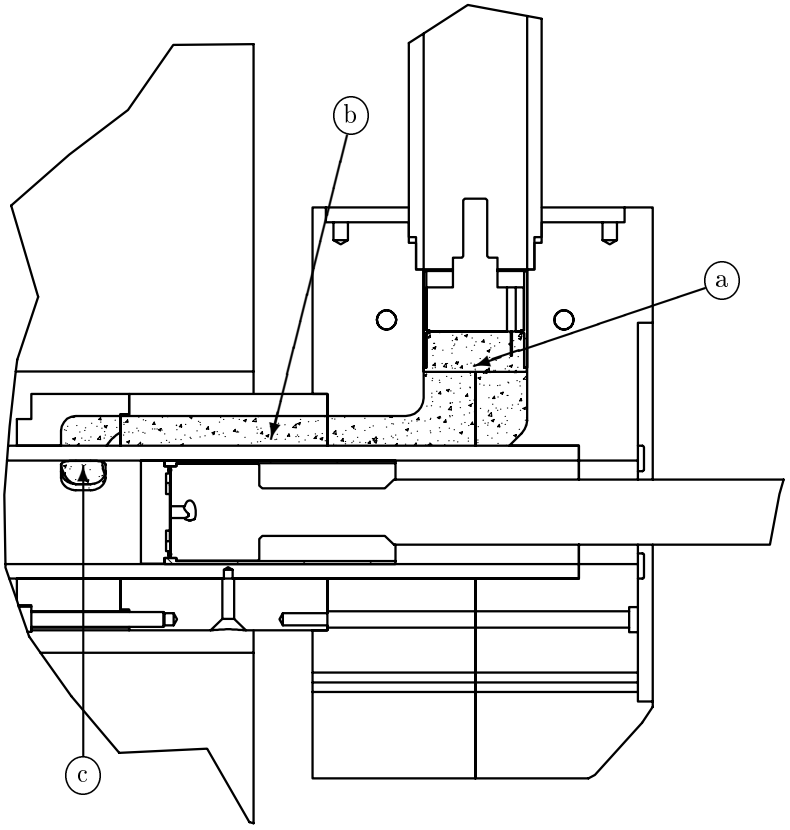

Figure 4.4: Material transfer phase flow areas (enlargement of Figure 4.1)

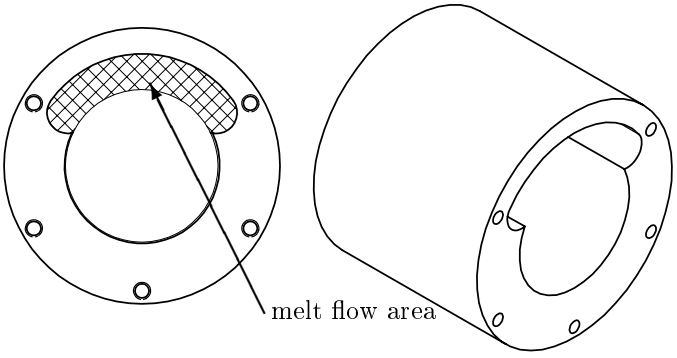

Figure 4.5: Semi-annular runner

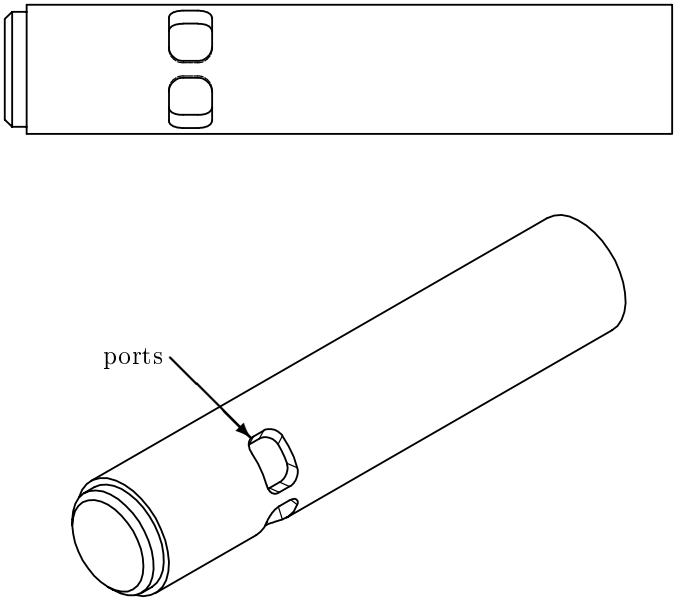

Figure 4.6: Moulding cylinder

is the radius of the tube, w is the width of the flow channel between the parallel plates and h is half of the channel height. Equation 4.4.2 applies to cases where h is much smaller than w. These equations take into account the total flow area as well as the shape of the flow area.

In the parametric model, since the real flow areas do not exactly correspond to either equation's geometry, half of the hydraulic diameter is substituted for R in the case of non-round flow areas and the pressure gradient given by both equations are evaluated for each part of the flow path. The largest of the two pressure gradients is compared to the pressure gradient at the entrance to the mould cavity to decide whether the flow area is large enough. It will be shown in the case studies that the melt flow runners are sized such that the material shear rate is a factor of 10 smaller in the runners compared to the shear rate at the ring gate.

4.5 Machine Part Material Selection

This subsection describes material selections that were made for some critical parts of the lomolding unit. Almost all parts are made from steel except for the parts described below. Quite extreme temperature differences exist during machine operation. The mould cavity is ideally cooled to a temperature in the range of 30 ℃ to 55 ℃, while the moulding- and metering cylinders are kept at temperatures above 200 ℃ to prevent melt solidification. These large temperature differences, and the associated start-up and shut-down variations, must be kept in mind while design-

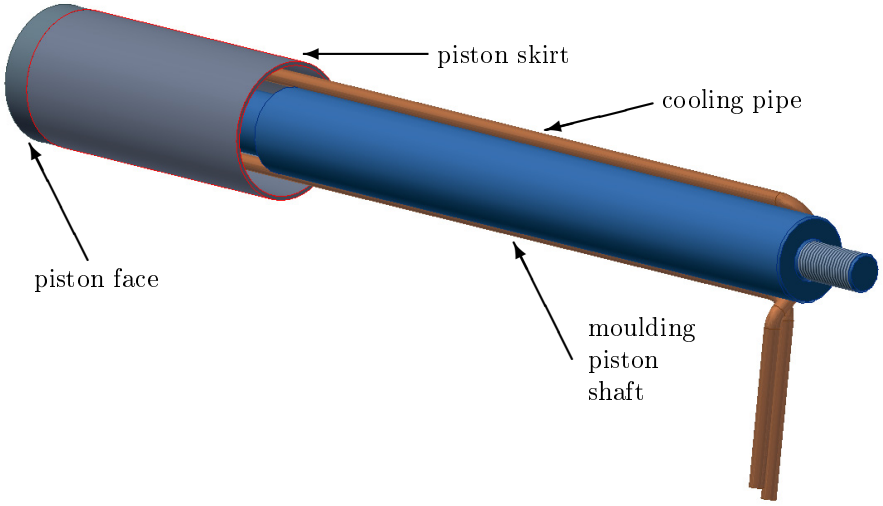

Figure 4.7: Moulding piston parts

ing the components, as their thermal expansion will be significant during machine operation. Any differences must be accounted for.

Figure 4.7 shows some details of the moulding piston assembly. The moulding cylinder (removed in Figure 4.7 for clarity) is typically made from honed hollow bar and hardened to resist frictional wear as a result of the moving piston skirt. The moulding piston and piston face are made from unhardened tool steel to withstand the cavity pressures. However, they are not affected by frictional wear.

Care must be taken to ensure that all the parts shown in Figure 4.7 should have approximately the same thermal expansion coefficient, otherwise the piston skirt might get stuck in the moulding cylinder which will result in machine failure, or it might become too loose which will result in melt leaking past the sleeve. Therefore, the piston skirt is made from cast iron which has the same thermal expansion coefficient as mild steel (Benham *et al.*, 1996) and some lubrication properties due to its graphite content. Large differences in thermal expansion coefficients are the reason why phosphor-bronze was not selected, even though it reduces frictional wear excellently in many applications.

The parametric model is applied to two case studies in the next sections to show the versatility of designing machines at extreme scale ends. Both the small and the large lomolder are sized to be able to manufacture a thin and a thick part with the same machine configuration.

4.6 Case Studies

The following two case studies are considered here to determine boundaries for the lomolder cost analysis that follows in Chapter 5. It also shows the versatility of the

parametric sizing model.

4.6.1 Small lomolder

This case study considers a small lomolder capable of manufacturing a cutting board sized disc (150 mm diameter). Two different thickness discs having the same diameter were considered: 1 mm and 3 mm. The thin disc determines the maximum injection pressure that the machine must cope with and the thick disc determines the volumetric requirements of the metering unit, runner system and moulding unit. The injection phase is done in 0,5 seconds and two part materials were considered, i.e. Novolen 1100 N (a homogeneous polypropylene) and Celstran PP GF30 (a polypropylene with 30% glass fibre). Both materials were simulated at the process parameters recommended by Cadmould (2002), which were given in Table 2.1.

4.6.1.1 Moulding cylinder

This subsection explains how the main components of the moulding cylinder assembly are sized in relation to the maximum speed required, maximum force needed and stroke length needed. The cavity filling time was chosen to be 0,5 seconds for both the thin and thick parts. A shorter time will result in very high pressure drops and high shear rates occurring in the case of the thin part, while a larger time will increase the cycle time up to a point where a short shot will result. Melt pressure drops and shear rates are less dependent on the injection time when the thicker part is considered, since the melt flow area is larger. Therefore the thin part will determine the maximum moulding force needed and the thicker part will determine the maximum speed and stroke length of the metering and moulding actuators required to manufacture a part in 0,5 seconds.

During a constant flow rate simulation (35,35 cm^3/sec to fill the 1 mm thick cavity in 0,5 seconds) a cavity pressure drop of 135 bar was reached at 75 % fill for the Celstran material and 225 bar for the Novolen material at 75 % fill. The machine was therefore sized for the Novolen material. The pressure drop was increased to 280 bar (a 25 % increase) to account for dynamic effects and friction of the moulding piston skirt against the moulding cylinder wall. The tolerance between these two components is quite small to prevent molten material leaking past the piston.

The moulding piston diameter (ϕ_{mol}) was chosen as 35 mm to ensure that the piston together with its cooling pipes (it is necessary to cool down the moulding piston face as it forms part of the cavity wall) can be conveniently manufactured and assembled. The maximum force (F_{max}) required to push the piston forward was calculated to be 27 kN (this includes the 25 % increase mentioned above to allow for dynamic effects and friction). This force was used to choose a ball screw shaft (in the case of an electric driven machine) and an equivalent hydraulic piston shaft.

In order to fill the smaller cavity size in 0,5 seconds, an average moulding piston speed of 37 mm/sec (during the first 75 % of cavity filling) was necessary when calculated on a volume basis and assuming that no material is pushed into the cavity by the metering piston.

Focussing on the thicker disc of 3 mm, a pressure of only 40 bar is needed to fill the cavity completely (i.e. no constant pressure injection phase will be required) at a constant flow rate of 106 cm^3/sec in 0,5 seconds for the Novolen material. The Celstran material gives a cavity pressure drop of 30 bar for the same conditions. In this example machine sizing was done for a constant melt flow rate up to the point where the cavity is 100 % filled (refer to Figure 4.2a). Thus 40 bar (the higher pressure drop is taken for machine sizing) must be delivered by the piston actuator at a speed of 106 mm/sec. This pressure drop of 40 bar relates to a piston force of 3,8 kN. Lower requirements will result if the flow rate diagram of Figure 4.2b is used.

Therefore machine sizing (servo-electric motor and accompanying pulley/belt assembly if necessary or hydraulic power pack) has to be done for these sizing thresholds:

- 37 mm/sec at a force of 27 kN (1 mm thick disc requirement)
- 106 mm/sec at a force of 3,8 kN for a distance of 55 mm (3 mm thick disc requirement)

4.6.1.2 Metering cylinder

Measurement accuracy is an important factor when choosing a diameter for the metering piston. A larger diameter will require a better encoding accuracy on the control side, while a smaller diameter will require a longer metering cylinder. A diameter of 30 mm was chosen for the metering piston. This is due to manufacturing constraints and assembly convenience. It is less than the moulding piston diameter, since no cooling of the metering piston face is required. Therefore the metering piston must be able to travel 75 mm, which was increased to 80 mm for design safety to be able to manufacture the thicker part.

The distance swept by the moulding piston (i.e. the distance from the start of the melt fed port to the ring gate) is 72 mm in this machine configuration as determined by the parametric sizing model. This swept volume is larger than the shot volume required for the thick part. This means that no mould filling is done by the metering piston and the metering pressure drop is equal to the pressure drop occurring as the material flows in the runners. The metering cylinder is designed for a pressure drop of 150 bar to be able to transport the molten material in front of the moulding piston through the runner system (shown in Figure 4.4) in the same time as the mould filling time, i.e. 0,5 seconds. This pressure is chosen by the user and takes into account dynamic effects and the friction of the piston sleeve against

the metering cylinder wall (with metering this tolerance is equally important, since any leakage will have a negative impact on the measuring accuracy). The metering actuator is rather over-sized in this scenario to ensure that the metering phase time will be reached. Therefore, no part defects will occur as a result of premature melt solidification in the moulding cylinder as the metering transfer time will be short enough to ensure a good part quality.

The maximum force on the metering piston was 10,6 kN and this force was again used to size the shaft of the actuating device (either hydraulic or electric) against buckling and fatigue. The maximum metering piston speed was calculated to be 150 mm/sec and this speed was again used to size the hydraulic power pack or servo motor drive. In order to do a costing analysis, different combinations of servo motors and belt/pulley drives, or hydraulic systems, are compared to find the optimum solution (Chapter 5).

4.6.1.3 Runner flow areas

The critical flow areas are discussed for the Novolen material in this section as the calculations are similar for the Celstran material. The pressure gradient of the material (Novolen which gives a higher pressure gradient than Celstran) at the entry to the cavity is 237 bar/m (for the 1 mm thick part which is higher than the pressure gradient for the 3 mm thick part), as calculated by Richardson's equation for flow between parallel plates (Equation 4.4.2). The channel width (w) was taken as the circumference of the moulding piston and the half-height (h) as half of the part thickness.

The pressure gradient of the melt flow in the moulding cylinder is 2,5 bar/m for flow in round tubes (Equation 4.4.1). For the metering cylinder this pressure gradient is equal to 3,5 bar/m as a result from the smaller diameter piston. These respective pressure gradients are much smaller than the limiting 237 bar/m and this is expected, since the chosen diameters of both cylinders were limited to fairly large values by manufacturing constraints. Keep in mind that these pressure gradients are not very accurate, since the requirements of Richardson's formulae (a fully developed velocity field) are generally not met due to the short distance of the flow geometry. However, it is noted that the predicted pressure gradients are in the order of ten times smaller than the critical limiting value. Therefore, it can be argued that the pressure gradient restriction is still met.

The semi-annular runner (Figure 4.5 and 4.8) was analysed with both of Richardson's equations. The highest pressure gradient was compared to the material pressure gradient at the cavity entry. The equivalent channel height ($2h$) was equal to 10 mm and the channel width (w) was taken to be 62 mm, i.e. the arc distance between the centres of the two R6 radii. These channel dimensions lead to a pressure gradient of 10,9 bar/m when Equation 4.4.2 is used. The hydraulic diameter of this runner computes to 17,9 mm. This gives a pressure gradient of 10,6 bar/m when

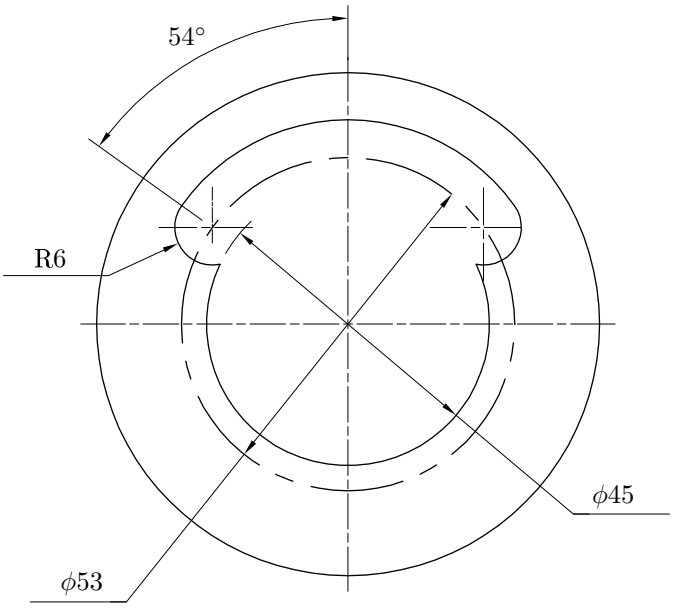

Figure 4.8: Semi-annular runner dimensions

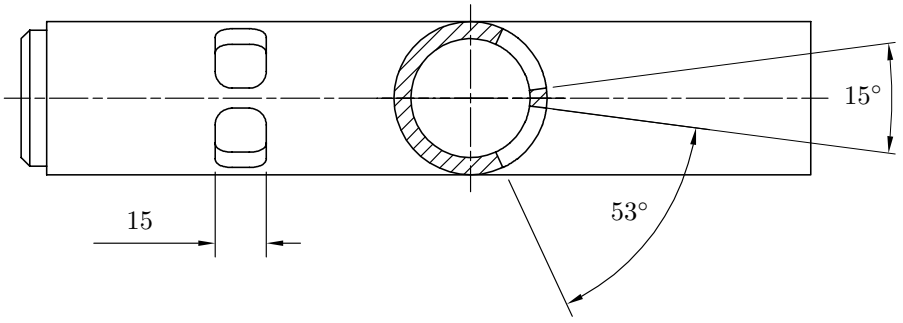

Figure 4.9: Moulding cylinder dimensions

Equation 4.4.1 is used for flow in tubes. Both these calculated pressure gradients are well below the limit of 237 bar/m and therefore the channel semi-annular runner dimensions are satisfactory.

The moulding cylinder's two ports were analysed by halving the material flow rate (Q) and calculating the dimensions of one hole (refer to Figure 4.9). Since these ports are almost circular it would not make sense to use Richardson's flow between parallel plates formula. The hydraulic diameter of the ports computes to 16,2 mm and this gives a pressure gradient of 10 bar/m which is also well inside the 237 bar/m barrier. Therefore all the flow areas conform to the principle of having the largest pressure gradient at the point where the molten material enters the cavity.

4.6.2 Large lomolder

As a second case study, a large lomolder unit's dimensions are considered. Since the calculations are similar to that in the previous section, this section will focus on the differences between the small and large lomolder and point out specific pitfalls. The large lomolder is a machine capable of manufacturing a plastic pallet (± 20 L volume) used in the transporting business. The same two polymers as for the small lomolder were used for the calculations in this section.

4.6.2.1 Moulding and metering cylinders

The plastic pallet has a projected area of 1,0 m^2. Typical wall thickness varies from 3 mm to 6 mm. To fill such a large cavity with only one moulding cylinder in a typical fill time of 3 seconds, will result in high cavity pressure drops (in the order of 300 bar for the thin wall sections at 75 % fill). This calculation was done with a moulding piston diameter of 252 mm. This diameter value was calculated in such a way that the moulding piston frontal area is 5 % of the part effective area. This 5 % area ratio was suggested in a European patent (Eckardt and Stemke, 2000) as ideal in order to lower the cavity injection pressures (case studies in Chapter 5 describe in detail how this area ratio influences the injection pressure drop).

The cavity pressure drop of 300 bar and the moulding piston diameter of 252 mm lead to a very high calculated axial force (1867 kN) for the moulding piston shaft actuator (either hydraulic or electric). In this calculation a 25 % increase in pressure drop was allowed for unknowns such as dynamic effects and friction. It was found to be impossible to drive this piston with an electric servo motor and ball screw shaft, since it is beyond the capabilities of currently available servomotors. On the other hand, it would be very expensive to build a hydraulic actuator with accompanying power pack to move such a large piston under such high loads.

A possible solution to this problem is to design the piston moulding machine with more than one moulding cylinder. Different configurations are possible with four or even nine moulding pistons. Each moulding piston can have its own metering unit attached or metering units can be shared. The injection cavity pressure drop drops to about 120 bar (at 75 % fill) when four moulding cylinders are used for cavity filling (these moulding cylinder diameters are also sized to the 5 % area ratio). Part design will obviously play an important role when more than one moulding cylinder is used as weld lines (the position where two melt fronts reach each other during the filling process) will form in the part. This is even more important when fibres are used, since the fibres will not cross over the weld lines. This phenomenon can drastically influence the strength of a part if the weld lines are not correctly positioned in the part. Multi lomolding unit filling is discussed as a case study in Chapter 6.

Costing decisions can be determined once the different costs are known for each configuration. Chapter 5 gives insight into the costs involved in the single piston design configuration. Spatial- and assembly constraints are important considerations. The metering cylinder configurations will be influenced by the required measuring accuracy. More metering cylinders may provide better metering accuracy, but the measuring volume error may well be less significant on such a large part when compared to a smaller part. Part defects as a result of inaccurate metering were discussed in Section 3.2.

4.6.2.2 Flow areas required

The calculations of the flow areas showed that all of these areas can easily be chosen to satisfy the maximum pressure gradient threshold as discussed in the small lomolder case study. One of the big design differences is the thicker stationary platen (it can be up to one metre thick for such a large part) on the larger machine. This leads to a proportionally longer semi-annular runner (refer to Figure 4.4) than required for the smaller lomolder.

4.7 Conclusion

Chapter 3 explained various machine concepts and evaluations were given for their suitability as candidates for further design development. In this chapter, the chosen concept was further developed and a parametric machine model created to assist in layout design. Different component material choices were highlighted.

This chapter described the parametric machine design model for the lomolding units of a piston moulding machine. Key aspects (material runner design, metering and moulding unit forces, stroke lengths and piston speeds) regarding the design of the machine were highlighted.

The user provides inputs to the semi-analytical model (Chapter 2) regarding part dimensions, material properties and process parameters. The semi-analytical model uses this information to calculate the cavity pressure drop required to fill the mould. Once this step is completed, the parametric model uses this information to calculate the required material flow areas, forces on the piston actuators, required piston speeds and required piston stroke lengths.

This parametric design information is then used to size either the electric or hydraulic actuators needed. The true value of the parametric model comes forth as it supplies the user with a machine layout design with very little user input. This parametric model therefore enables thorough machine optimisation as it allows a designer to quickly compare a large number of design options.

The parametric model was applied to two case studies to show the versatility of designing machines at extreme ends. It is an essential element in predicting cost for the piston moulding machines.

Chapter 5

Parametric Cost Model

5.1 Introduction

This chapter describes a method to approximately determine the purchase cost of a lomolding unit (i.e. metering unit, moulding unit and melt transfer runners). Brief consideration is also given to the maintenance- and operating cost of these units. Focus is placed on the small and large lomolders discussed in Chapter 4 and a medium sized lomolder is also analysed. All prices obtained at the end of 2006 and beginning of 2007 do not include value added tax (VAT). It is noted that these costs are intended for different machine design cost evaluation and not for quoting purposes. As in the previous chapters, the subsystems of a lomolding machine also found in injection moulders, e.g. the clamping unit, are not considered here.

Figure 5.1 (Blanchard and Fabrycky, 1997) shows where life cycle cost fits into the value that is added by different levels of design consideration. As can be seen from the figure the life cycle cost elements considered in this study cover only a small percentage of the overall picture. However, specifically in the case of the South African market, these are typical costs that are mainly considered by companies in decisions about purchasing machines.

The following key design decisions influence the purchase cost of machine components considerably:

- The frontal area of the moulding piston face compared to the effective area of the part strongly influences cavity pressure and the related injection force. This is discussed in Section 5.2.
- The choice between hydraulic and servo electric actuators. Advantages of both will be highlighted in the sections that follow.
- The choice between one and multiple lomolding units per part which becomes relevant when large parts are manufactured. This aspect is discussed as a case study in Chapter 6.

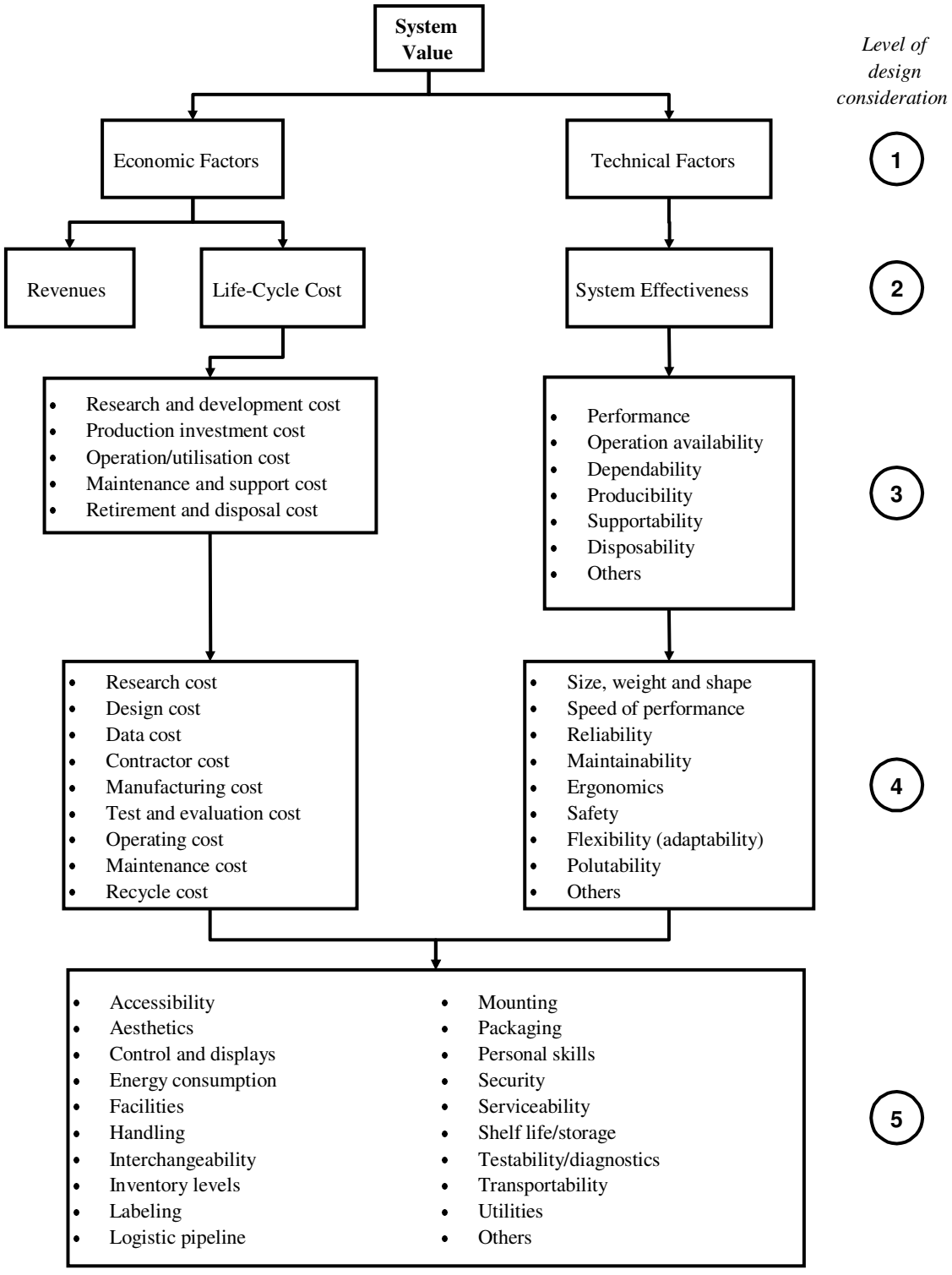

Figure 5.1: Design consideration hierarchy (Blanchard and Fabrycky, 1997)

Choosing the type of actuator (hydraulic or electric) is not always driven by cost alone. This paragraph highlights the differences between hydraulic and electric actuators and where one will be chosen above the other for certain reasons. Servo electric configurations are more accurately controlled than hydraulics. They are suitable for clean environments (for instance food and beverages industries), since no oil leaks can develop over time. They are up to 40 % more energy efficient according to Bracke (2006). However, the control of hydraulic systems becomes increasingly intelligent and thereby improving energy efficiency. For instance the electric motor driving the hydraulic pump can be speed controlled to supply flow only when power is needed.

Electric configurations also offer quieter working environments than their hydraulic counterparts. Simultaneous actuation of the metering and moulding pistons are easier to incorporate, since the electric system is easily simplified in subsections, while it is more difficult with hydraulics, where the power pack has to be upgraded when alterations resulting in exceeding the design pressure and flow rate are needed. With an electric configuration, only the relevant subsystem has to be replaced. Better part cycle times are generally obtained with electric machines (in the injection moulding industry). Fewer part rejects are manufactured with electric machines, as a result of the better accuracy and better repeatability (no oil heating time that affects both at start-up). Electric machines require less maintenance. However, their initial purchase cost is about on average 20 % to 30 % higher than that of hydraulic systems (Bracke, 2006).

The possibility also exists to design a hybrid lomolder, where hydraulic actuation of the moulding piston where high forces are required is combined with electric actuation of the metering piston when high accuracy is required. The above paragraphs highlighted the considerations to be made when selecting a hydraulic or electric configuration for a specific application.

The effect of moulding piston face area to part effective area is discussed in the next section. A detailed cost analysis of hydraulic actuation versus electrical actuation follows that. The costing of the custom lomolder manufactured parts is analysed and this is followed by a brief discussion regarding control-, maintenance- and operating cost. Chapter 6 gives a design case study of a medium sized lomolder that combines all the steps already described in the preceding chapters.

5.2 Moulding Piston to Part Area Ratio

The area ratio between the frontal area of the moulding piston face and the effective area of the moulded part is one of the most important machine sizing and costing factors, since the melt injection force is driven by this relation. The effective area of the part is related to the aspect ratio (longest melt flow path divided by the average thickness of the flow path) of the part. A good approximation is to take it equal

to the volume of the part divided by the average part thickness. It is noted that the part projected area in the direction of the platens is used to size the clamping unit.

The area ratio trade-off positions itself between having a long moulding piston stroke (small diameter piston) and a short stroke with accompanying larger piston face area. The area ratio is explored for hydraulic and electric actuators on a purchase cost basis as well as a manufacturing constraints basis. Three sizes of lomolders are considered: a small lomolder capable of manufacturing a $\phi 15\,\text{cm}$ disc (breadboard size), a medium sized lomolder that can produce a $\phi 50\,\text{cm}$ disc (serving tray size) and a large lomolder capable of manufacturing a $1\,\text{m}^2$ square plate (transport palette size). Two typical part thicknesses are considered for each part size. Specifications of the different part sizes are given in Table 5.1.

Advantages of a small diameter piston include:

- The volume swept by the moulding piston becomes small enough to require that the metering piston inject some of the melt into the cavity during the melt transfer phase. This decreases the cycle time per part and shortens the time that the melt is in contact with the cold cylinder wall near the ring gate (minimising potential solidification problems mentioned in Chapter 4).
- The moulding piston force required reduces as the face area decreases. However, a trade-off exists as the longer actuator shaft is more costly. Shaft buckling becomes a factor as well as the speed limitations on the hydraulic seals ($\pm 1\,\text{m/s}$) or the precision screw nut (function of screw and nut size - discussed in Section 5.4). Advantages include smaller sized actuators, smaller servo motors (pulleys and belts as well) or hydraulic power packs.
- A smaller sized hole in the stationary platen is an advantage, since the platen is weakened less at the position of maximum cavity pressure drop as discussed in Chapter 4. This also means that more space is available for the part ejection system.

Disadvantages of a small diameter piston include:

- Cooling of the moulding piston becomes more difficult as the space for the cooling pipes is decreased. The length of these pipes also increases and therefore the pipes become more costly. As the pipe length increases, the water flow pressure drop across the pipe length also increases.
- A smaller diameter face will result in a higher melt shear rate at the ring gate.
- A larger diameter piston will hide an error in melt volume measurement better as the extra/lack of material will result in a thinner extension/indent on/in the part (refer to Figure 3.2).

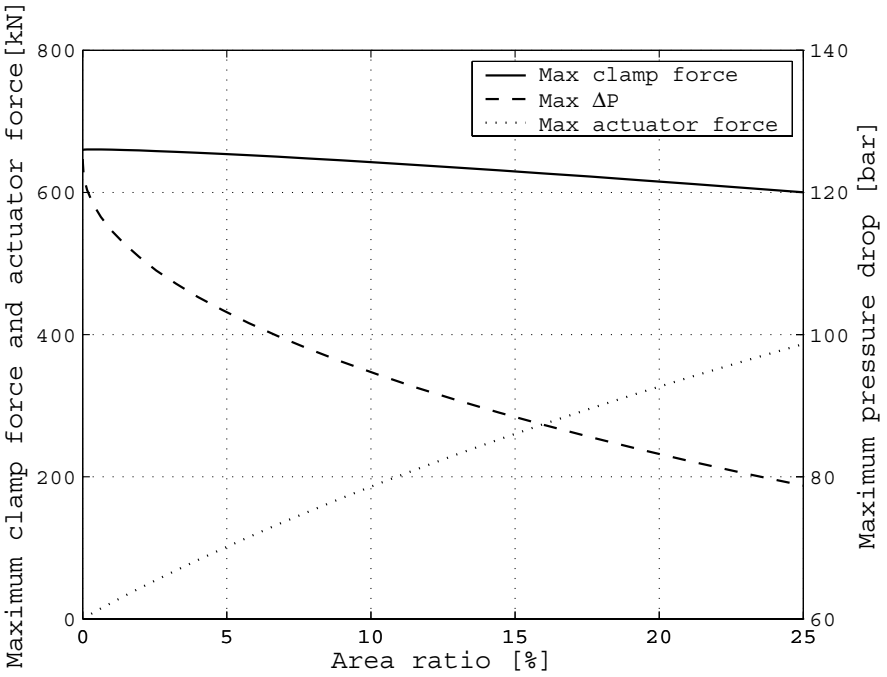

Figure 5.2: Piston area influence on cavity pressure drop, clamp force and actuator force

The piston face area also plays an important role in the metering cylinder. A smaller diameter piston will result in a longer actuator shaft (increased cost), but the metering accuracy will be improved.

Table 5.1: Range of lomolder units investigated

	Mini LM	**Midi LM**	**Maxi LM**
Part type	ϕ15 cm disc	ϕ50 cm disc	1 m^2 square plate
Part effective area [cm^2]	176,7	1963,5	10 000
Thin part thickness [mm]	1	2	3
Thick part thickness [mm]	3	4	6
Thin part volume [cm^3]	17,67	392,7	3000
Thick part volume [cm^3]	53,01	785,4	6000
Injection time [sec]	0,5	1	3

Figure 5.2 show the typical influence of the ratio of piston face area to part effective area on the injection pressure drop, clamp force required and injection force required. The graph shows Cadmould results for the Celstran material (material properties given in Table 2.1) injected into a disc cavity of 500 mm in diameter and 3 mm thick. Injection is done in 1 second and the values are calculated when the cavity is completely filled at a constant fill rate.

Figure 5.2 shows a 17 % drop in the total cavity pressure drop in the area ratio range of 0 % to 5 %. From an area ratio of 5 % onwards, the advantage of the decrease in pressure drop is less rewarding considering the increase in actuator force required to push the melt into the cavity. Figure 5.2 shows that the clamping force required to prevent opening of the moulding platens is less dependent on the area ratio. A clamping force drop of 9,1 % is noted over the range of area ratios considered.

It is necessary to know the piston to part area ratio in order to calculate the purchase cost of a certain configuration machine. However, this area ratio is very vaguely defined by Eckardt and Stemke (2000). They explored ratios from 0,5 % to 5 % and never came to a conclusion of what will be an optimum ratio or if there is one. The next part of this section will explain a route that the author investigated to determine a good estimate (based on lomolder unit purchase cost and physical constraints) of area ratios for different sizes of lomolder units.

First of all it is necessary to define the range of lomolders considered in this study. Table 5.1 shows properties of the different sizes of lomolders considered. Two types of parts are considered: round and rectangular. Different thickness parts are considered for the following reasons:

- A thin part leads to a higher cavity pressure drop. This determines the injection force required from the actuators as well as the power rating of the hydraulic power pack or servo electric motors.
- A thick part determines the volume of the part and therefore the injection stroke required by the metering cylinder actuators.

The same melt injection time is used in both part thickness cases for the three ranges of lomolders considered. These times are comparable to typical injection times if the parts are made with injection moulding machines. The larger volume part (thicker part) can be injected in the same time as the thin part, as the pressure drop across the cavity is much less as a result of the larger flow area available. Therefore a higher injection speed can be used, but keeping the higher material shear rates in mind. The Novolen material is taken as reference material to calculate the cavity pressure drop, since it gives a higher pressure drop than the Celstran material. The melt inlet temperature is 220 ℃ and the cavity wall temperature 40 ℃. The parts are cooled to 120 ℃ and ejected.

Table 5.2 shows the following information for the mini, midi and maxi lomolder configurations. The labels thin and thick refer to the part thickness in each case.

- a range of ratios of moulding piston face area to part effective area that was selected for consideration
- the moulding piston diameter was calculated from the area ratio

Table 5.2: Lomolder design data

Area ratio [%]	Piston dia [mm]	ΔP [bar]	Piston force [kN]	Piston stroke [mm]		Piston speed [mm/sec]	
				thin	thick	thin	thick
Mini Lomolder							
0,5	10,6	280	2,5	200	600	400	1200
1,0	15,0	271	4,8	100	300	200	600
2,0	21,2	256	9,0	50	150	100	300
3,0	26,0	247	13,1	33	100	67	200
5,0	33,5	230	20,3	20	60	40	120
7,0	39,7	215	26,6	14	43	29	86
10,0	47,4	196	34,9	10	30	20	60
Midi Lomolder							
0,5	35,4	352	34,6	400	800	400	800
1,0	50,0	341	66,9	200	400	200	400
2,0	70,7	326	127,9	100	200	100	200
3,0	86,6	312	184,0	67	133	67	133
5,0	111,8	292	286,7	40	80	40	80
7,0	132,3	278	381,4	29	57	29	57
10,0	158,1	257	504,7	20	40	20	40
Maxi Lomolder							
0,5	79,8	448	224	600	1200	200	400
1,0	112,8	433	433	300	600	100	200
2,0	159,6	416	833	150	300	50	100
3,0	195,4	399	1197	100	200	33	67
5,0	252,3	373	1867	60	120	20	40
7,0	298,5	355	2488	43	86	14	29
10,0	356,8	328	3284	30	60	10	20

- the cavity pressure drop as calculated by Cadmould at 75 % part fill multiplied by 1,25 to account for uncertainties as mentioned in Chapter 4
- the force on the piston face as a result of the pressure drop
- the required piston stroke, determined from the shot volume
- the required piston speed to fill the cavity in the time specified in Table 5.1

5.3 Hydraulic Actuation for Moulding Cylinder

This section describes the different costs associated with the different lomolders studied. Most (70 % to 80 %) of the hydraulic system cost is contributed by the cylinder, hydraulic pump and electric motor cost. Focus is placed on these three cost elements, since the rest of the hydraulic system cost is dependent on client configuration, control requirements and so forth.

Two choices are available when it comes to selecting a power pack configuration: fixed and variable displacement pump solutions. The fixed displacement pump is driven by an AC electric motor at constant speed (usually at 1450 rpm). The system will provide pressure (normally 250 bar) up to a certain maximum flow rate. When this flow rate is exceeded, the pressure generated by the pump will drop. A hydraulic pressure control valve ensures that the pressure will not rise higher than a certain safety preset value. If this preset value is reached, the excess hydraulic oil is bypassed to the tank by a pressure release valve, to keep the pressure constant. This method of pressure regulation generates heat that has to be removed from the oil again and is not favourable. However, this system option is available in smaller sizes than the variable displacement pump solution. It is costly to achieve the same versatility as that of the variable displacement pump solution. More valves and accumulators can be added to the fixed displacement pump solution, but this increases the total hydraulic system cost and complexity. Over time it will cost as much as the variable displacement pump solution to maintain, as a result of the complexity. Therefore, the author decided to opt for the variable displacement pump solution, even if it is oversized in the case of the mini lomolder. It is realised that many different combinations of pumps, motors, actuators, accumulators, valves and control configurations can be used in a lomolder. The variable pump configuration is explored as a basis to which other combinations can be compared if necessary. This comparison falls outside the scope of this research.

With the variable displacement pump solution, the generated pressure in the system is measured and the motor speed adjusted to keep the pressure constant at a preset value. The AC motor will reach a maximum speed at a certain required flow rate and this is the upper limit of the system. Thereafter, the generated pressure will drop. A pressure relief valve is also included in this system for safety reasons. The pressure limits are preset beforehand. This system option lends itself to easy expansion and producing parts with varying volumes. Small accumulators are also fitted occasionally to these variable displacement pump solutions to even out oil flow spikes that may occur.

From the data presented in Table 5.2, the hydraulic equipment is selected as follows: Hydraulic cylinder tubing comes in standard diameters - 40 mm, 63 mm, 80 mm, 100 mm, 125 mm, 160 mm, 200 mm and 250 mm. Special sizes can be manufactured, but the costs involved are about three to four times more than that of the nearest available diameter. Hydraulic power packs usually deliver pressure at 250 bar as an industry standard. For each size cylinder a maximum force can be calculated according to equation 5.3.1.

$$F = pA \tag{5.3.1}$$

where F is the force, p is the pressure and A is the area of the cylinder. The force generated by the hydraulic cylinder must just be higher that the force required

by the moulding cylinder in Table 5.2. Once the cylinder size is selected, the hydraulic flow rate can be calculated, since the injection time, cylinder area and piston stroke (determined by the thickest part i.e. highest volume) are known. A hydraulic pump can then be selected on the same basis as the cylinders. The smallest pump that satisfies the flow rate requirement of the system is selected. The variable displacement pumps have efficiencies of 94 %. The motor size is selected by calculating the power required as given in equation 5.3.2. The four pole 50 Hz electric motors run at 1450 rpm and have efficiencies of 80 %. The highest of the two power requirements as prescribed by the thin or thick part are used. The pumps and motors are selected by dividing the required flow and power by their respective efficiencies. Since the melt cavity pressure drop is already increased to account for unknowns, the motor size is not further adjusted.

$$P = pQ = Fv \tag{5.3.2}$$

where P is the power required, p is the pressure, Q is the hydraulic flow rate, F is the piston force and v is the piston speed. Table 5.3 shows the hardware selections for the different area ratios and Table 5.4 gives the corresponding cost estimates. The cylinder stroke is prescribed by the thickest part (highest volume). The electric motor power is driven by the thin part as it generates the higher pressure drop. It is noted that the combination of the longer stroke (and therefore higher oil flow rate to manufacture the thicker part in the same time as the thin part) and the higher force required to manufacture the thin part is not used to size the electric motor needed to drive the hydraulic pump. The thicker part requires less force to produce a part as discussed before. Normally the power requirement is higher for the thinner part as a result of the large increase in force required.

From Table 5.3 (refer to Table A.1 in Appendix A) it can be seen that the smallest motor size (3 kW) satisfies the requirements of all the cases of the mini lomolder. The smallest standard hydraulic cylinder diameter (40 mm - Figure A.4) satisfies all the corresponding cases except the one with the area ratio of 10 %. This is the reason that a larger hydraulic pump is necessary for the first two cases (higher required volume), since the required piston stroke decreases as the area ratio increases.

The midi lomolder cases are not restricted by hydraulic cylinder diameter, electric motor size or hydraulic pump flow rate. Therefore, no extreme values exist as in the case of the mini lomolder.

The maxi lomolder requires larger diameter cylinders than available in the standard range for the last three cases. This result in custom made cylinders which are expensive as can be seen in Table 5.4 for area ratios 5,0 %, 7,0 % and 10,0 %.

Table 5.3: Lomolder hydraulic selection

Mini Lomolder				
Area ratio [%]	**Cylinder dia [mm]**	**Cylinder stroke [mm]**	**Pump flow rate [cc/rev]**	**Power rating [kW]**
0,5	40	600	71	3,0
1,0	40	300	45	3,0
2,0	40	150	18	3,0
3,0	40	100	18	3,0
5,0	40	60	18	3,0
7,0	40	43	18	3,0
10,0	50	30	18	3,0
Midi Lomolder				
0,5	63	800	125	18,5
1,0	80	400	125	18,5
2,0	100	200	71	18,5
3,0	100	133	71	18,5
5,0	125	80	45	18,5
7,0	160	57	71	15,0
10,0	160	40	45	15,0
Maxi Lomolder				
0,5	125	1200	250	75,0
1,0	160	600	180	75,0
2,0	250	300	180	55,0
3,0	250	200	180	55,0
5,0	320	120	180	55,0
7,0	380	86	180	55,0
10,0	420	60	125	45,0

5.4 Electric Actuation for Moulding Cylinder

Selecting a servo motor - ballscrew configuration is a bit trickier than for the hydraulic counterpart. First of all a screw is selected that is able to handle the force/speed requirements of the configuration. A matching servo motor is then added to the system that will deliver the necessary torque. The speed is not as important, except that a maximum exists for the motor as well as the screw. A pulley/belt configuration is required even if the speed range of the servo motor is well matched to that required by the system, since the ballscrew nut is turned in all configurations. The lomolder configurations have varying speeds and loads and therefore the average load the screw will see in its service life is given by equation 5.4.1. Equations 5.4.1 to 5.4.5 comes from a manual by the Rexroth Bosch Group (2002).

$$F_m = \sqrt[3]{F_1^3 \frac{n_1}{n_m}\frac{q_1}{100} + F_2^3 \frac{n_2}{n_m}\frac{q_2}{100} + ... + F_n^3 \frac{n_n}{n_m}\frac{q_n}{100}} \tag{5.4.1}$$

where the average speed is given by equation 5.4.2:

Table 5.4: Lomolder hydraulic system costs

Area ratio [%]	Cylinder cost [R]	Motor cost [R]	Pump cost [R]	Total cost [R]
Mini Lomolder				
0,5	3724	2208	59 187	65 118
1,0	3514	2208	51 789	57 511
2,0	3409	2208	42 222	47 839
3,0	3374	2208	42 222	47 804
5,0	3346	2208	42 222	47 776
7,0	3334	2208	42 222	47 764
10,0	3439	2208	42 222	47 870
Midi Lomolder				
0,5	4794	8966	127 225	140 985
1,0	5747	8966	127 225	141 938
2,0	6301	8966	59 187	74 453
3,0	6134	8966	59 187	74 287
5,0	8972	8966	51 789	69 727
7,0	11 608	7302	59 187	78 096
10,0	11 510	7302	51 789	70 601
Maxi Lomolder				
0,5	13 161	28 450	176 403	218 014
1,0	14 702	28 450	140 317	183 469
2,0	28 386	23 376	140 317	192 079
3,0	27 060	23 376	140 317	190 753
5,0	85 240	23 376	140 317	248 933
7,0	172 545	23 376	140 317	336 238
10,0	188 980	18 952	127 225	335 157

$$n_m = \frac{q_1}{100} n_1 + \frac{q_2}{100} n_2 + ... + \frac{q_n}{100} n_n \tag{5.4.2}$$

where q_i is a percentage of the time that the screw will operate at a certain speed (n_i). The average speed (n_m) is influenced by the lead of the screw, but the average load is not.

The different lomolder screws were chosen to last for two years under continuous operation. This choice was made as Bracke (2006) mentioned that Engel's electric injection moulding machines requires service/replacement of its ballscrews every two years on average. The accuracy of the ballscrews becomes less as more play in the screw/nut develops as a result of wear over time. From this the service life in hours (L_h) and the service life in revolutions (L) can be calculated:

$$L = 60 n_m L_h \tag{5.4.3}$$

The dynamic load rating (C) is calculated as in equation 5.4.4 and from this the screw is selected from a catalogue.

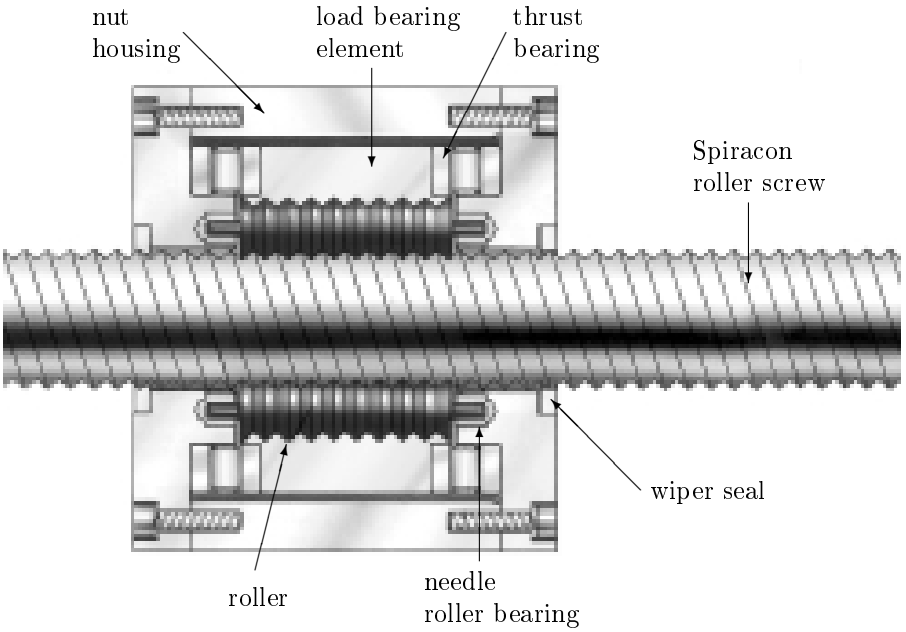

Figure 5.3: Roller screw (Spiracon, 2007)

$$C = F_m \sqrt[3]{\frac{L}{10^6}} \tag{5.4.4}$$

If more than one screw with different leads satisfy the dynamic load rate requirement, then the one with the smallest lead will often be selected, since this will lower the torque requirements (T) of the servo drive as calculated in equation 5.4.5. The operating rotational speed of the screw must not exceed its safe operating speed, or else a screw with a higher lead has to be selected.

$$T = \frac{Fp}{2\pi\eta} \tag{5.4.5}$$

where F is the operating load, p is the screw lead and η is the screw mechanical efficiency (normally in the range of 90 % for Bosch Rexroth ballscrews). Once again the lomolder cases presented here has relatively short strokes and therefore screw buckling did not present any problems. Bosch Rexroth manufactures screws with mainly a 10 mm or 20 mm lead. From their catalogue screws could be selected for the mini lomolder dynamic load requirements, as well as the first two area ratio cases of the midi lomolder. However, the company stopped manufacturing their highest dynamic load rating range, since it is very expensive and not often requested by clients. The reason for the high cost is that a grinding process is necessary in the case of the large screws/balls assemblies to achieve a good tolerance. The smaller assemblies' components are rolled.

The author explored roller screws (Figure 5.3) as a good alternative to ball screws when high dynamic load ratings are required. These screws were distributed by Yale Engineering products, but they stopped producing them due to high costs and low sales volume. SKF still distributes similar screws to Yale Engineering in South Africa. These screws have a short roller screw that runs on a few consecutive threads in place of the balls of the ball screw. Their higher cost (compared to ballscrews) is offset by the following advantages:

- higher dynamic load capacity
- larger diameters and higher leads
- higher positional accuracy
- longer life
- higher stiffness
- higher speed and acceleration
- low temperature operation
- lower noise
- nut easily removed with rollers retained

These roller screws have the capabilities required by all of the midi lomolder cases as well as the first two area ratio cases of the maxi lomolder. However, it will be seen that current available servo motors are only able to drive screws up to the first two cases of the midi lomolder configuration. Therefore, these screws will play a role when higher torque servo motors come to the market in future.

Ballscrews are used in this study, since they are cheaper and their accuracy can be improved by current feedback control technology. The selected lomolder ballscrews, screw costs, nut costs, servo motor costs and drive costs are shown in Tables 5.5 and 5.6 for the mini and midi lomolder configurations. It can be seen from Table 5.6 that the motor and drive cost shadows the screw and nut costs by about a factor of 10 across the range of area ratios for the mini- and midi lomolders. A screw cannot be selected for the mini lomolder case at the 0,5 % area ratio. The reason is that the rotational speed is higher than the allowed safe speed for the screw and nut combination. At such speeds excessive friction occurs at the ball bearings and screw contact area. The large amount of generated heat cannot be conducted quickly enough and this leads to lubrication failure and nut seizure. Therefore, no costs were calculated for this area ratio mini lomolder case.

Table 5.5: Lomolder screw and motor selection

Mini Lomolder					
Area ratio [%]	**Stroke [mm]**	**Screw lead [mm]**	**Rotational speed [rpm]**	**Torque required [Nm]**	**Selected screw [#]**
0,5	600	20	3600	-	Rotational speed too high
1,0	300	20	1800	15,6	32x20Rx3.969-2
2,0	150	10	1800	14,8	32x10Rx3.969-5
3,0	100	10	1200	21,3	32x10Rx3.969-5
5,0	60	10	720	33,1	40x10Rx6-4
7,0	43	10	516	43,1	40x10Rx6-4
10,0	30	10	360	56,4	40x10Rx6-4
Midi Lomolder					
0,5	800	20	2400	112,7	50x20Rx6.5-3
1,0	400	10	2400	108,8	63x10Rx6-6

The selected servo motors for the mini lomolder cases are all standard servo motors. The midi lomolder cases require asynchronous AC motors that can be controlled to operate as a servo motor and drive combination. It is more expensive, but can deliver higher torques that are required in these cases. If the client specifically requests an electric configuration for the higher torque requirement cases, a much more costly linear electric motor is available. Simply explained, these motors have a linear stator and the rotor rolls along the stator in a straight line. The high cost is contributed by a special linear encoder, linear bearings and water cooled stator. The reason that the stator is water cooled is that a fan cannot be connected to it as in the normal servo motor case. These motors are extremely accurate and can handle forces up to 20 tons.

The servo electric drives quoted in this section use absolute encoders, meaning that their position is exactly known at any given time. Again, this was a choice of the author and it is realised that less expensive incremental encoders could have been used. The absolute encoders offers the same versatility as the hydraulic variable displacement pump configuration and are therefore comparable on a cost basis. Incremental encoders use homing switches to calculate their position. A disadvantage of the homing switches is that the servo drive has to be reset in case of a power failure or system configuration change. The total electric configuration costs are shown in Table 5.6 for the mini and midi lomolder configurations. These costs include all necessary power and communication cables.

Table 5.6: Lomolder electrical actuator costs

Mini Lomolder					
Area ratio [%]	**Screw cost [R]**	**Nut cost [R]**	**Motor cost [R]**	**Drive cost [R]**	**Total cost [R]**
0,5	-	-	-	-	-
1,0	1295	3333	15 030	27 342	47 000
2,0	826	3158	15 030	27 342	46 356
3,0	708	3158	17 712	27 342	48 920
5,0	685	3690	21 969	27 342	53 686
7,0	643	3690	22 725	38 334	65 392
10,0	611	3690	27 289	38 334	69 924
Midi Lomolder					
0,5	3034	5097	38 696	47 877	94 704
1,0	2429	5940	38 696	47 877	94 942

5.5 Comparison of Hydraulic and Electric Actuation

5.5.1 Optimal area ratio

Optimal area ratios on a hardware purchase cost basis for the mini-, midi- and maxi lomolder are derived in this subsection. It must be stressed that interpolation between different area ratios to predict hardware cost is only a first approximation, since high non-linearities exist between these points.

From Table 5.4 it can be seen that an area ratio of 2,0 % to 3,0 % gives a minimum hydraulic purchase cost for the range of lomolder sizes analysed here. If cost is not the main design requirement, design outside of these regions are possible, but the hardware limitations mentioned below must be kept in mind. Non-standard hardware are extremely expensive as it is made in small volumes where standard types of hardware are produced in series. Standard hydraulic cylinder seals can operate up to 1,0 m/s. Larger speeds can be obtained, but special seals and rod surface finish requirements make this choice very expensive. Only the mini lomolder's 0,5 % area ratio requires a speed higher than 1,0 m/s, but is discarded on a cost basis. Shaft buckling is not a problem in any of the analysed cases, since the rod lengths are relatively short in the 2,0 % to 3,0 % area ratio region and the rods are well supported at the ends.

Area ratios of 2,0 % to 3,0 % provide a long enough stroke to work with regarding control (discussed in Section 5.7) and may be changed to suite the client's needs. For instance, moulding against skins may require a larger piston diameter to decrease the injection speed and decrease the shear rate as a result. In this case the area ratio is not selected with a minimum cost objective.

No conclusions regarding optimum piston to part area ratio can be obtained

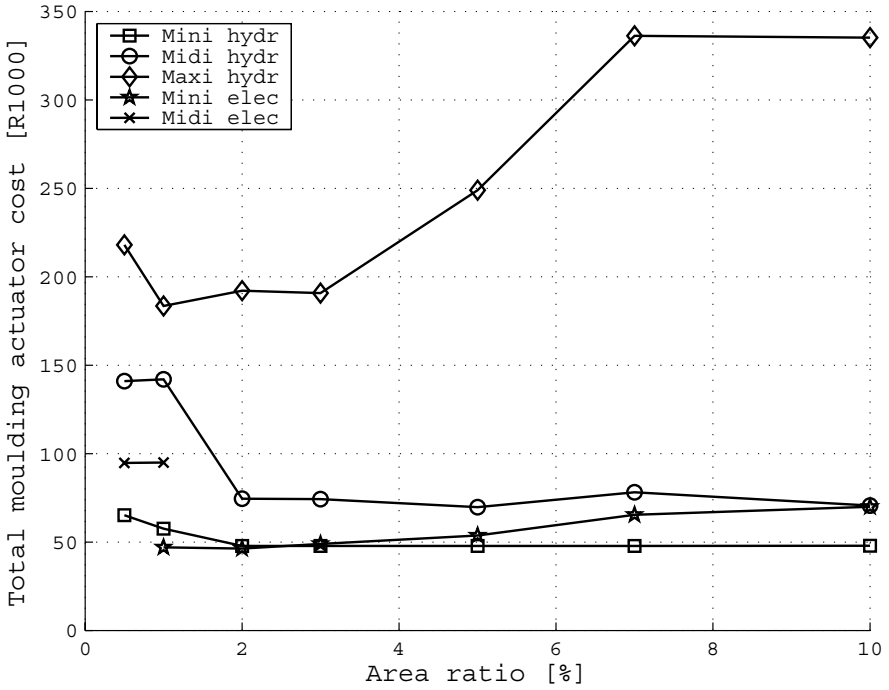

Figure 5.4: Total moulding actuator cost for hydraulic and electric actuation

from the midi lomolder electrical case, since only two area ratio cases can be evaluated with the components currently available in South Africa according to Venter (2007). Therefore, electric configuration machines are limited to a 0,5 % and 1,0 % area ratio for the midi lomolder case. An area ratio of 2,0 % to 3,0 % is again favourable on a purchase cost basis considering the mini lomolder electrical configuration.

Thus, for both hydraulic and servo electric configurations it seems that a 2,0 % to 3,0 % area ratio is good initial choice on a purchase cost view (refer to Figure 5.4). It is also noted that there is not much of a difference between the costs of the hydraulic and the electric configurations for the mini lomolder cases in the 2,0 % to 3,0 % area ratio range.

5.5.2 Metering actuator cost

For all three size lomolders, the hydraulic power pack is sufficient to drive the metering units. The reason is that only at the end of the moulding phase, maximum piston force is needed. This force requirement determines the power pack size in the cases considered here. Simultaneous actuation of the metering- and moulding cylinders is not necessary in the lomolding configuration, since the metering phase is done during the part cooling and ejection phase. Therefore, only the cost of the

Table 5.7: Metering unit design data

	Cylinder diameter [mm]	**Actuator stroke [mm]**	**Injection time [sec]**	**Actuator speed [mm/s]**	**Maximum force [kN]**
Mini LM	30	75	0,5	150	13,3
Midi LM	60	278	1,0	278	53,0
Maxi LM	110	630	3,0	210	178,2

Table 5.8: Metering unit hydraulic configuration cost

	Cylinder diameter [mm]	**Actuator stroke [mm]**	**Cylinder cost [R]**
Mini LM	40	75	3357
Midi LM	63	278	4241
Maxi LM	100	630	7376

cylinder has to be added to the total system cost. It must be kept in mind that mould opening and part ejection actuation is not considered in the cost analysis.

Table 5.7 shows the design data for the actuators of the lomolder metering cylinders. The forces are computed for a metering melt backpressure of 150 bar. The diameters of the cylinders were chosen to assist accurate metering, while the speed limitations of the ball screws and hydraulic piston seals were kept in mind. Too large metering cylinder diameters will result in a short metering piston stroke and therefore better control encoder accuracy is required to measure the shot size accurately. As the metering cylinder diameter is decreased, the total cylinder length increases, resulting in a cost increase.

The mini lomolder metering cylinder has a diameter of 30 mm, since it becomes very difficult to manufacture and assemble the unit if this diameter is further decreased. It may be desirable to have the metering actuator stroke longer for the mini lomolder case to achieve a good measuring accuracy. Since this is not possible, a more accurate position encoder may be needed for the mini lomolder metering cylinder compared to the midi- and maxi lomolder cases. The hydraulic cylinder costs are given in Table 5.8. The cylinder cost is not as much influenced by the length as the diameter and therefore its cost is mainly driven by the metering force required to transfer the melt to the moulding cylinder. This force is very dependent on the area of the metering piston. A straight line is fitted through the three force and cost points and equation 5.5.1 shows the relation:

$$C_{hydmet} = 24.5F_{met} + 2991.9 \tag{5.5.1}$$

where C_{hydmet} is the hydraulic metering unit cost and F_{met} is the required metering piston force in kN. Figure A.1 in Appendix A shows the fit accuracy.

Table 5.9: Metering unit electric configuration cost

	Torque required [Nm]	**Nut cost [R]**	**Screw cost [R]**	**Servo motor cost [R]**	**Servo drive cost [R]**	**Total cost [R]**
Mini LM	23,5	2733	502	21 969	27 342	52 546
Midi LM	93,7	5097	1251	38 696	47 877	92 921
Maxi LM	-	-	-	-	-	-

Table 5.10: Moulding unit costs

	Piston force [kN]	**Total hydraulic cost [R]**	**Total electric cost [R]**
Mini LM	13,1	47 804	48 920
Midi LM	184,0	74 287	94 942
Maxi LM	1197,1	190 753	-

The electric configuration cost is shown in Table 5.9. It is noted that the costs are much higher, compared to the hydraulic actuation, since a servo motor and drive must also be included. Again, the maxi lomolder metering cylinder requirements fall outside the range of currently available servo motors. A straight line (equation 5.5.2) is also used to interpolate for any electric metering cylinder between the mini and midi lomolder configurations. Care must be taken if this equation is used outside the interpolated region.

$$C_{elecmet} = 1017F_{met} + 39020 \tag{5.5.2}$$

where $C_{elecmet}$ is the electric metering actuator cost and F_{met} is the required metering piston force in kN. It is noted that equations 5.5.1 and 5.5.2 are derived for a metering cylinder melt backpressure of 150 bar. For other user defined backpressures, these equations will be different. The next step is to compute equations for the moulding cylinder actuators in a similar manner.

5.5.3 Moulding actuator cost vs. machine size

The costs in Table 5.10 are from Sections 5.3 and 5.4. All costs are for a piston to part area ratio of 3 %, except the midi electrical moulding unit cost, which is for a 1 % area ratio, since the 3 % area ratio is out of range.

Again a linear relationship (Equation 5.5.3) is assumed between the hydraulic cost data and the force required by the system.

$$C_{hydmol} = 118.7F_{mol} + 49104 \tag{5.5.3}$$

Table 5.11: Mini and maxi lomolder parts cost

	Mass [kg]	**Material cost [R]**	**Manufacturing cost [R]**	**Assembly cost [R]**	**Total cost [R]**
Mini LM	80	960	25 577	18 600	45 137
Maxi LM	3343	40 116	42 541	41 920	124 577

where C_{hydmol} is the hydraulic actuator cost for the moulding cylinder and F_{mol} is the force on the moulding piston in kN. Figure A.2 in Appendix A shows the fit accuracy.

Equation 5.5.4 shows a linear relationship for the moulding cylinder actuation. It is noted that this equation is fitted for a moulding piston face area to part effective area ratio of 3,0 % for a mini lomolder, but a 1,0 % area ratio for a midi lomolder. Therefore, this equation is not valid for moulding piston forces larger than 66,9 kN (refer to Table 5.2).

$$C_{elecmol} = 855.11F_{mol} + 37718 \tag{5.5.4}$$

where $C_{elecmol}$ is the electric moulding actuator cost and F_{mol} is the required moulding piston force in kN.

This concludes the costs involved for the metering and moulding actuators. The equations developed in this chapter will be used to determine the cost of a medium sized lomolder in Chapter 6.

5.6 Custom Manufactured Part Costs

This section describes the purchase cost of the manufactured parts for the lomolder assembly. These parts were designed before the cost analysis in the previous section was available. They were designed to withstand forces generated by a 5,0 % moulding piston area to part area ratio configuration. Therefore, these costs will not be exceeded if the area ratio is reduced to a more optimum point as determined earlier in this chapter.

The purchase cost of all the hardware that has to be manufactured (i.e. moulding unit, metering unit and runner system parts) is broken down into material cost, manufacturing cost and assembly cost. The parametric machine model (discussed in Chapter 4) was used to create layout designs for the mini, midi and maxi lomolder. TF Design quoted for the manufacturing and assembly of the lomolder parts (see Appendix A for cost data). Table 5.11 shows the parts' cost for the mini and maxi lomolder configurations.

The parametric design model was used to generate parts for the midi lomolder as well. The accumulated mass of these parts amounted to 523 kg.

Table 5.12: Midi lomolder mass calculation and verification

	Produced part volume [cm^3]	**Piston force [kN]**	**Mass of manufactured parts [kg]**
Mini LM	53	20	80
Midi LM	785	287	523
Maxi LM	6000	1867	3343

Table 5.12 shows the produced part volumes, piston forces (5 % area ratio and 75 % cavity fill multiplied by 1,25) and the total mass of the manufactured parts for the three sizes of lomolders. The author explored whether a linear relationship could be found between the produced part volume, the required moulding piston force and the total mass of the lomolding unit's components. If such a relationship exists, the lomolding unit component material cost can be estimated for any size of lomolder between the mini- and maxi lomolder limits.

The mass of the midi lomolder was linearly calculated on a part volume basis (m_V) as well as a force basis (m_F). The determined mass of the midi lomolder is listed below:

- determined by parametric sizing model: 523 kg
- linear interpolation by part volume (m_V): 482 kg
- linear interpolation by piston force (m_F): 552 kg

This shows that the manufactured parts' mass of the lomolding unit has an approximately linear relationship with the part volume and force exerted on the piston. Since both produced part volume and required piston force interpolations gave reasonable answers, the author decided to compute the lomolding unit components mass as the average of the two interpolated masses. The following equation will therefore be used to calculate the mass of a specific lomolder m_{lom} between the mini and maxi lomolder extremes:

$$m_{lom} = 3343 - \frac{1}{2}\left[1.767(1867 - F_p) + 0.5487(6000 - V_p)\right] \tag{5.6.1}$$

where F_p is the piston force in kN and V_p is the part volume in cm^3. The estimated lomolder parts mass is then multiplied by R12 /kg (mild steel price at the end of 2006 in South Africa) to obtain the manufactured parts material cost. This mild steel price is used similarly to a costing index for comparative studies. Using these equations, the midi lomolder manufactured parts will have a mass of 516 kg and the material cost will be R6196 . Figure A.3 in Appendix A shows the accuracy of the fit of equation 5.6.1.

According to manufacturing companies, the part manufacturing cost is also approximately linearly dependent on the parts mass and even more so in the cases

studied here, since the manufacturing operations do not differ between the different sizes of lomolders. The same can be argued regarding the lomolding unit assembly cost, since the complexity stays the same. Therefore, both the manufacturing cost and lomolder assembly cost are linearly interpolated as a function of the total lomolding unit mass between the mini- and maxi lomolder extremes. The next two equations show the equations used to approximate the manufacturing cost (C_{man}) and assembly cost (C_{assy}):

$$C_{man} = 42541 - 5.199(3343 - m_{lom}) \tag{5.6.2}$$

$$C_{assy} = 41920 - 7.147(3343 - m_{lom}) \tag{5.6.3}$$

The costing data used to derive these equations are given in Appendix A. When these equations are used, the midi lomolder manufacturing cost will amount to R27 843 and its assembly cost will be R21 715 .

5.7 Control Cost

The control system cost is very dependent on the hardware used in the lomolder design. No costing is done here, but it is shown that the control cost is not dependent on the mass of the manufactured lomolder parts. Rather, the control cost varies very little across the range of lomolders considered.

Lomolding has to distinct material injection phases. Molten material is injected at a constant flow rate during the first phase. This is followed by material injection at a constant pressure that will result in reducing the material flow rate. Once the cavity is filled, packing of the material commences under a constant pressure. These constant flow rate and constant injection pressure phases are easily controlled by the servo valve(s) of the hydraulic power pack. The equivalent of these phases when electric motors are used will be the following: The first phase will be done with a constant rotational velocity by varying the current supplied to the servo motor. The second phase will be achieved with a constant torque supplied by the motor i.e. a constant current.

Servo motor drives are programmed to achieve the requested velocity of the constant filling phase if possible. If this is not possible the controller will respond with a servo alarm. This is a built in electronic protection feature. The controller is able to do the pressure phase requirement by using basically the same logic. The programmer has to supply a force output and the controller will try to achieve it.

The control system of the lomolder can mainly be configured after the design phase. Provision must be made for control feedback elements for instance thermocouple probes, linear translation sensors, etc. The lomolder control system will

be PLC (Programmable Logic Controller) based as many inputs and outputs exist. Two types of PLC's exist today: the traditional PLC ('hard' PLC) and the computer based PLC ('soft' PLC). Traditional PLC's are build to withstand life on the factory floor, can easily connect to industrial wiring and are good at real-time control. Personal Computer (PC) based PLC's are easy to program and very versatile. As computer processing speed increased rapidly during the last decade, 'soft' PLC's are now able to do real-time control. One of the drawbacks with 'soft' PLC's is the rapidly changing PC technology. Traditional PLC's are easily supported for up to five years. System stability, when using 'soft' PLC's, is often achieved by redundancy for instance using dual CPU (Central Processing Unit) systems, etc.

The following information is important when selecting PLC's:

- Number of outputs
- Number of inputs
- Sampling rate (current technology PLC's sufficient in most cases - not as important factor anymore)
- Type of CPU required (modern PLC CPU's can do floating point operations - ease of programming increased)
- Decisions where control is needed, for instance: linear displacement sensor can have an integrator/differentiator on board for calculating displacement, velocity and acceleration and the output is fed to the PLC versus a simple sensor where all calculations have to be done by the PLC
- Type of output cards (relay or transistor) to be used. Relay types are preferred due to lower maintenance (easier to replace only one relay than whole card)
- Availability of local system integrators and/or programmers for the specific PLC brand

The most important cost driver for PLC based systems is the number of inputs and outputs required to control the system. This determines the number of input/output cards required. The PLC unit becomes more expensive when all the control calculations have to be done by the PLC's CPU. This computing load can be distributed by using intelligent feedback components. The total control system cost can also be altered by substituting expensive control cards with combinations of less expensive controllers. An example is the replacement of a dedicated temperature control card with a converter/transducer that feeds the thermocouple output to an analogue card. The computational load is then shifted to the PLC's CPU. It can therefore be seen that numerous options exist to control the lomolder. Finding

an optimum solution can therefore only be done once the lomolder hardware is set, which narrows down the control component combinations.

A typical control system for a lomolder will require control elements for the following:

- hydraulic actuators
- electric motor/ball screw combinations
- linear displacement sensors
- pressure sensors
- temperature control

The control system will be sized according to the specific lomolder being designed. The control system will be more or less the same for any given lomolder, since the type hardware does not differ between different sizes of lomolders. Therefore the PLC based control system (number of input/output cards etc.) can be scaled for any size of lomolder to estimate the control cost if needed.

5.8 Maintenance and Operating Cost

This section provides maintenance and operating information gathered mainly from the South African industry for injection moulding machines. Most of the information is for hydraulic machines, since the hydraulic technology has been in use much longer than the electric machine technology. A few companies are replacing their old hydraulic machines with electric machines. Companies that have electrical machines in use have not had them long enough in order to make conclusions on life cycle maintenance costs, since most of the machines have not gone through a major overhaul yet. Information gathered for electrical machines are from Engel South Africa.

Comparing maintenance and operating costs is also difficult since the technology has improved and large differences between different manufacturers exist. An example from Circuit Breaker Industries confirms this: A Ferromatic machine has at least four proportional hydraulic valves with a replacement cost of approximately R7800 . An Engel hydraulic injection moulding machine has only two. A Ferromatic machine has three limit switches and two hydraulic valves to prevent the opening of the safety gate while the machine is operating. An equivalent Engel machine has only four limit switches. An equivalent Chinese machine has a warning sign informing the operator of moving parts with no safety gate and no limit switches or valves - i.e. no maintenance costs. A medium sized Engel machine has one hydraulic oil filter on the pressure side of the pump. A Ferromatic machine has two - one on the

suction side and one on the pressure side. This illustrates that maintenance costs vary significantly from one manufacturer to the other and that a generally valid prediction of a lomolder's maintenance cost is not possible. However, to illustrate the type of maintenance that should be anticipated, the following:

Hydraulic machines undergo a yearly service where the following are checked (Viehweg, 2006):

- The cylinders and power packs are checked for leaks and seals are replaced if necessary. Usually equipment is run until it fails.
- Hydraulic accumulators are checked for leaks and undergo a pressure test every three years.
- Hydraulic oil pipes are checked for leaks and replaced if necessary.
- Hydraulic oil is tested and usually replaced together with the filters if due. Oil costs about R10 /l and a filter in the order of R1230 . Obviously the amount of oil increases as the size of the machine increases - a 20 ton clamp force machine takes about 150 litre of oil and a 250 ton machine 600 litre.
- The control system is cleaned.
- The linear slides are greased.
- The screw and barrel are measured and reworked/replaced if necessary.
- All safety switches are checked.

In general hydraulic machines become very dirty machines as they get older. The cylinders start leaking oil, the pipes are sweating and the solenoid valves start leaking, for instance. The repair is time consuming and costly. Maintenance, especially on the screw and barrel, is very dependent on the type of material that is processed. PVC is more corrosive than other materials and Nylon and fibre reinforced material (glass fibres for instance) are very abrasive.

Most manufacturers of electric machines state that the components are almost maintenance free. However, the belts are replaced approximately every two years (Bracke, 2006). The ballscrews and nuts are also checked yearly and replaced when the tolerance levels are outside the specifications. The screw drag force also becomes larger as they get older.

5.9 Conclusion

This chapter showed why a moulding piston to part effective area ratio of 2 % to 3 % is a good choice regarding the lomolding unit purchase cost. The differences between electric and hydraulic configurations were highlighted as well as their specific

application fields. High speed, low pressure (force) requirements (metering cylinder for instance) can easily be met by electric motor/screw combinations. High pressure requirements (moulding cylinder) especially in the larger area ratio cases of the midi lomolder and all the area cases of the maxi lomolder can be delivered by hydraulic actuators. Therefore, the possibility exists for hybrid lomolders when large parts are to be manufactured, where the moulding phase is performed by hydraulic actuators and the metering phase is done with electric actuators where high accuracy is required. Cost analysis was not done for hybrid lomolders.

Equations for the purchase cost of the manufactured parts were formulated for the metering and moulding unit configurations. These equations can be used to estimate the cost of machines lying between the mini and maxi lomolder configurations. Such an example is given by the case study of Chapter 6.

The last part of the chapter showed why it is not possible to draw generally applicable conclusions regarding the maintenance and operating cost of electrical versus hydraulic machine configurations. Another cost issue that is very difficult to determine, before detailed design has been completed, is the control cost of the lomolders. It is very dependent on the client's needs. One point that can be argued is that the control system will not differ significantly for the range of lomolders, since the operating sequence is identical. The next chapter uses the equations developed here to approximately determine the purchase cost of a medium sized lomolder.

Chapter 6

Design Case Studies

6.1 Introduction

The first part of this chapter describes a general design optimisation procedure to estimate the machine purchase cost. The second part of the chapter shows how the information given in Chapters 2 to 5 is used to estimate the purchase cost of a medium sized (midi) lomolder capable of making a dust bin. This relatively simple 3D part is used to illustrate the cost estimating process' capability. The third part of the chapter considers a large lomolder and shows why it is better to use four lomolding units per machine (if possible) from a cost perspective.

6.2 Design Optimisation Process

The optimisation objective function is the minimisation of the lomolder purchase cost. This purchase cost, combined with part material cost and part cycle time, drive the moulded part's cost. The optimisation problem is complex as can be seen from the information described in the previous chapters. Various discontinuities exist in the parameter values e.g. discrete steps exist in the available hardware. Therefore, it is difficult to formulate a fully automatic optimisation process that will run without any user intervention. Rather, it was decided that the user is allowed to influence the optimisation process by specifying the independent variables and some constraints on the process. These constraints are labelled "designer constraints" in the rest of the chapter.

Two other constraint types exist in the optimisation model. The specific part to be manufactured places constraints (e.g. geometric) on the optimisation process. The last type of constraints are grouped under hardware constraints, e.g. limitations of actuator speed. This concludes the constraint types to be discussed in the next subsections. The independent variables, as well as intermediate variables calculated by the model, are described first.

6.2.1 Independent variables

Ideally an optimisation algorithm should be used to systematically vary the independent variables until a minimum objective function value (lomolder purchase cost) is found. However, the optimisation model is not sufficiently robust for this approach. Therefore, the optimisation algorithm currently relies on the user to make realistic choices for the independent variable values.

The user has to decide on a melt injection profile similar to those described in Figure 2.19. Caution must be exercised during selection as a too high flow rate will lead to an unnecessary increase in machine purchase cost, as well as higher material shear rates that could cause fibre attrition for instance. A too low flow rate will lead to a short shot, i.e. when the melt solidifies prematurely during cavity filling, but this would not occur as long as the Graetz number remains above the 100 limit (Section 2.4). The point where the constant melt flow rate phase is followed by cavity filling under constant pressure, determines the actuator sizing and cost as shown in Chapter 5.

The moulding piston face area to part effective area ratio is treated as an independent variable. Chapter 5 showed that an area ratio of 2 % to 3 % is ideal when lomolder purchase cost is the objective function.

6.2.2 Intermediate variables

Intermediate variables are calculated by the optimisation model as the process progresses. The following variables are considered as intermediate:

- Metering cylinder pressure drop: can be calculated once the metering cylinder diameter, melt transfer time to the moulding cylinder and runner areas are known.
- Moulding piston diameter: this is calculated from the independent area ratio variable.
- Melt solidification layer thickness: this is calculated by the semi-analytical model in order to compute the cavity melt pressure drop (refer to Chapter 2).
- Injection time and Graetz number: a range of injection times is used to compute the cavity melt pressure drop. The one that gives the lowest pressure drop (more or less at the point where the flow Graetz number reaches 100) is suggested to the user.
- Cavity pressure drop (ΔP): using the injection time, the user can check the semi-analytical model's estimate of the pressure drop against numerical simulation predictions.

- Shaft forces for metering (F_{met}) and moulding (F_{mol}) cylinders: these variables are easily calculated once the cavity pressure drop is known.
- Maximum piston speeds needed for metering (v_{met}) and moulding (v_{mol}) cylinders: these variables are calculated once the injection time is known.
- Runner sizing according to equations 4.4.1 and 4.4.2.

6.2.3 Optimisation procedure constraints

These constraints are divided into part, designer and hardware constraints.

6.2.3.1 Part constraints

- Part volume, thickness and shape: these constraints are essential for the semi-analytical model to calculate the cavity melt pressure drop. The part shape can be approximated as circular, square or rectangular. If the shape of the part is too complex to be categorised as either of the three, then the semi-analytical model may be used to calculate an initial flow rate that will minimise the cavity pressure drop. This flow rate can then be used as an initial estimate for a numerical analysis in order to compute the cavity pressure drop.
- Material properties that include:
  - melt unit shear rate viscosity, μ^*
  - melt viscosity shear rate exponent, m
  - melt melting temperature, T_m
  - thermal conductivity of melt, k_L
  - melt density, ρ_L
  - melt thermal diffusivity, α

  The material selection could have been part of the optimisation process. However, the impact of different materials on the moulded part properties are not considered in this dissertation.
- Material related constraints that consist of the following two process constraints:
  - melt inlet temperature, T_i
  - uniform cavity wall temperature, T_w

These constraints are not independent of the material selected. A too high melt inlet temperature will lead to melt degradation and a too low inlet temperature to premature solidification (in combination with the cavity wall temperature) and higher cavity pressure drops due to the increased melt viscosity. The cavity wall temperature influences the part cycle time.

- Number of moulding cylinders: this constraint is considered as a part constraint. Multiple moulding cylinders may be used when parts are manufactured with a high aspect ratio. The position of the injection points will determine the position of the weld lines (a weld line is the line where two melt flow fronts meet). It creates a weak line in the part when the part is reinforced with fibres, as no fibres are binding the matrix of the separate flow fronts. The part geometry therefore plays a role when the positions of the injection points are determined.

6.2.3.2 Designer constraints

- Metering cylinder diameter: this choice is influenced by the following:
  - measuring resolution of the linear encoder versus acceptable volumetric error on the moulded part (refer to Figure 3.2): the encoder determines the accuracy of positioning of the metering piston face.
  - the ratio of metering cylinder area to melt runner flow area: arguments regarding the melt shear rate mentioned in Chapter 4 must be kept in mind.
  - actuator speed: the designer can place a limitation on the metering and moulding actuator speed (either electric or hydraulic). The optimum melt injection flow rate may then be altered if necessary to incorporate this actuator enforced constraint.
  - assembly constraints: metering and moulding cylinder assembly becomes increasingly difficult as the cylinder diameter is reduced.
- Percentage increase on metering and moulding calculated pressure drop: the designer can decide on the level of uncertainty e.g. unknown effects such as the piston frictional forces. Also, a larger metering unit pressure drop will enable the metering unit to do some of the cavity filling if required.
- Actuator selection: the following selections can be made by the designer:
  - Either hydraulic or electric actuation
  - Variable or fixed displacement hydraulic pump (in case of hydraulic selection)

– Incremental or absolute encoding servo drives (in case of electrical selection)

6.2.3.3 Hardware constraints

- Ball screw speed or hydraulic cylinder speed: this determines the service life of the actuators.
- Ball screw or hydraulic shaft maximum allowed force.
- Servo motor torque constraints: some machine configurations (especially on the larger lomolder sizes) cannot be driven electrically.

6.3 Midi Lomolder Purchase Cost

The purchase cost is estimated in the following manner: First of all the cavity melt pressure drop is calculated. This is followed by sizing the metering and moulding cylinder as well as the melt flow runners. Once component sizing is completed, the approximate machine mass is determined with equation 5.6.1. The author realises that since few lomolding unit masses in the higher mass region were used to fit equation 5.6.1, a linear relationship (refer to Figure A.3) might be a crude estimation. The manufactured parts material cost is calculated from the parts' mass by multiplying with a price per kilogram of steel. The parts' manufacturing cost is then calculated by equation 5.6.2. This is followed by estimating the assembly cost by equation 5.6.3. Costing for the lomolder actuator units is then done with equations 5.5.1 to 5.5.4. The author used a metering unit pressure drop of 150 bar in the formulation of equations 5.5.3 and 5.5.4. Other metering pressure drops will influence these equations. At the end all the different costs are added to give the final lomolding unit pressure drop.

Figure 6.1 shows the dimensions in millimetre of the dust bin. It has a uniform thickness of 3 mm and a volume of 625 cm^3.

6.3.1 Cavity pressure drop calculation

The Novolen material is used as example, since from previous experience (refer to Chapter 2) it is known that Novolen leads to higher cavity pressure drops than the Celstran material. The material properties and process parameters were given in Table 2.1. The dust bin is closest to a flattened out round disc and therefore, "round" is selected as the part shape for use in the semi-analytical model. The effective part area is calculated as the dust bin volume divided by the thickness and is equal to 2081 cm^2. A part area to moulding piston face area ratio of 3 % results in a moulding piston diameter of 9 cm. A constant melt flow rate is prescribed for

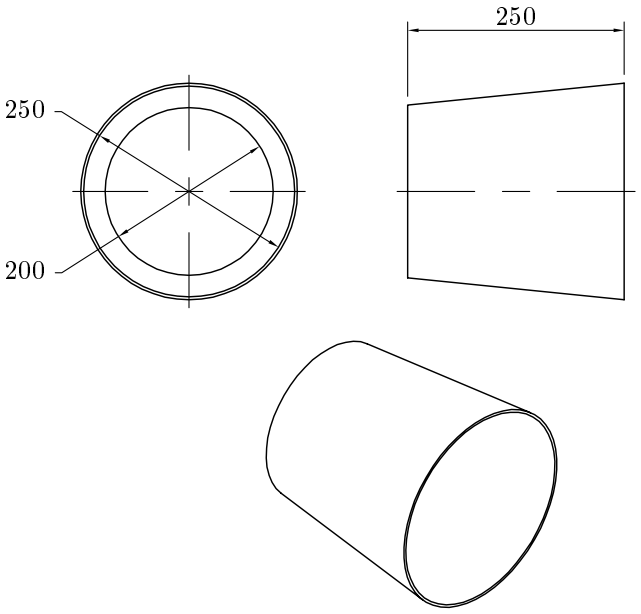

Figure 6.1: Dust bin size

75 % of the fill volume and the cavity pressure drop at this point multiplied by 25 % will be used for moulding unit sizing.

Figure 6.2 shows the results of the semi-analytical model for melt injection times ranging from 0,5 sec to 2,0 sec. Verification of the semi analytical calculated cavity pressure drops is done with Cadmould. The cavity pressure drops at 75 % fill are already multiplied by 1,25 in Figure 6.2. The user chose an injection time of 1 sec, since if longer injection times are used, the advantage of a smaller cavity pressure drop is cancelled by the increase in moulding cycle time. At 1 sec, the calculated pressure drop by Cadmould (multiplied by 1,25) is 25 bar higher than calculated by the semi-analytical model. The Cadmould result will be used in this case study, since it is the higher value and therefore provides more design safety.

6.3.2 Component sizing

The following values are calculated by the parametric sizing model.

6.3.2.1 Metering cylinder

A metering melt pressure drop of 150 bar is selected and a metering cylinder diameter of 5,0 cm. This gives a metering cylinder stroke of 318 mm. The metering cycle time was selected to be equal to the moulding cycle time (i.e. 1 sec). The

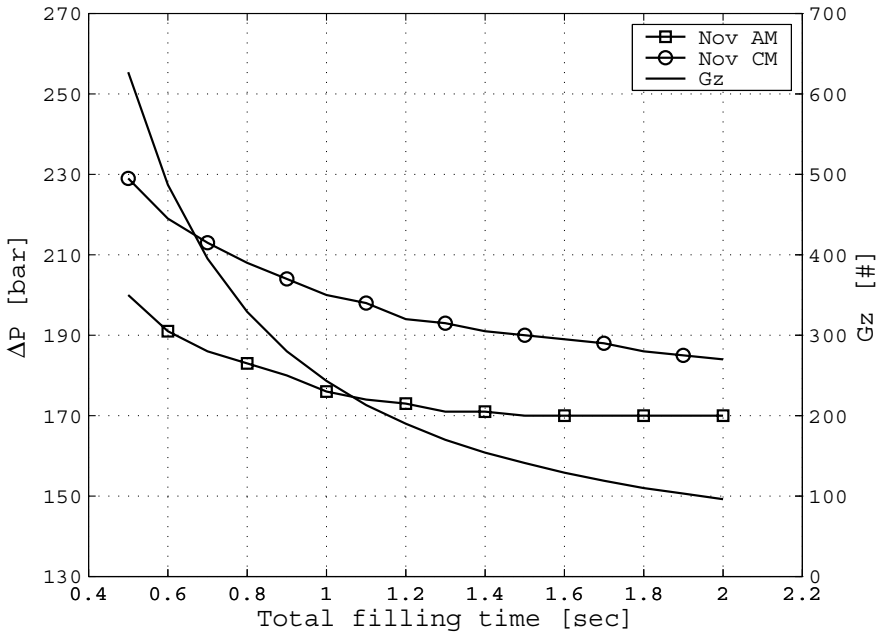

Figure 6.2: Dust bin melt injection time and resulting cavity pressure drop

required metering cylinder force is 29,5 kN and the required piston speed equal to 318 mm/s.

6.3.2.2 Moulding cylinder

The moulding melt pressure drop of 200 bar means that an actuator force of 127,2 kN is needed for the ϕ9 cm moulding piston. A moulding cylinder stroke of 98,2 mm is needed and a moulding piston speed of 98,2 mm/s to fill the cavity in 1 sec.

6.3.2.3 Runner areas and pressure drop

Figures 6.3 and 6.4 show the dimensions of the semi-annular runner and moulding cylinder ports. Again, the parametric sizing model checks the pressure drops per unit length and makes sure that all values are lower than the pressure drop occurring at the ring gate. Equations 4.4.1 and 4.4.2 are used for the Novolen material as it generates higher pressure drops than Celstran.

The pressure gradient of the material at the ring gate is 71 bar/m. The pressure gradient of the melt flow in the moulding cylinder is 0,65 bar/m for flow in round tubes (Equation 4.4.1). For the metering cylinder this pressure gradient is equal to 2,3 bar/m as a result from the smaller diameter piston. These respective pressure gradients are much smaller than the limiting 71 bar/m. Again, keep in mind that these pressure gradients are not very accurate as discussed in Chapter 4. However,

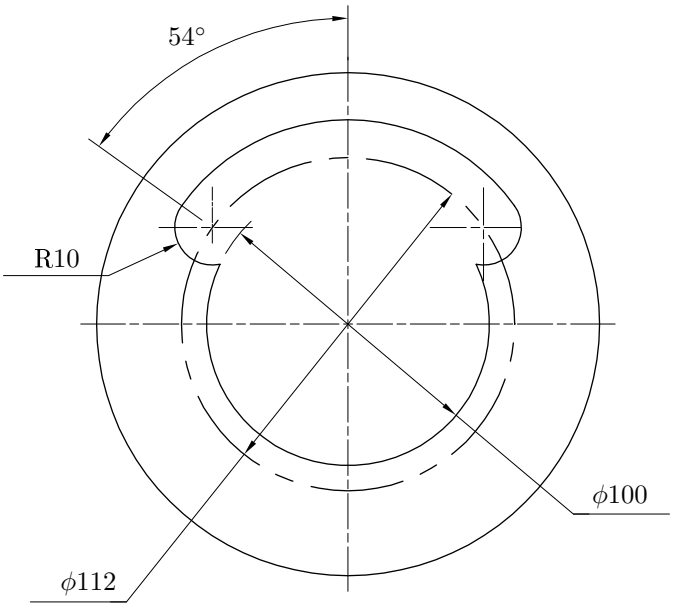

Figure 6.3: Semi-annular runner dimensions

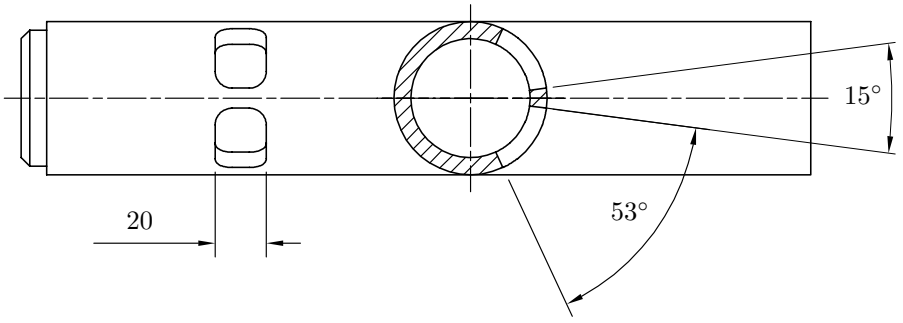

Figure 6.4: Moulding cylinder dimensions

the predicted pressure gradients are so much lower than the critical limiting value, that the inaccuracies are acceptable.

The semi-annular runner (Figure 6.3) was analysed with both of Richardson's equations. The highest pressure gradient was compared to the material pressure gradient at the cavity entry. The equivalent channel height ($2h$) was equal to 16 mm and the channel width (w) was taken to be 125 mm, i.e. the arc distance between the centres of the two R10 radii. These channel dimensions lead to a pressure gradient of 5,1 bar/m when Equation 4.4.2 is used. The hydraulic diameter of this runner computes to 29,3 mm. This gives a pressure gradient of 7,2 bar/m when Equation 4.4.1 is used for flow in tubes. Both these calculated pressure gradients are well below the limit of 71 bar/m and therefore the semi-annular runner dimensions are satisfactory.

The moulding cylinder's two ports were analysed by halving the material flow rate (Q) and calculating the dimensions of one hole (refer to Figure 6.4). Since these ports are almost circular it would not make sense to use Richardson's flow between parallel plates formula. The hydraulic diameter of the ports computes to 27,0 mm and this gives a pressure gradient of 6,6 bar/m which is also well inside the 71 bar/m barrier. Therefore all the flow areas conform to the principal of having the largest pressure gradient at the ring gate.

6.3.3 Cost estimation

The equations derived in Chapter 5 are used to estimate the total cost of the lomolding unit required to manufacture the dust bin. First of all the mass of the manufactured components are calculated with equation 5.6.1. The dust bin part volume is 625 cm^3 and the moulding piston force required equal to 127,2 kN. According to equation 5.6.1, the lomolder mass is 331 kg. The material cost will then be R3975 if a steel cost of R12 /kg is used. The parts manufacturing cost amounts to R26 882 when equation 5.6.2 is used and the lomolder assembly cost to R20 393 (equation 5.6.3).

If hydraulic actuators are chosen, the moulding actuator will cost R64 203 when equation 5.5.3 is used. Note that this cost includes the hydraulic power pack. Equation 5.5.1 gives a metering actuator cost of R3715 .

When electrical actuators are chosen, it is noted that this lomolder size falls outside the validity range of equation 5.5.4. The screw is the limiting factor and the largest screw size available from Bosch Rexroth can be used, but it might not survive the 2 year requirement. It may be a good option to manufacture a hybrid lomolder (hydraulic moulding unit and electrical metering unit) in this case if high melt measuring accuracy is needed. This will however increase the cost considerably. Equation 5.5.2 gives a metering actuator cost of R69 022 .

The total hydraulic lomolder cost is then R119 168 . The hybrid lomolder will cost R184 475 .

6.4 Number of Lomolding Units for Maxi Lomolder

This case study compares the total purchase cost between a maxi lomolder with a single lomolding unit and a maxi lomolder with four units to distribute the processing load. A transport pallet of 1,0 m by 1,0 m is considered as a product and a piston face area to part area ratio of 3 % is used. Again, the melt injection time is 3 seconds. The 3 % area ratio gives a moulding piston diameter of 195,4 mm when a single moulding cylinder is used and a diameter of 97,7 mm when four cylinders are used. Figure 6.5 shows the material flow inside the square cavity when four

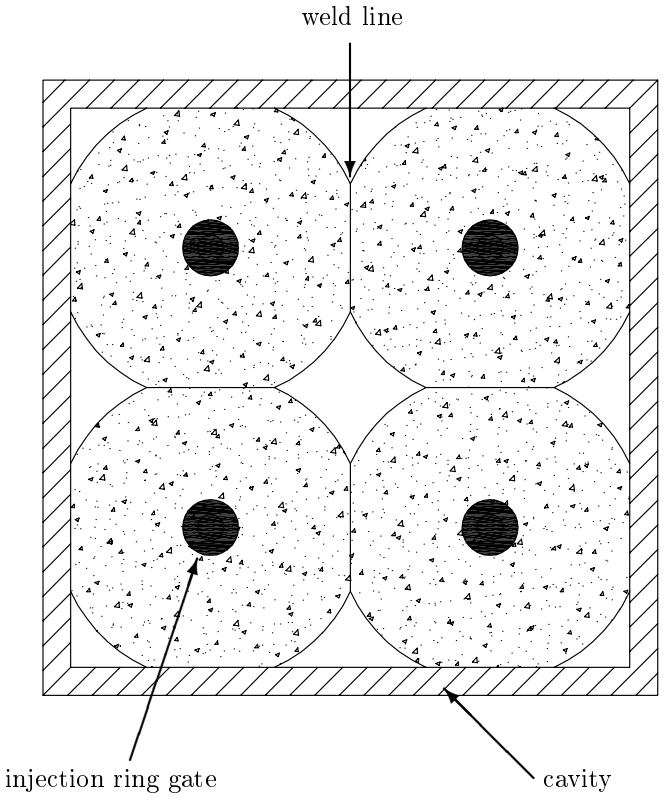

Figure 6.5: Flow front pattern of a lomolder with four lomolding units

moulding cylinders are used. Note the weld lines formation at the position where the melt flow fronts meet.

A cavity injection pressure drop (when four moulding cylinders are used) of 115 bar is needed at 75 % cavity fill as calculated by Cadmould. The semi-analytical result is inaccurate for this case study, since the Graetz number requirement is not met. Again, this pressure drop is increased by 25 % to account for friction and miscellaneous effects. Therefore, the design pressure drop is 144 bar. This compares to a design pressure drop of 399 bar if a single moulding cylinder is used. Therefore, the piston forces generated are 108 kN for four cylinders and 1197 kN for one cylinder.

The hydraulic cylinder cost for a single moulding cylinder amounted to R27 060 (refer to Table 5.4). Note that this cost was calculated as a combination of the high force needed to produce the 3 mm thick pallet and the stroke length needed to produce the 6 mm thick pallet. The cost for the four cylinders is calculated next. A hydraulic cylinder with a bore diameter of 80 mm is able to deliver a force of 125,7 kN at a 250 bar working pressure. The stroke of each of the four cylinders is

equal to 20 cm to produce a 6 mm thick pallet. According to Table A.4 the cost for a single cylinder (front flange type) is R5455 . Therefore, four cylinders will cost R21 820 .

The hydraulic moulding unit cost equation (5.5.3) developed in Chapter 5 cannot be applied directly, as this equation was developed specifically for a single lomolding unit per lomolder. The hydraulic power pack cost is included in this equation. However, the four moulding cylinders will still be driven by a single power pack and the power pack cost does not scale linearly between the number of lomolding units used as shown in the next paragraph.

The hydraulic power pack costs R164 128 to drive a single cylinder. This was calculated by using equation 5.5.3 and subtracting the cost (R27 060) of the single moulding cylinder. The power pack cost for the multi moulding piston is calculated as follows: A hydraulic fluid flow rate of 42,8 l/min is necessary when the 3,0 mm thick part cavity is filled. The pressure in each of the four cylinders is equal to 214,9 bar when a force of 108 kN is delivered. This means that an electric motor of at least 19,1 kW is required if an efficiency of 80 % is used. A 22 kW motor is selected from Table A.1 and costs R9922 . The hydraulic pump with an efficiency of 94 % must be able to deliver flow at 59 cc/rev . Therefore, a 71 cc/rev pump is selected from Table A.2 and costs R59 187 . Adding the pump and motor cost amounts to R69 109 for the hydraulic power pack.

It can be argued that the power pack size must be the same, since the same part is made in the same time under identical processing conditions. However, no linear relationship exists between the melt pressure drop occurring across the melt flow path. From the costs calculated above, it can be seen that a four moulding cylinder configuration is better sized (for hydraulic power pack optimisation) than a single cylinder configuration in the case study presented here.

The material, manufacturing and assembly costs are considered next. Four lomolding units will have a combined mass of 1394 kg, compared to the total mass of 3343 kg of one unit. These masses are calculated with equation 5.6.1. Therefore, the material cost difference will be R23 388 at R12 /kg. The manufacturing cost (equation 5.6.2) amounts to R107 892 , compared to the R42 541 needed to manufacture the single lomolding unit configuration (refer to Table 5.11). The assembly cost (equation 5.6.3) is R82 076 compared to the R41 920 needed to assemble the single lomolding unit configuration. Therefore, the total cost for the multi-piston lomolder is R297 625 , compared to the R315 765 of the single lomolding unit configuration. Table 6.1 summarises the calculated costs.

From these cost figures, it is cheaper in this case to use four lomolding units than one. Part quality must not be neglected when lomolder costing is considered. A multi-piston environment leads to weld lines forming in moulded parts. If not properly controlled and positioned, it can decrease the strength of the part considerably. This negative aspect must be weighed against the advantage of a smaller cavity melt pressure drop that can be obtained with multiple piston configurations.

Table 6.1: Cost comparison between single- and multi-piston lomolder configurations

	Single piston	**Multi-piston**
Moulding cylinder cost [R]	27 060	21 820
Power pack cost [R]	164 128	69 109
Manufactured parts' mass [kg]	3343	1394
Manufactured parts' material cost [R]	40 116	16 728
Manufacturing cost [R]	42 541	107 892
Assembly cost [R]	41 920	82 076
Total cost [R]	315 765	297 625

It must be noted that no maintenance and operating costs are considered. It is expected that the maintenance cost will be higher to maintain the multi-piston configuration lomolder. Melt distribution from a plasticiser or compounder to each lomolding unit is also ignored. This aspect will obviously have cost influences. Other configurations are also possible, for instance using a single metering cylinder to measure the melt for all four moulding cylinders. Cost estimation for this configuration can also be done in a similar fashion, but the equations developed in Chapter 5 have to be altered. This aspect is not covered in this study.

6.5 Conclusion

This chapter showed the application of the work described in Chapters 2 to 5. Firstly, the semi-analytical model was used to determine the cavity pressure drop to produce a dust bin size part. This pressure drop, together with the required user information, were used to size the lomolder with the parametric sizing model. The cost equations of Chapter 5 were used to determine the purchase cost of the lomolding unit components.

The second case study in the chapter showed a cost comparison between a single- and multi-piston lomolding unit configuration for a large lomolder. The purchase cost of the multi-piston configuration is slightly less than the single piston configuration. It was argued that this is not the only cost that has to be considered.

The author realises that many different lomolding unit component configurations and lomolder sizes exist and that two case studies are not enough to test the cost model thoroughly. However, this work provides a basis to study other configurations and component combinations and illustrates the value of the models developed in this dissertation.

Chapter 7

Conclusions

This dissertation discusses the critical design factors that have a large impact on machine cost for a range of different sized lomolders. Three questions are posed as objectives to this dissertation:

- What is the optimal ratio of part area to moulding piston face area?
- What type of actuator (hydraulic or electric) must be used?
- What is the optimal number of melt injection moulding cylinders when larger parts are manufactured?

To answer these types of questions, a parametric sizing and cost model was developed. First of all, a semi-analytical model (Chapter 2) was derived to ease the calculation of part cycle time and cavity pressure drop calculations. The model proved to be useful for machine costing studies. The model's limitations regarding part complexity and its dependence on the melt flow Graetz number were discussed. Estimations can easily be checked with numerical simulation packages, after the injection time has been estimated using the semi-analytical model.

Various machine layout concepts were discussed in Chapter 3 and the layout with the least complexity and disadvantages was chosen for further development. A refined design and parametric sizing model, which includes a parametric CAD model, were developed in Chapter 4. This sizing model is useful in determining machine component sizes for various ranges of lomolders. It also provides information regarding actuator shaft forces, cylinder stroke lengths and actuator speeds required.

In Chapter 5 equations were developed to estimate the purchase cost of different sized lomolders. This chapter builds on all the information of Chapters 2 to 4 and is used as input to answer the first two questions posted above. Chapter 5 shows that a moulding piston face to effective part area ratio of 2,0 % to 3,0 % is a good choice for both hydraulic and servo electric configurations from a purchase cost point of

view. This ratio may be changed if other factors like material shear rate is very important to produce quality parts. Such aspects were, however, not considered here.

The parametric and cost models were validated for only three lomolder configurations and more costing research can be done considering more lomolder sizes as well as different actuator technologies, e.g. cheaper encoders for the servo motors and fixed hydraulic pump power packs with accumulators. However, a basis is set for further research regarding these aspects.

The question whether electric or hydraulic actuation is "best" does not have a precise answer and is very dependent on the purpose of the lomolder. For instance, it was shown that large lomolders (capable of manufacturing large parts) require very high moulding actuator forces and that electrical configurations are not capable of achieving this. However, on the smaller lomolder cases, the client may request that electrical actuators have to be used. Reasons may include accuracy, low noise and clean environments. It was shown that electrical actuators are more expensive, and therefore hydraulic actuators must be used if cost is the only basis of decision. The main reason is that one power pack can drive both the metering and moulding actuators, where electrical configurations need two servo motors and two drives.

Further, it should be noted, that the costs predicted in Chapter 5 are not intended for accurate estimates, but to enable machine designers to evaluate design options. These costs were calculated on a quotation basis for the different components. It is too expensive to validate these quoted costs against costs gathered by building the different sized lomolders.

In Chapter 6, two design case studies show the usefulness of the work presented in this dissertation. A medium sized lomolder was evaluated and a sizing and costing analysis was performed. It showed the limitations of the electric configurations when the lomolders become larger. The second case study in Chapter 6 considers the option of having multiple moulding units injecting melt into the part cavity. It was shown that a multi-piston configuration was slightly cheaper on a purchase cost point of view than a single piston configuration for a large part. However, disadvantages are introduced (e.g. weld lines inside the part where the melt flow fronts meet during injection).

The cost model (in particular the equations developed in Chapter 5) can in future be improved by analysing more lomolder sizes and actual prototype machines' cost. Also, different types of hydraulic and electric configurations must be evaluated and compared, since many actuation combinations exist.

Finally, as shown in Chapter 6, this dissertation achieved the objectives set out in Chapter 1, and the parametric sizing and cost model provides a useful tool to optimise lomolder design configurations.

Appendix A

Cost Data

This appendix contains all the hardware cost data that was collected during the research done in this dissertation.

Electric motors for
hydraulic power packs
4 pole 50 Hz 1450 rpm flange mounted
Contact: Zest Automation (021) 551-2710
Leon Christians, Jolene Hall

Size	Cost
[kW]	[R] ex vat
3	2208
4	2455
5.5	2974
7.5	3676
11	5678
15	7302
18.5	8966
22	9922
30	11940
37	16277
45	18952
55	23376
75	28450
90	32361
110	39177
132	47095
160	50989

Table A.1: Electric motor cost

Hydraulic pumps for hydraulic power packs

Contact: Hytec (021-551 4747)

Herman van Rensburg

Description	Size	Cost
[#]	[cc/rev]	[R] ex vat
SYDFE1-2X/018R-PSC12N00-0000-A0X0XX6	18	42222
SYDFE1-2X/045R-PPA12N00-0000-A010PXX	45	51789
SYDFE1-2X/071R-PPA12N00-0000-A0X0XX5	71	59187
A A4VSO 125 HS3P /30R-PPB13N00	125	127225
A A4VSO 180 HS3P /30R-PPB13N00	180	140317
A A4VSO 250 HS3P /30R-PPB13N00	250	176403

Table A.2: Hydraulic pump cost

Contact: Hytec (021-551 4747)

Herman van Rensburg

	RETAIL	RETAIL	RETAIL	RETAIL	RETAIL
	PRICE	PRICE	PRICE	PRICE	PRICE
BORE	220	280	320	380	420
ROD	160	180	220	220	300
STROKE	300	200	120	85	60
FRONT FLANGE	R 73,820	R 80,240	R 85,240	R 172,545	R 188,980

Table A.3: Hydraulic non-standard cylinder cost

Contact: Hytec (021-551 4747)
Herman van Rensburg
ISSUE DATE 01/01/2006
VALUED TILL 01/01/2007

H250B SERIES STANDARD CYLINDERS

DEL: 10-15 WORKING DAYS

BORE	40	50	63	80	100	125	160	200	250
ROD	20	32	40	50	65	80	100	125	160
STROKE	RETAIL PRICE	RETAIL PRICE	RETAIL PRICE	RETAIL PRICE	RETAIL PRICE	RETAIL PRICE	RETAIL PRICE	RETAIL PRICE	RETAIL PRICE
BASIC PRICE	R 2,302	R 2,974	R 3,419	R 4,394	R 4,952	R 7,267	R 9,496	R 13,986	R 12,804
PRICE/100mm	R 70	R 86	R 106	R 146	R 250	R 374	R 570	R 810	R 1,326
PRICE (incl str)	R 2,302	R 2,974	R 3,419	R 4,394	R 4,952	R 7,267	R 9,496	R 13,986	R 12,804
BODY MOUNTING									
MALE CLEVIS (MC)	R 3,091	R 3,196	R 3,652	R 4,746	R 5,428	R 8,070	R 10,794	R 15,468	R 23,202
FEMALE CLEVIS (FC)	R 3,130	R 3,227	R 3,686	R 4,785	R 5,515	R 8,186	R 10,925	R 15,851	R 23,777
FRONT FLANGE (FF)	R 3,304	R 3,414	R 3,946	R 5,163	R 5,801	R 8,673	R 11,282	R 16,272	R 24,408
REAR FLANGE (RF)	R 3,304	R 3,401	R 3,932	R 5,076	R 5,714	R 8,575	R 11,086	R 16,174	R 24,260
FOOT MOUNT (FO)	R 3,599	R 3,628	R 4,107	R 5,267	R 5,991	R 9,034	R 11,977	R 17,270	R 25,906
MALE TRUNNION (MT)	R 3,316	R 3,360	R 3,833	R 4,974	R 5,769	R 8,507	R 11,321	R 17,336	R 26,004
SPHERICAL BEARING (SB)	R 2,964	R 3,244	R 3,641	R 4,735	R 5,460	R 8,053	R 11,461	R 18,040	-
ROD END MOUNTING									
MALE CLEVIS (MC)	R 213	R 227	R 252	R 375	R 630	R 929	R 1,643	R 2,069	R 1,503
FEMALE CLEVIS (FC)	R 317	R 325	R 419	R 486	R 556	R 1,291	R 2,059	R 2,509	R 1,879
SPHERICAL BEARING (SB)	R 198	R 214	R 349	R 458	R 619	R 1,286	R 2,857	R 6,464	-

Table A.4: Hydraulic standard cylinder cost

Rexroth Precision Screw Assembly
Tectra Automation - 011 971-9400
Kevin Lombard

Part No	Length (mm)	Description	Unit Price
151224013		FLANGED SINGLE NUT, FEM-E-S 25 X 10RX3-4	R 2,732.90
151237013		FLANGED SINGLE NUT, FEM-E-S 32 X 20RX3,969-2	R 3,333.30
151234013		FLANGED SINGLE NUT, FEM-E-S 32 X 10RX3,969-5	R 3,158.30
151234013		FLANGED SINGLE NUT, FEM-E-S 32 X 10RX3,969-5	R 3,158.30
151244013		FLANGED SINGLE NUT, FEM-E-S 40 X 10RX6-4	R 3,690.10
151244013		FLANGED SINGLE NUT, FEM-E-S 40 X 10RX6-4	R 3,690.10
151244013		FLANGED SINGLE NUT, FEM-E-S 40 X 10RX6-4	R 3,690.10
151254013		FLANGED SINGLE NUT, FEM-E-S 50 X 10RX6-6	R 5,097.20
151264013		FLANGED SINGLE NUT, FEM-E-S 63 X 10RX6-6	R 5,940.20
150294002		FLANGED SINGLE NUT, FEM-E-S 125 X 10RX6,5-6	R 24,336.50
151124700	704	BALL SCREW SPINDLE, CUT TO LENGTH, SIZE 25 X 10R X 3	R 1,766.60
151137710	409	BALL SCREW SPINDLE, CUT TO LENGTH, SIZE 32 X 20R X 3,969	R 1,294.50
151134710	272	BALL SCREW SPINDLE, CUT TO LENGTH, SIZE 32 X 10R X 3,969	R 825.70
151134710	222	BALL SCREW SPINDLE, CUT TO LENGTH, SIZE 32 X 10R X 3,969	R 707.90
151144700	190	BALL SCREW SPINDLE, CUT TO LENGTH, SIZE 40 X 10R X 6	R 684.80
151144700	173	BALL SCREW SPINDLE, CUT TO LENGTH, SIZE 40 X 10R X 6	R 643.10
151144700	160	BALL SCREW SPINDLE, CUT TO LENGTH, SIZE 40 X 10R X 6	R 611.10
151154700	970	BALL SCREW SPINDLE, CUT TO LENGTH, SIZE 50 X 10R X 6	R 3,034.20
151164700	590	BALL SCREW SPINDLE, CUT TO LENGTH, SIZE 63 X 10R X 6	R 2,429.00

Table A.5: Ballscrew and nut cost

Rexroth Precision Screw Assembly
Tectra Automation - 011 971-9400
Georg Venter

Mini	**Torque req**	**Selected servo motor**	**Cost (ex vat)**	**Selected servo drive**	**Cost (ex vat)**
Area ratio	**by servo**				
	[Nm]		**[R]**		**[R]**
0.50%	4.17	MSK050C-0600	11301	HCS02.1E-W0028-A-03-NNNN	21898
1.00%	15.60	MSK070D-0300	15030	HCS02.1E-W0054-A-03-NNNN	27342
2.00%	14.84	MSK070D-0300	15030	HCS02.1E-W0054-A-03-NNNN	27342
3.00%	21.26	MSK070E-0300	17712	HCS02.1E-W0054-A-03-NNNN	27342
5.00%	33.15	MSK100C-0300	21969	HCS02.1E-W0054-A-03-NNNN	27342
7.00%	43.09	MSK101D-0200	22725	HCS03.1E-W0070-A-05-NNNV	38334
10.00%	56.38	MSK101E-0200	27289	HCS03.1E-W0070-A-05-NNNV	38334
Midi	**Torque req**	**Selected servo motor**	**Cost (ex vat)**	**Selected servo drive**	**Cost (ex vat)**
Area ratio	**by servo**				
	[Nm]		**[R]**		**[R]**
0.50%	112.77	MAD130C-0250	38696	HCS03.1E-W0100-A-05-NNNV	47877
1.00%	108.83	MAD130C-0250	38696	HCS03.1E-W0100-A-05-NNNV	47877

Table A.6: Servo motor and drive cost

MINI LOMOLDER METERING UNIT ASSEMBLY
Contact: Grant Hailmer 021 887 9288

THERMODYNAMICS FLUIDS & DESIGN

COMPONENTS

METERING UNIT ASSEMBLY (MI_LM01_A)

			Material cost	Manufacturing
Description	**Drawing No.:**	**Mass (kg)**	**R12/kg**	**Cost**
Welding of Metering Support Tube	MI_LM0111_A			R 525.00
Machining of Lower Flange	MI_LM01111_P	0.31	R 3.72	R 222.00
Machining of Motor Support Tube	MI_LM01112_P	1.7	R 20.40	R 285.00
Machining of Upper Flange	MI_LM01113_P	0.38	R 4.56	R 287.00
Machining of Cylinder	MI_LM0112_P	1.27	R 15.24	R 1,250.00
Machining of Bearing Bottom Cover	MI_LM0121_P	10.2	R 122.40	R 1,250.00
Machining of Bearing Sleeve Nut	MI_LM0122_P	0.041	R 0.49	R 225.00
Machining of Bearing Sleeve Top	MI_LM0123_P	1.46	R 17.52	R 605.00
Machining of Piston Skirt	MI_LM0131_P	0.22	R 2.64	R 275.00
Machining of Ball Screw Shaft	MI_LM0132_P	supplied	supplied	R 250.00
Machining of Piston Clamp	MI_LM0133_P	0.3	R 3.60	R 325.00
Machining of Piston Face	MI_LM0134_P	0.106	R 1.27	R 125.00
Machining of Motor Plate	MI_LM014_P	4.48	R 53.76	R 435.00
Machining of Piston Stationary Guide	MI_LM015_P	0.6	R 7.20	R 236.00
Machining of Sliding Rod	MI_LM016_P	2.22	R 26.64	R 620.00
Machining of piston Moving Guide	MI_LM017_P	2.45	R 29.40	R 399.00
	Totals	**25.737**	**R 308.84**	**R 7,314.00**

Table A.7: Mini lomolder metering unit parts cost

THERMODYNAMICS FLUIDS & DESIGN

MINI LOMOLDER MOULDING UNIT ASSEMBLY
Contact: Grant Hailmer 021 887 9288

COMPONENTS

MOULDING UNIT ASSEMBLY (MI_LM02_A)

			Material cost	Manufacturing
Description	**Drawing No.:**	**Mass (kg)**	**R12/kg**	**Cost**
Machining of Transfer Block A	MI_LM02111_P	11.9	R 142.80	R 2,400.00
Machining of Transfer Block B	MI_LM02112_P	10.9	R 130.80	R 2,400.00
Machining of Transfer Unit Runner	MI_LM02113_P	1.89	R 22.68	R 1,050.00
Machining of Transfer Unit End Cap	MI_LM02114_P	1.5	R 18.00	R 1,150.00
Machining of Transfer Unit Cylinder	MI_LM02115_P	1.143	R 13.72	R 1,250.00
Machininig of Alignment Screw	MI_LM0212_P	0.008	R 0.10	R 210.00
Welding of Pipe Support Assembly	MI_LM022_A			R 525.00
Machining of Pipe Support	MI_LM0221_P	2.13	R 25.56	R 725.00
Machining of Pipe Flange	MI_LM0222_P	1.01	R 12.12	R 452.00
Machining of Moulding Piston	MI_LM0231_P	1.935	R 23.22	R 725.00
Machining of Piston Skirt	MI_LM0232_P	0.369	R 4.43	R 375.00
Machining of Moulding Piston Face	MI_LM0233_P	0.076	R 0.91	R 825.00
Machining of Moulding Piston Guide	MI_LM0234_P	0.98	R 11.76	R 1,550.00
Machining of Piston Ball Screw	MI_LM0235_P	supplied	supplied	R 250.00
Machining of Bearing Bottom Cover	MI_LM0241_P	5.69	R 68.28	R 475.00
Machining of Bearing Sleeve Nut	MI_LM0242_P	0.083	R 1.00	R 275.00
Machining of Bearing Sleeve Top	MI_LM0243_P	1.471	R 17.65	R 650.00
Machining of Moulding Motor Plate	MI_LM025_P	7.7	R 92.40	R 580.00
Machining of Platen Stud	MI_LM03_P	1.08	R 12.96	R 900.00
Machining of Sliding Rod	MI_LM04_P	3.59	R 43.08	R 1,700.00
	Totals	**53.46**	**R 641.46**	**R 18,467.00**

Table A.8: Mini lomolder moulding unit parts cost

THERMODYNAMICS FLUIDS & DESIGN

MAXI LOMOLDER METERING UNIT ASSEMBLY
Contact: Grant Hailmer 021 887 9288

COMPONENTS

METERING UNIT ASSEMBLY (MA_LM01_A)

			Manufacturing	Material cost
Description	**Drawing No.:**	**Mass (kg)**	**Cost**	**R12/kg**
Welding of Metering Support Tube	MI_LM0111_A			R 525.00
Machining of Lower Flange	MA_LM01111_P	4.89	R 58.68	R 391.00
Machining of Motor Support Tube	MA_LM01112_P	27.62	R 331.44	R 1,650.00
Machining of Upper Flange	MA_LM01113_P	8.15	R 97.80	R 476.00
Machining of Cylinder	MA_LM0112_P	10.4	R 124.80	R 1,165.00
Machining of Bearing Bottom Cover	MA_LM0121_P	53.27	R 639.24	R 1,450.00
Machining of Bearing Sleeve Nut	MA_LM0122_P	0.179	R 2.15	R 325.00
Machining of Bearing Sleeve Top	MA_LM0123_P	13.98	R 167.76	R 725.00
Machining of Piston Skirt	MA_LM0131_P	4.59	R 55.08	R 385.00
Machining of Ball Screw Shaft	MA_LM0132_P	supplied	supplied	R 250.00
Machining of Piston Clamp	MA_LM0133_P	6.16	R 73.92	R 425.00
Machining of Piston Face	MA_LM0134_P	1.48	R 17.76	R 250.00
Machining of Motor Plate	MA_LM014_P	101.03	R 1,212.36	R 1,698.00
Machining of Piston Stationary Guide	MA_LM015_P	10.93	R 131.16	R 688.00
Machining of Sliding Rod	MA_LM016_P	20.714	R 248.57	R 1,250.00
Machining of piston Moving Guide	MA_LM017_P	66.32	R 795.84	R 1,848.00
	Totals	**329.71**	**R 3,956.56**	**R 13,501.00**

Table A.9: Maxi lomolder metering unit parts cost

MAXI LOMOLDER MOULDING UNIT ASSEMBLY
Contact: Grant Hailmer 021 887 9288

COMPONENTS

MOULDING UNIT ASSEMBLY (MI_LM02_A)

			Material cost	Manufacturing
Description	Drawing No.:	Mass (kg)	R12/kg	Cost
Machining of Transfer Block A	MA_LM02111_P	400.39	R 4,804.68	R 2,400.00
Machining of Transfer Block B	MA_LM02112_P	400.39	R 4,804.68	R 2,400.00
Machining of Transfer Unit Runner	MA_LM02113_P	690.52	R 8,286.24	R 4,000.00
Machining of Transfer Unit End Cap	MA_LM02114_P	125.4	R 1,504.80	R 2,850.00
Machining of Transfer Unit Cylinder	MA_LM02115_P	80.15	R 961.80	R 2,950.00
Machininig of Alignment Screw	MA_LM0212_P	0.122	R 1.46	R 235.00
Welding of Pipe Support Assembly	MA_LM022_A			R 525.00
Machining of Pipe Support	MA_LM0221_P	86.3	R 1,035.60	R 2,350.00
Machining of Pipe Flange	MA_LM0222_P	13.76	R 165.12	R 808.00
Machining of Moulding Piston	MA_LM0231_P	469.4	R 5,632.80	R 725.00
Machining of Piston Skirt	MA_LM0232_P	4.68	R 56.16	R 375.00
Machining of Moulding Piston Face	MA_LM0233_P	9.03	R 108.36	R 825.00
Machining of Moulding Piston Guide	MA_LM0234_P	29.67	R 356.04	R 1,550.00
Machining of Piston Ball Screw	MA_LM0235_P	supplied	supplied	R 250.00
Machining of Bearing Bottom Cover	MA_LM0241_P	85.5	R 1,026.00	R 750.00
Machining of Bearing Sleeve Nut	MA_LM0242_P	2.23	R 26.76	R 325.00
Machining of Bearing Sleeve Top	MA_LM0243_P	37.5	R 450.00	R 1,050.00
Machining of Moulding Motor Plate	MA_LM025_P	207.24	R 2,486.88	R 2,980.00
Machining of Platen Stud	MA_LM03_P	25.28	R 303.36	R 1,240.00
Machining of Sliding Rod	MA_LM04_P	345.26	R 4,143.12	R 5,400.00
	Totals	**3012.82**	**R 36,153.86**	**R 33,988.00**

Table A.10: Maxi lomolder moulding unit parts cost

ASSEMBLY COSTS FOR MINI/MAXI LOMOLDER ASSEMBLIES
Contact: Grant Hailmer 021 887 9288

ASSEMBLE AND TEST COST

		Number of		Cost per hour		
Description	Hours	Engineers	Technicians	Eng	Tech	Total cost
Mini Lomolder Assembly	40	1	1	R 275.00	R 190.00	R 18,600.00
Maxi Lomolder Assembly	64	1	2	R 275.00	R 190.00	R 41,920.00

Table A.11: Mini- and maxi lomolder assembly cost

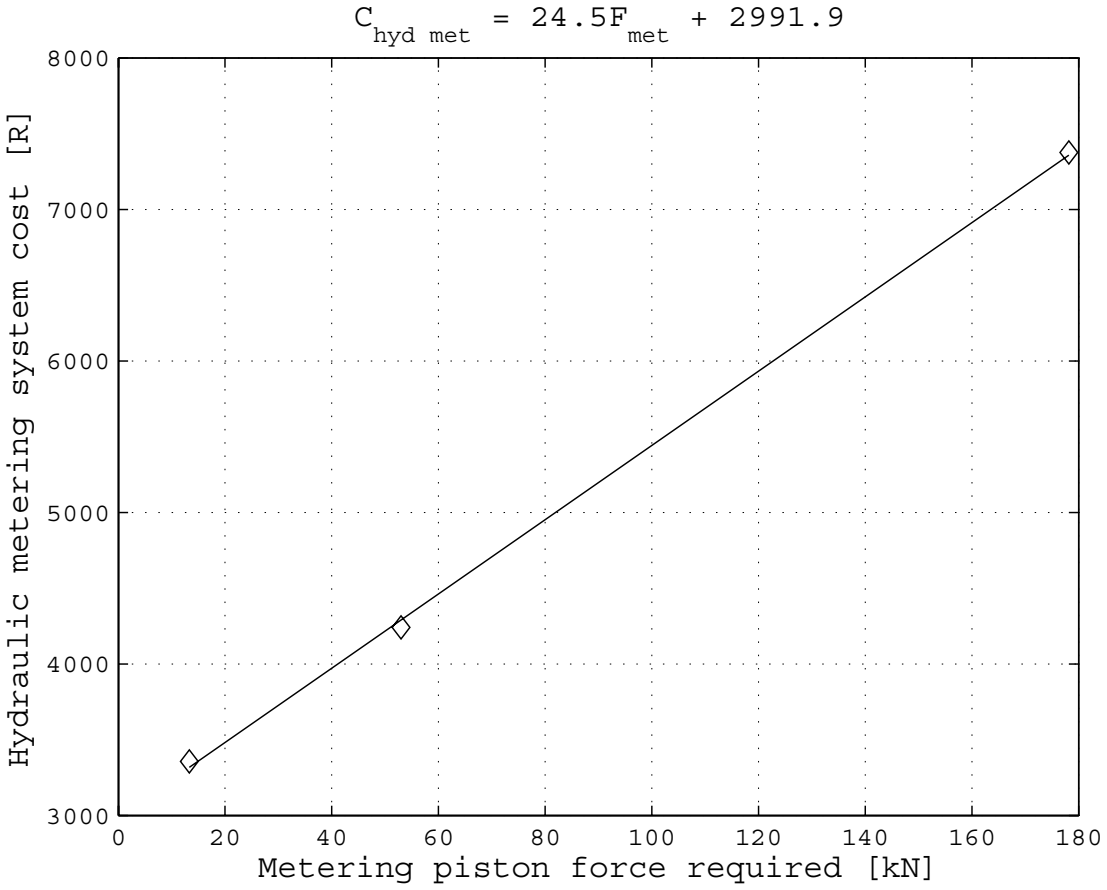

Figure A.1: Equation fit for hydraulic metering unit cost

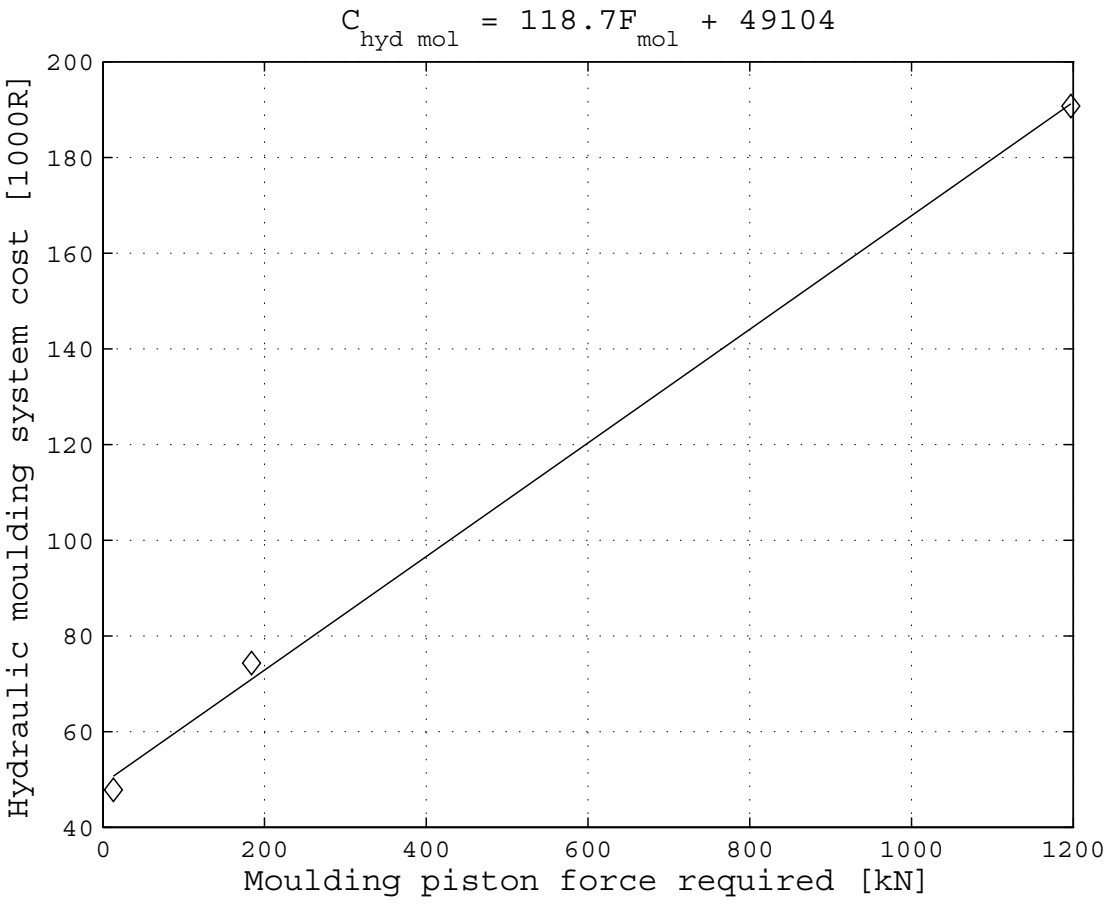

Figure A.2: Equation fit for hydraulic moulding unit cost

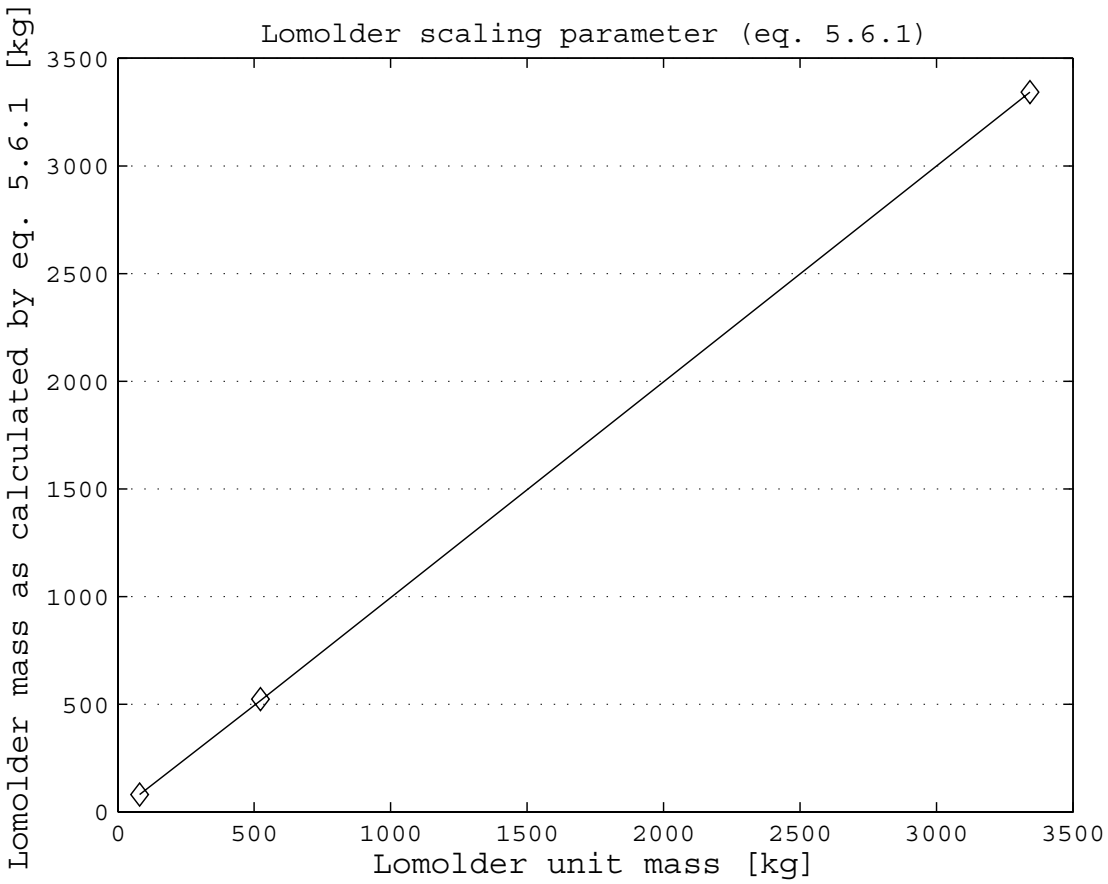

Figure A.3: Equation fit for lomolding unit mass

List of References

Benham, P.P., Crawford, R.J. and Armstrong, C.G. (1996). *Mechanics of Engineering Materials*. 2nd edn. Addison Wesley Longman Limited, England.

Bernhardt, E.C. (1983). *Computer Aided Engineering for Injection Moulding*. Hanser Publishers.

Blanchard, B.S. and Fabrycky, W.J. (1997). *Systems Engineering and Analysis*. 3rd edn. Prentice Hall International, Upper Saddle River, New Jersey 07458.

Bracke, P. (2006). Personal Communication: CEO of Engel, South Africa.

Cadmould (2002). v6. Simcon Kunststofftechnische Software GmbH, Germany. Available at: `www.simcon-worldwide.com`

Chen, Y-M. and Liu, J-J. (1999). Cost-effective design for injection moulding. *Robotics and Computer-Integrated Manufacturing*, vol. 15, pp. 1–21.

Dietz, W., White, J.L. and Clark, E.S. (1978). Orientation development and relaxation in injection moulding of amorphous polymers. *Polymer Engineering and Science*, vol. 18, no. 4, pp. 273–281.

Dymond, J.A.D. (2004). *The simulation of the flow of polymer melt in lomolding*. Master's thesis, Stellenbosch University.

Eckardt, H. and Stemke, L. (2000). Verfahren und vorrichtung zum spritzgiessen von kunststoff-formteilen. *European Patent Office*. EP1090734A1.

Gao, D.M., Nguyen, K.T., Girard, P. and Salloum, G. (1994). Effect of variable injection speed in injection mould filling. In: *Proceedings of the 52nd Annual Technical Conference*. Published by the Society of Plastic Engineers, Brookfield, CT, USA, pp. 712-715.

Goussard, C.L. and Basson, A.H. (2006a). Cavity pressure estimation for a piston moulding life cycle cost model. In: *Proceedings of the TMCE 2006*, pp. 767–774. Ljubljana, Slovenia.

Goussard, C.L. and Basson, A.H. (2006b). Parametric design model for the optimisation of a piston moulding machine. In: *The 16th CIRP International Design Seminar*, pp. 786–792. Alberta, Canada.

Goussard, C.L. and Basson, A.H. (2006c). Cavity pressure estimation for a piston moulding life cycle cost model. *Journal of Mechanical Engineering, Slovenia.* Accepted.

Goussard, C.L. and Basson, A.H. (2007). Concept evaluation and layout design of a piston moulding machine. In: *International Conference on Engineering Design 2007.* Paris, France. Accepted.

Hill, D. (1996). Further studies of the injection moulding process. *Applied Math Modelling*, vol. 20, pp. 719–730.

Hsing-Lung, L. and Hwang, G.J. (1977). An experiment on liquid solidification in thermal entrance region of a circular tube. *Letters in Heat Mass Transfer*, vol. 4, pp. 437–444.

Janeschitz-Kriegl, H. (1977). Injection moulding of plastics: Some ideas about the relationship between mould filling and birefringence. *Rheol. Acta*, vol. 16, pp. 327–339.

Janeschitz-Kriegl, H. (1979). Injection moulding of plastics: II. Analytical solution of heat transfer problem. *Rheol. Acta*, vol. 18, pp. 693–701.

Johnson, B.A. (2006). *The influence of processing on properties of injection-moulded and lomolded components.* Master's thesis, Stellenbosch University.

Jones, R.F. (1998). *Guide to Short Fiber Reinforced Plastics.* Society of Plastic Engineers, Hanser Publishers, Munich.

Joubert, F. (2005). *Rapid tooling and the lomold process.* Master's thesis, Stellenbosch University.

Kim, S-W. and Turng, L-S. (2004). Developments of three-dimensional computer-aided engineering simulation for injection moulding. *Modelling and Simulation in Materials Science and Engineering*, vol. 12, pp. 151–173.

Lee, D.G. and Zerkle, R.D. (1969). The effect of liquid solidification in a parallel-plate channel upon laminar flow heat transfer and pressure drop. *ASME Journal of Heat Transfer*, vol. 91, pp. 583–585.

Lee, R-S., Chen, Y-M. and Lee, C-Z. (1997). Development of a concurrent mold design system: A knowledge-based approach. *Computer Integrated Manufacturing Systems*, vol. 10, no. 4, pp. 287–307.

Manzione, L.T. (1987). *Applications of Computer Aided Engineering in Injection Moulding.* Hanser Publishers, New York.

Matsuoka, T., Takabatake, J-I., Koiwai, A., Inoue, Y., Yamamoto, S. and Takahashi, H. (1991). Integrated simulation to predict warpage of injection moulded parts. *Polymer Engineering and Science*, vol. 31, no. 14, pp. 1043–1050.

Mavridis, H., Hrymak, A.N. and Vlachopoulos, J. (1986). Mathematical modeling of injection mold filling: A review. *Advances in Polymer Technology*, vol. 6, no. 4, pp. 457–466.

Osswald, T.A. and Menges, G. (1995). *Materials Science of Polymers for Engineers.* Hanser Publishers, Munich, Vienna, New York.

Rexroth Bosch Group (2002). *Rexroth Precision Ball Screw Assemblies, End Bearings and Nut Housings*, RE 83 301/2002-09 edn.

Richardson, S.M. (1983). Injection moulding of thermoplastics: Freezing during mould filling. *Rheol. Acta*, vol. 22, pp. 223–236.

Richardson, S.M. (1985a). Injection moulding of thermoplastics. I. Freezing-off at gates. *Rheol. Acta*, vol. 24, pp. 497–508.

Richardson, S.M. (1985b). Injection moulding of thermoplastics. II. Freezing-off in cavities. *Rheol. Acta*, vol. 24, pp. 509–518.

Richardson, S.M. (1986a). Injection moulding of thermoplastics: Freezing of variable-viscosity fluids. Developing flows with very high heat generation. *Rheol. Acta*, vol. 25, pp. 180–190.

Richardson, S.M. (1986b). Injection moulding of thermoplastics: Freezing of variable-viscosity fluids. Developing flows with very low heat generation. *Rheol. Acta*, vol. 25, pp. 308–318.

Richardson, S.M. (1986c). Injection moulding of thermoplastics: Freezing of variable-viscosity fluids. Fully-developed flows. *Rheol. Acta*, vol. 25, pp. 372–379.

Richardson, S.M. (1987). Freezing-off in disc cavities. *Rheol. Acta*, vol. 26, pp. 102–105.

Richardson, S.M., Pearson, H.J. and Pearson, J.R.A. (1980). Simulation of injection moulding. *Plastic and Rubber: Processing*, vol. 5, pp. 55–60.

Schacht, T., Maier, U., Esser, K., Kretzschmar, O. and Schmidt, T. (1985). CAE/CAD in injection moulding, blow moulding, and foam moulding - the shortest way to mould design. *Advances in Polymer Technology*, vol. 5, no. 2, pp. 99–137.

Singh, K.J. and Wang, H.P. (1982). Computer analysis to optimise mould cooling process. *Society of Plastics Engineers: Technical Papers*, vol. 28, pp. 330–331.

Spiracon (2007). Spiracon roller screws. Power Jacks Ltd., South Harbour Road, Fraserburgh AB43 9BZ Scotland. (23 March 2007).
Available at: `http://www.powerjacks.com`

Venter, G. (2007). Personal Communication: Sales Division of Tectra Automation South Africa.

Viehweg, W. (2006). Personal Communication: Maintenance Engineer at Circuit Breaker Industries, South Africa.

Wang, V.W., Hieber, C.A. and Wang, K.K. (1986). Filling of an arbitrary three-dimensional thin cavity. *Journal of Polymer Engineering*, vol. 7, no. 1, pp. 21–45.

Weigand, B. and Beer, H. (1991). Heat transfer and solidification of a laminar liquid flow in a cooled parallel plate channel: The stationary case. *Wärme- und Stoffübertragung*, vol. 19, pp. 233–240.

Weir, C.J. (1975). *Introduction to Injection Moulding.* Society of Plastic Engineers, 656 West Putnam Avenue, Greenwich, Conn. 06830.

Yang, L.C., Chen, S.J. and Charmchi, M. (1991). Steady solidification of non-Newtonian fluid flowing in a round tube. *Polymer Engineering and Science*, vol. 31, no. 3, pp. 191–196.

Zerkle, R.D. and Sunderland, J.E. (1968). The effect of liquid solidification in a tube upon laminar flow heat transfer and pressure drop. *ASME Journal of Heat Transfer*, vol. 90, pp. 183–190.

Zhang, G. and Thompson, M.R. (2005). Reduced fibre breakage in a glass-fibre reinforced thermoplastic through foaming. *Composites Science and Technology*, vol. 65, pp. 2240–2249.